

N-CAP MUTANTS OF CHICKEN SKELETAL TROPONIN C :
STRUCTURE/AFFINITY RELATIONSHIPS OF PAIRED
CALCIUM BINDING SITES

by

Louise Ellen Leblanc

B.Sc. (Honours) Simon Fraser University, 1993

Thesis submitted in partial fulfillment of the requirements
for the degree of Master of Science

in the Department of Chemistry and
Institute of Molecular Biology and Biochemistry

© Louise Ellen Leblanc, 1996

SIMON FRASER UNIVERSITY

June 1996

All rights reserved. This work may not be reproduced in whole or in part, by photocopy or other means, without expressed permission from the author.

APPROVAL

Name: Louise Ellen Leblanc
Degree: Master of Science
Title of thesis: N-cap Mutants of Chicken Skeletal Troponin C:
Structure/Affinity Relationship of Paired Calcium
Binding Sites

Examining Committee:

Chairman : Dr. Rosemary Cornell

Dr. ~~Thor~~ J. Borgford
Senior Supervisor
Associate Professor

Dr. William Richards
Professor

Dr. Steven Holdcroft
Associate Professor

Dr. Andrew J. Bennet
Internal Examiner
Assistant Professor

Date Approved :

June 27/96

PARTIAL COPYRIGHT LICENSE

I hereby grant to Simon Fraser University the right to lend my thesis, project or extended essay (the title of which is shown below) to users of the Simon Fraser University Library, and to make partial or single copies only for such users or in response to a request from the library of any other university, or other educational institution, on its own behalf or for one of its users. I further agree that permission for multiple copying of this work for scholarly purposes may be granted by me or the Dean of Graduate Studies. It is understood that copying or publication of this work for financial gain shall not be allowed without my written permission.

Title of Thesis/Project/Extended Essay:

N-cap mutants of chicken skeletal
troponin C: Structure/Affinity
relationships of paired calcium
binding sites

Author:

(signature)

Louise Leblanc

(name)

June 28/96
(date)

ABSTRACT

Chicken skeletal troponin-C is a calcium-binding protein with a pair of helix-loop-helix motifs in each of its two domains. In the high-affinity ion binding domain, each loop is capable of binding calcium or magnesium ions while the two binding loops of the low-affinity domain are calcium specific. This protein has several features which make it a good candidate for use in protein folding studies: its small size (162 amino acids), lack of naturally occurring tyrosine or tryptophan residues, ease of purification, stability when stored in the presence of calcium and the existence of established protocols to examine how structural changes influence the functional properties of this protein. In this thesis, various physical properties of TnC were studied in order to determine the relationship of the N-cap residue of the paired calcium-binding sites to ion affinity and protein stability. Site-directed mutagenesis was used to substitute a threonine residue with either a glycine, alanine, valine or serine residue at position 54, the N-cap of the C-helix located in the low-affinity domain. These substitutions were compared to N-cap mutants of the G-helix from a previous study. Calcium titration of the C-helix mutants was followed via fluorescence of a single tryptophan residue previously engineered into the sequence at position 29 (Phe₂₉ > Trp). The selected substitutions were found to decrease the calcium affinity of this domain. Flow dialysis experiments using radiolabelled calcium confirmed the presence of 4 functional binding sites in the valine mutants. Far UV Circular Dichroism was used to look at the secondary structure of the proteins. The greatest variation in the ellipticity values of the mutant proteins was observed for the fully-folded calcium-bound state. This change represented a change in the helical content of the protein which did not always predict the attenuated calcium affinity to TnC. Fluorescence emission spectra of the apoproteins and the calcium-bound proteins confirmed that the N-cap mutations

had not changed the overall structure of the protein. Differences in stability were uncovered when the apoproteins were denatured by urea. Stopped-flow analysis of the C-helix mutant proteins at 21°C measured the calcium off-rates for the low-affinity domain: a fast rate which ranged from 890sec⁻¹ to 1450sec⁻¹ depending on the mutation, and a second, much slower rate of 100sec⁻¹ for all of the proteins. Overall, these studies indicate that attenuation of the calcium affinity by substitution of the N-cap residue may be a general property of paired calcium-binding sites. Since protein stability is observed to be altered by these substitutions, a change in helix stability is likely playing a role in the ion affinity of the mutant protein. Other factors play a contributing role since the mutations introduced in structurally equivalent positions of the protein did not play equivalent roles in both domains of the protein. In the case of the valine substitution, the protein was more stable when located in the high-affinity domain as opposed to the low-affinity domain and yet calcium affinity was lower for the high-affinity domain.

To my Dad for his love and support - Two down and one to go.

Hey, maybe we can read this together sometime!

To my Mom who taught me how to give myself a swift kick whenever I thought all of this was more than I could handle

To Lowell who knew firsthand when I thought it was more than I could handle and yet stood by me anyway.

I also have two great sisters, Suzanne and Diane, who always took the time to cheer me on. You're the best!

I'd also like to thank my senior supervisor, Dr. Thor Borgford, for giving me the opportunity to work on this project.

Thanks to all in the lab: Dev, Grace, Jason, Jeff and Kathy - life was seldom dull.

And as they say, last but not least, thanks Gabe - You were always there when I needed a hand.

I would like to dedicate this to my children, Melissa and Adrienne who still love me as much as ever even though I've been just a little distracted in the doing and the writing of this "thing".

TABLE OF CONTENTS

	Page
Title.....	i
Approval.....	ii
Abstract.....	iii
Dedication.....	v
Acknowledgements.....	vi
Table of contents.....	vii
List of Figures.....	xiv
List of Tables.....	xvii
List of Abbreviations.....	xviii
 1. INTRODUCTION	
1.1 Organization of Muscle Fiber components.....	1
1.2 Structure of troponin-C	
1.2.1 The Functional Domains of Troponin C.....	4
1.2.2 The Calcium-binding Loops.....	7
1.2.3 The α -Helix and the N-cap Residue.....	11
1.2.4 The Calcium Induced Folding of Troponin C.....	14
1.2.5 Interactions of Troponin C Within the Thin Filament fo Muscle Fibers.....	15
1.3 Analyzing the Folded States of Troponin C.....	17
1.4 Methods of Study	
1.4.1. Far UV Circular Dichroism.....	18

1.4.2. Fluorescence Spectroscopy.....	19
1.4.3. Urea Denaturation.....	21
1.4.4. Flow Dialysis.....	25
1.4.5. Stopped Flow Measurement of the Off-rates for Calcium-binding.....	28

2. MATERIALS AND METHODS

2.1 Buffers and other solutions.....	29
2.2 Bacterial Strains.....	32
2.2.1 <i>Escherichia coli</i> strain QY13.....	32
2.2.2 <i>Escherichia coli</i> strain K12cI.....	32
2.2.3 <i>Escherichia coli</i> strain DH5a.....	33
2.3 Media.....	33
2.4 Preparation of Competent <i>Escherichia coli</i> cells.....	34
2.4.1 QY13 strain.....	34
2.4.2 K12cI strain.....	34
2.4.3 DH5 α strain.....	35
2.4.4 Preparation of Electrocompetent cells.....	35
2.5 Transformation of Competent <i>Escherichia coli</i> cells.....	35
2.5.1 Transformation of <i>Escherichia coli</i> strain QY13.....	35
2.5.2. Transformation of <i>Escherichia coli</i> strain K12cI.....	36
2.5.3 Transformation of <i>Escherichia coli</i> strain DH5 α	36
2.5.4 Electroporation of electrocompetent cells.....	36

2.6 Plasmids

2.6.1. pLcII-Fx-Tnc.....	37
2.6.2. pUC 18.....	37
2.6.3. Preparation of plasmid DNA.....	37
2.6.4. Purification of plasmid DNA for sequencing.....	38
2.6.5. Sequencing of plasmid DNA.....	39

2.7 Cloning procedures

2.7.1 Purification of DNA for cloning.....	39
2.7.2. Restriction digest of constructs.....	39
2.7.3. Ligation of pLcII fragments into pUC 18	40

2.8 Site-directed Mutagenesis

2.8.1 Primer extension

2.8.1.1 Primers selected for PCR mutagenesis.....	40
2.8.1.2 Preparation of mutant DNA using PCR....	42
2.8.1.3 Ligation of PCR products into pLcII-Fx-TnC.....	42

2.8.2 Triple ligation of PCR products into pLcII

vector

2.8.2.1 Selection of PCR primers.....	45
2.8.2.2 Preparation of DNA fragments.....	45
2.8.2.3 Triple ligation.....	46
2.8.2.4 Identification of mutant clones.....	46
2.8.2.5. PCR amplification of triple ligation mixture.....	48

2.8.2.6. PCR amplification of blunt end ligation.....	48
2.8.3. Triple ligation of PCR products into pUC18.....	49
2.8.3.1. Identification of mutant clones from pUC18.....	49
2.9 Expression vector constructs.....	50
2.9.1 Preparation of pLcII-Fx-TnC (F29W) expression vector.....	50
2.9.2 Verification of fragment insertion into the expression vector.....	51
2.10 Protein expression from pLcII-Fx-TnC mutants	
2.10.1 Test for expression.....	52
2.10.2 Preparation of large scale cultures.....	52
2.11 Purification of the recombinant proteins	
2.11.1 Release of fusion-TnC by cell lysis.....	53
2.11.2 Purification by ion exchange chromatography.....	53
2.11.3 De-salting by gel filtration.....	54
2.12 Preparation of Factor X _a	
2.12.1 Isolation and purification of Factor X.....	54
2.12.2 Preparation of CNBr-Sepharose 4B column.....	55
2.12.3 Activation of Factor X	56
2.12.4 Assay of Factor X _a activity.....	56

2.13 Preparation of recombinant proteins for spectroscopic analysis	
2.13.1 Factor X _a digestion of fusion TnC.....	56
2.13.2 Purification of digested proteins by FPLC.....	57
2.13.3 Dialysis of proteins.....	57
2.13.4 Quantitation of proteins.....	57
2.14 Metal binding properties of mutant proteins	
2.14.1 Spectroscopic analysis of purified proteins	
2.14.1.1 Fluorescence spectroscopy.....	57
2.14.1.2 Circular dichroism spectroscopy.....	58
2.14.1.3 Flow dialysis.....	58
2.14.1.4 Stop flow fluorescence spectroscopy.....	61
2.15 Unfolding of proteins using urea as the denaturant	
2.15.1 Steady state fluorescence spectroscopy.....	62
2.15.1.1 Preparation of urea stock solutions.....	62
2.15.1.2 Procedure for denaturation of proteins.....	63
2.15.2 Circular dichroism spectroscopy.....	63
2.16 Preparation of Antibodies and Immunoblotting of troponin C	
2.16.1 Immunization of Rabbits.....	63
2.16.2 Isolation of rabbit anti-cII-TnC	
immunoglobulin G.....	64
2.16.3 SDS PAGE identification of IgG fraction.....	64
2.16.4 Enzyme linked immunosorbant assay of FPLC	
fractions.....	64

2.16.5 Immunoblotting of proteins.....	65
--	----

3. RESULTS

3.1 Cloning of the Troponin C gene into pUC18.....	67
3.2 PCR mutagenesis	
3.2.1 Primer extension.....	67
3.2.2 Triple ligations.....	74
3.2.3 Analysis of clones from the PCR amplification of triple ligations.....	76
3.2.4 Analysis of clones from the PCR amplification of blunt end ligations.....	76
3.2.5 Analysis of clones from blunt end ligation of PCR fragments into pUC18.....	76
3.3 Preparation of pLcII-Fx-TnC (F29W) expression vector.....	77
3.4 Expression and purification of the fusion mutant proteins.....	77
3.5 Preparation of Factor X_a	79
3.5.1 Isolation and purification of Factor X_a	79
3.5.2 Activation of Factor X_a	80
3.6 Preparation and purification of the Troponin C mutant proteins.....	80
3.7 Metal binding properties of the mutant proteins	
3.7.1 Far UV Circular Dichroism	90
3.7.2 Fluorescence.....	90
3.7.3 Flow dialysis.....	104
3.7.4. Stopped flow analysis of binding sites.....	106
3.8. Stability of the calcium free mutant proteins measured by urea denaturation	

3.8.1 Unfolding of the calcium free mutant proteins followed by Far UV Circular Dichroism.....	111
3.8.2. Unfolding of calcium free mutant proteins followed by steady state fluorescence emission spectroscopy.....	117
3.9. Analysis of polyclonal antibody raised against cII-fusion-chicken skeletal Troponin C	
3.9.1 Western Blot analysis of polyclonal antibody.....	125
3.9.2. Enzyme Linked Immunosorbant Assay of polyclonal antibody.....	125
4. DISCUSSION.....	128
5. CONCLUSION.....	149
6. REFERENCES.....	150

LIST OF FIGURES

	Page
Figure 1.1. Organization of Skeletal Muscle.....	2
Figure 1.2. Model for the Arrangement of the Thin Filament of Myofibrils.....	3
Figure 1.3. Partial Plasmid Map of the pLcII-Fx-TnC Vector.....	5
Figure 1.4. Amino Acid Sequence of Fusion Troponin C.....	6
Figure 1.5. Ribbon Diagram of Troponin C	8
Figure 1.6. Ribbon Diagram Showing the Formation of the Helix-Loop-Helix Motif in the presence of calcium.....	10
Figure 2.1. Primer Extension PCR Mutagenesis.....	43
Figure 2.2. DNA Sequence of cII-Fx-Troponin C.....	44
Figure 2.3. Triple Ligation Protocol.....	47
Figure 2.4. Flow Dialysis Apparatus.....	59
Figure 3.1. Cloning the Gene for Troponin C From the pLcII Vector into into the pUC18 Vector.....	68
Figure 3.2. Ligation of Fusion TnC gene into pUC18.....	69
Figure 3.3. Agarose Gel Electrophoresis of the Primer Extension PCR Mutagenesis Products.....	71
Figure 3.4. Agarose Gel Electrophoresis of the Restriction Digests of PCR Products.....	72
Figure 3.5. Identification of Potential Mutant Clones Using Restriction Digests followed by Agarose Gel Electrophoresis.....	73
Figure 3.6. SDS-PAGE of the Protein Expression Test.....	75
Figure 3.7. Analysis of Blunt End Ligation of PCR Fragments into pUC18.....	78
Figure 3.8. Anion Exchange Chromatography of Cell Lysate.....	81
Figure 3.9. SDS Polyacrylamide Gel Electrophoresis of Fusion TnC.....	82

Figure 3.10. Gel Filtration Chromatography of Fusion Protein.....	83
Figure 3.11. Anion Exchange Chromatography of Bovine Blood Extract.....	84
Figure 3.12. SDS PAGE of Factor X Eluted from DEAE Sepharose CL-6B column.....	85
Figure 3.13. Gel Filtration Chromatography of Factor X.....	86
Figure 3.14. SDS PAGE of Troponin C digested with Factor X _a	87
Figure 3.15. FPLC Chromatography of TnC Digested with Factor X _a	88
Figure 3.16. SDS PAGE of Mutant TnC from the FPLC Mono-Q Column.....	89
Figure 3.17. Far UV CD Spectra of Mutant Proteins in the Absence of Calcium.....	93
Figure 3.18. Far UV CD Spectra of Mutant Proteins at Saturating Calcium Concentrations.....	94
Figure 3.19. Far UV Circular Dichroism Spectroscopy of F29W/54X Proteins.....	95
Figure 3.20. Far UV Circular Dichroism Spectroscopy of F105W/54X Proteins.....	96
Figure 3.21. Calcium Titration of Tryptophan Fluorescence of F29W/54X Mutant Proteins.....	98
Figure 3.22. Calcium Titration of the Tryptophan Fluorescence of the Valine Mutant Proteins.....	99
Figure 3.23. Fluorescence Emission Spectra of F29W/54X Mutant Proteins.....	100
Figure 3.24. Fluorescence Emission Spectra of F105W/130X Mutant Proteins.....	101
Figure 3.25. Fluorescence Emission Spectra of F105W/130T and F105W/130V Mutant Proteins.....	102
Figure 3.26. Measurement of Calcium-binding to Mutant Proteins.....	105

Figure 3.27. Non-Linear Regression Analysis of the Stopped-Flow Data for the F29W/54T Protein.....	108
Figure 3.28. Urea Denaturation of the Calcium Free, F29W/54X Mutant Proteins Followed by Far UV CD Spectroscopy.....	113
Figure 3.29. Free Energy Change of Unfolding of the Calcium Free, F29W/54X Mutant Proteins Measured by CD Spectroscopy.....	114
Figure 3.30. Urea Denaturation of the Calcium Free F105W/130X Mutant Proteins Followed by Far UV CD Spectroscopy.....	115
Figure 3.31. Free Energy Change of Unfolding of the Calcium Free, F105W/130X Mutant Proteins Measured by CD Spectroscopy.....	116
Figure 3.32. Urea Denaturation of the Calcium Free F29W/54X Mutant Proteins Followed by Steady State Fluorescence Emission Spectroscopy.....	118
Figure 3.33. Free Energy Change of Unfolding of the Calcium Free, F29W/54X Mutant Proteins Measured by Steady State Fluorescence Emission Spectroscopy.....	119
Figure 3.34. Urea Denaturation of the Calcium Free, F105W/130X Mutant Proteins Followed by Steady State Fluorescence Emission Spectroscopy.....	120
Figure 3.35. Western Blot of Polyclonal Antibody Binding to TnC.....	126
Figure 3.35. Western Blot Analysis of Rabbit Skeletal TnC and cII-Fusion Skeletal TnC.....	127
Figure 4.1. Hydrogen Bonding Pattern of the α -Helix.....	129

LIST OF TABLES

	Page
Table 2.1. Mutagenic Possibilities from the Two Oligonucleotides.....	41
Table 3.1. Circular Dichroism Spectroscopy Values at 222nm as a Measure of the Helical Content for the Three Folded States of Each Mutant Protein.....	97
Table 3.2. Binding Parameters Determined by Calcium Titration of the F29W/54X and the F105W/130V Mutant Proteins.....	103
Table 3.3. The Rates of Release of Calcium Ions from Calcium-Loaded Troponin C Studied by Stopped Flow Fluorescence Spectroscopy....	109
Table 3.4. The Rates of Release of Calcium Ions from the Calcium-Loaded F29W/54V Mutant Protein Studied at varying Protein, Calcium and EGTA Concentrations.....	110
Table 3.5. Summary of Data from the Free Energy of Unfolding with Urea by Non-Linear Regression Analysis.....	121
Table 3.6. Free Energy of Unfolding of Troponin C Using the Linear Extrapolation Method.....	122
Table 3.7. Summary of the Change in Stability with N-cap Mutation in Going From a Threonine Residue to Mutant X for Each Domain.....	123
Table 3.8. Summary of the Change in Stability with N-cap Mutation in Going from a Threonine Residue to Mutant X for Each Domain.....	124

ABBREVIATIONS

Ala (A)	Alanine
Arg (R)	Arginine
Asp (D)	Aspartic acid
Asn (N)	Asparagine
bp	base pairs
Ca	Calcium
CD	Circular dichroism
Cys (C)	Cysteine
dATP	2'-deoxyadenosine 5'-triphosphate
ddH ₂ O	Deionized, distilled water
DNA	Deoxyribonucleic acid
DTT	DL-dithiothreitol
EDTA	Ethylene diamine tetraacetic acid
EGTA	Ethylene glycol-bis-N,N,N',N'-
Tetraacetic	acid
ELISA	Enzyme linked immunosorbent assay
EtBr	Ethidium Bromide
FPLC	Fast protein liquid chromatography
Gln (Q)	Glutamine
Glu (E)	Glutamic acid
Gly (G)	Glycine
His (H)	Histidine
LEM	Linear extrapolation method
Ile (I)	Isoleucine
Leu (L)	Leucine
Lys (K)	Lysine

Met (M)	Methionine
MOPS	3-(N-morpholino) propanesulfonic
acid	
PAGE	Polyacrylamide gel electrophoresis
PBS	Phosphate-buffered saline
Phe (F)	Phenylalanine
PMSF	Phenylmethyl sulfonyl fluoride
Pro (P)	Proline
SDS	Sodium dodecyl sulfate
Ser (S)	Serine
TBS	Tris-buffered saline
TEMED	N,N,N',N'-tetramethylenediamine
Thr (T)	Threonine
Tris	Tris (hydroxymethyl) methylamine
TnC	Troponin C
Trp (W)	Tryptophan
TWEEN 20	Polyoxyethylene Sorbitan Monolaurate
Tyr (Y)	Tyrosine
UV	Ultra violet
Val (V)	Valine

1. INTRODUCTION

1.1 Organization of the Muscle Fiber Proteins

Whole muscle is arranged in fiber bundles which are subdivided into skeletal muscle cells, known as muscle fibers (Figure 1.1). Muscle cells are further subdivided into myofibrils which consists of a repeated unit known as a sarcomere. Every sarcomere is composed of two types of filaments. The large molecules of the ATPase enzyme myosin are the major protein component of the thick filaments while actin is the major constituent of the thin filaments. Myosin molecules are arranged such that the "tail" forms the core of the filament and the "head" of the protein projects outward. Cross-bridges are formed between the two filaments at regular intervals to bridge a 130\AA gap between them. When a muscle contracts the myosin "head" is observed to bind with the actin units in the thin filaments.

The thin filament also contains the proteins tropomyosin and troponin. Figure 1.2 (adapted from Stryer's Biochemistry) illustrates the arrangement the proteins of the thin filament. Tropomyosin is a double stranded helical protein which winds around an actin fiber preventing the attachment of myosin to actin. The troponin complex consists of three proteins: troponin-C (TnC) which binds calcium, troponin-I (TnI) which binds to actin and troponin-T (TnT) which binds tropomyosin. When calcium is released from the sarcoplasmic reticulum following a nerve impulse, the regulatory sites of troponin-C are proposed to bind calcium, inducing a conformational change in the protein which enables it to bind TnI. The interaction between troponin-I and actin is broken allowing tropomyosin to move from its blocking position on actin. Myosin is now able to bind to actin, ATP is hydrolyzed and the muscle contracts.

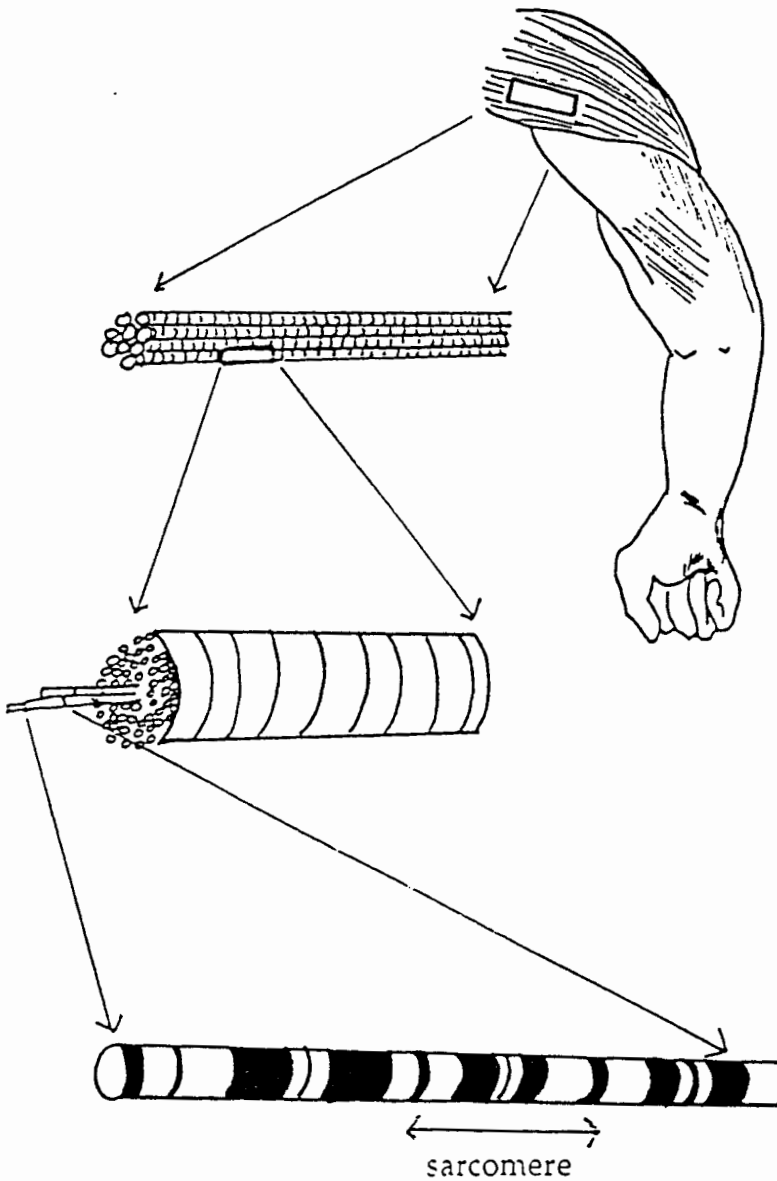


Figure 1.1. Organization of Skeletal Muscle.

Whole muscle is subdivided into bundles called fasciculi. These are further subdivided into single muscle cells called muscle fibers. Each muscle cell consists of myofibrils which are composed of repeating structures known as sarcomeres. (Figure adapted from *Physiology*, Edited by Ewald E. Selkurt, Little, Brown and Company, Boston, 1976).

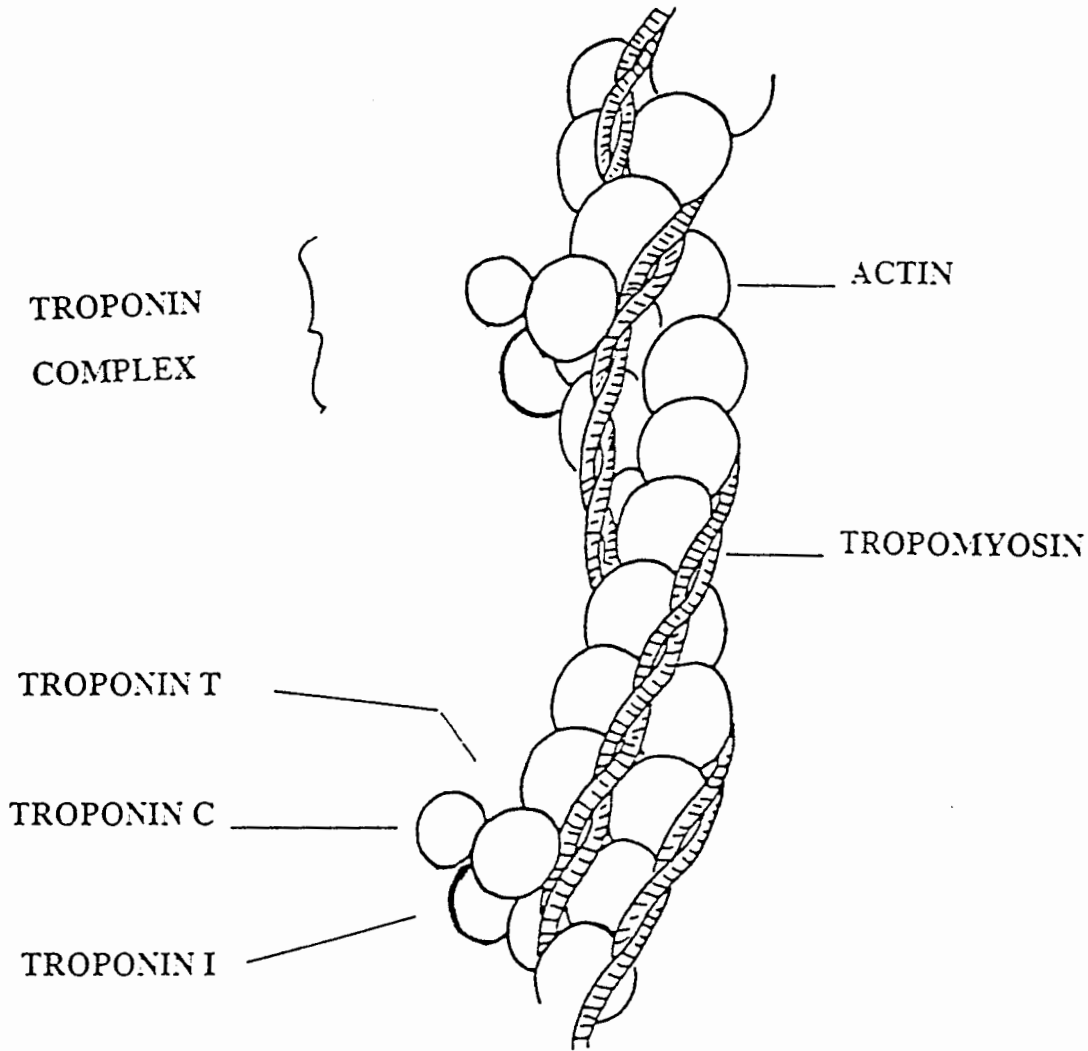


Figure 1.2. Model for the Arrangement of the Thin Filament of Myofibrils.

The myofilaments which make up the sarcomere are subdivided into thick and thin filaments. This cartoon depicts the proteins of the thin filament at rest with troponin T bound to tropomyosin which is blocking the myosin binding sites on actin. (Figure adapted from **Biochemistry**, Stryer, 2nd edition.)

1.2. The structure of Troponin C

1.2.1. The Functional Domains of Troponin C

This research project was centered on the structure and function of skeletal TnC. Structurally, skeletal TnC is divided into 2 functional domains: a high-affinity calcium-binding domain (C-terminal domain) which is involved in the binding of the protein to the thin filament (Robertson et al, 1981) and a low-affinity calcium-binding domain (N-terminal domain) which is believed to regulate muscle contraction. The protein is 66% α -helical with each domain consisting of two helix-loop-helix motifs with a long helix (D/E) linker connecting the two domains. Under physiological conditions the high-affinity binding sites (loops III and IV) are believed to be occupied by either calcium or magnesium ions at all times (Robertson et al, 1981). It is not known whether the binding of magnesium is important in the function of TnC. The binding affinity for these sites is $2 \times 10^7 \text{M}^{-1}$ for calcium and $2 \times 10^3 \text{M}^{-1}$ for magnesium (Gagne et al, 1994). The low-affinity binding sites (loops I and II) are calcium specific with a K_{Ca} of $3 \times 10^5 \text{M}^{-1}$. The gene for chicken skeletal TnC used in this study was available in a vector known as the pLcII-FX vector (Figure 1.3) All mutant proteins were expressed as a fusion with the cII protein of lambda phage (Nagai and Thogersen, 1987). Figure 1.4 is the amino acid sequence of chicken skeletal TnC with the helices and loops labelled. It includes the sequence of the fusion portion of the protein and identifies the Factor X_a recognition sequence at the junction of the cII peptide and TnC. Factor X_a , a serine protease also known as the Stuart Factor in the blood clotting cascade, cleaves the peptide bond immediately following an Arg residue in the recognition sequence, to remove the cII peptide before the final purification step in the preparation of TnC.

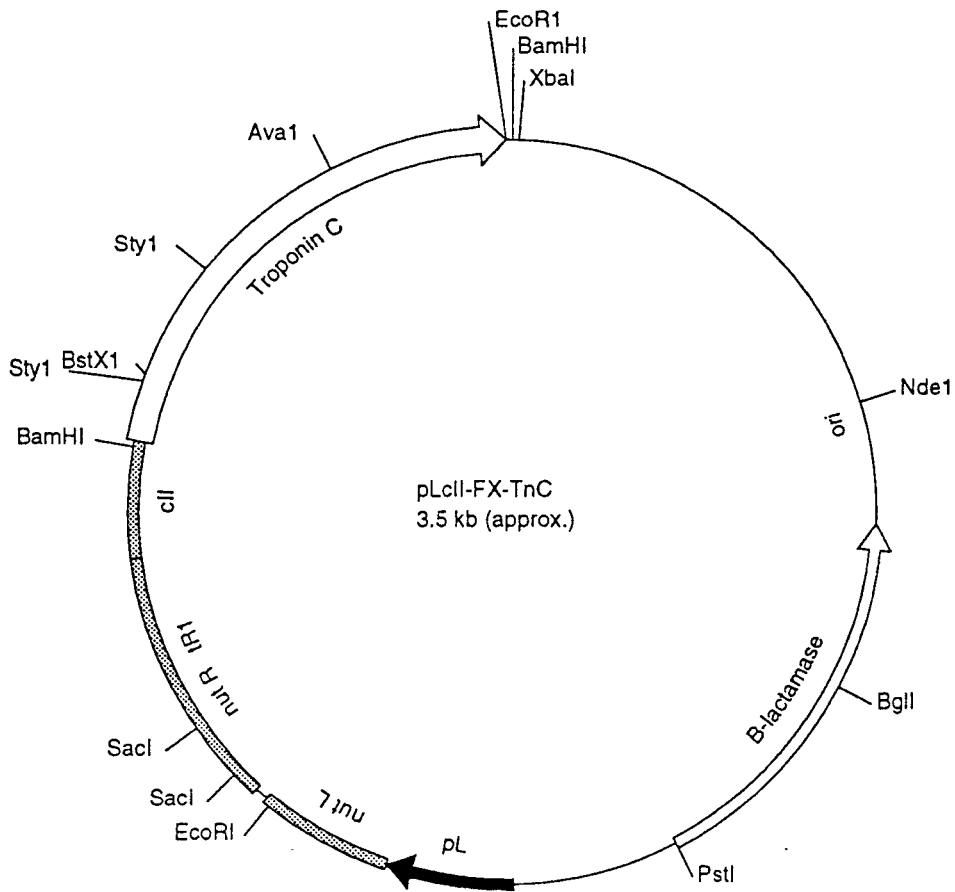


Figure 1.3. Partial Plasmid Map of the pLcII-Fx-TnC Vector.

Troponin C is produced as a fusion protein. Expression is driven by the leftward promoter (PL) from bacteriophage λ . The labelled restriction sites within the gene for TnC were used for cloning mutant fragments into the gene.

—cII

—FX_a—

M V T A N K R N E A L R I E S A L L N K I A M L G T E K T A E G G S I E G R

1 N-Helix 15

M A S M T D Q Q A E A R A F L S

16 A-Helix 29

Loop I

B-Helix

Linker 54

E E M I A E F K A A F D M F D A D G G G D I S T K E L G T V M R M L G Q N P T *

55 C-Helix 65

Loop II

D-Helix

90

K E E L D A I I E E V D E D G S G T I D F E E F L V M M V T Q M K E D A

91 E-Helix 105

Loop III

F-Helix

130

K G K S E E E L A N C F R I F D K N A D G F I D I E E L G E I L R A T G E H V T *

131 G-Helix 141

Loop IV

H-Helix

162

E E D I E D L M K D S D K N N D G R I D F D E F L K M E G V Q

FIGURE 1.4. Amino Acid Sequence of Fusion Troponin-C

This figure is a representation of the organization of the wild type sequence for chicken skeletal troponin-C and includes the cII fusion portion of the protein with the Factor X_a recognition site labelled. This is the form of the protein which is obtained from the expression of the pLcIIRX-TnC vector in the QY13 strain of *Escherichia coli*. The two N-cap residues which were studied are labelled with an asterisk. The high affinity domain includes loops III and IV while loops I and II are part of the low affinity domain of troponin-C. The two domains are joined by the D/E linker helix.

In 1988, a crystal structure was elucidated for chicken skeletal TnC with 2 calcium ions bound in the high-affinity domain. Figure 1.5 is a ribbon diagram of TnC based on the crystal structure of the protein with two calcium ions bound. A crystal of TnC with calcium-bound to all four sites has not been isolated to date. Therefore, the conformational change in TnC on binding calcium to the low-affinity domain is not yet fully understood. NMR studies have recently shown that there is a straightening of the B-helix with a shift of both the B- and C-helix away from the N-, A- and D-helices of the regulatory domain (Sykes, 1995).

1.2.2. The Calcium Binding Loops

In structure/function studies, site-directed mutagenesis allows us to alter the 1^o structure of a protein and measure its effect on the 2^o and 3^o structure and ultimately establish the relevance of that residue in the function of the protein. It is important however to select a mutation site which does not significantly change the structure of the final folded conformation of the protein as this would not accurately reflect the role of the single residue. To quantitate the change in stability as a result of mutation it is important that the folding pathway is unchanged. Otherwise the $\Delta\Delta G$ calculations would compare two unrelated events and be meaningless.

A search for consensus sequences between proteins of like function can identify highly conserved residues as a starting point in selecting mutation sites. When a crystal structure is available, residues are selected based on their interactions within the protein. The goal is to decipher the role each structural unit plays in the functioning of the protein such as those involved in catalysis, or in the case of TnC, those residues which affect the binding of the ligand. The calcium-binding loop itself has been mutated extensively to correlate the

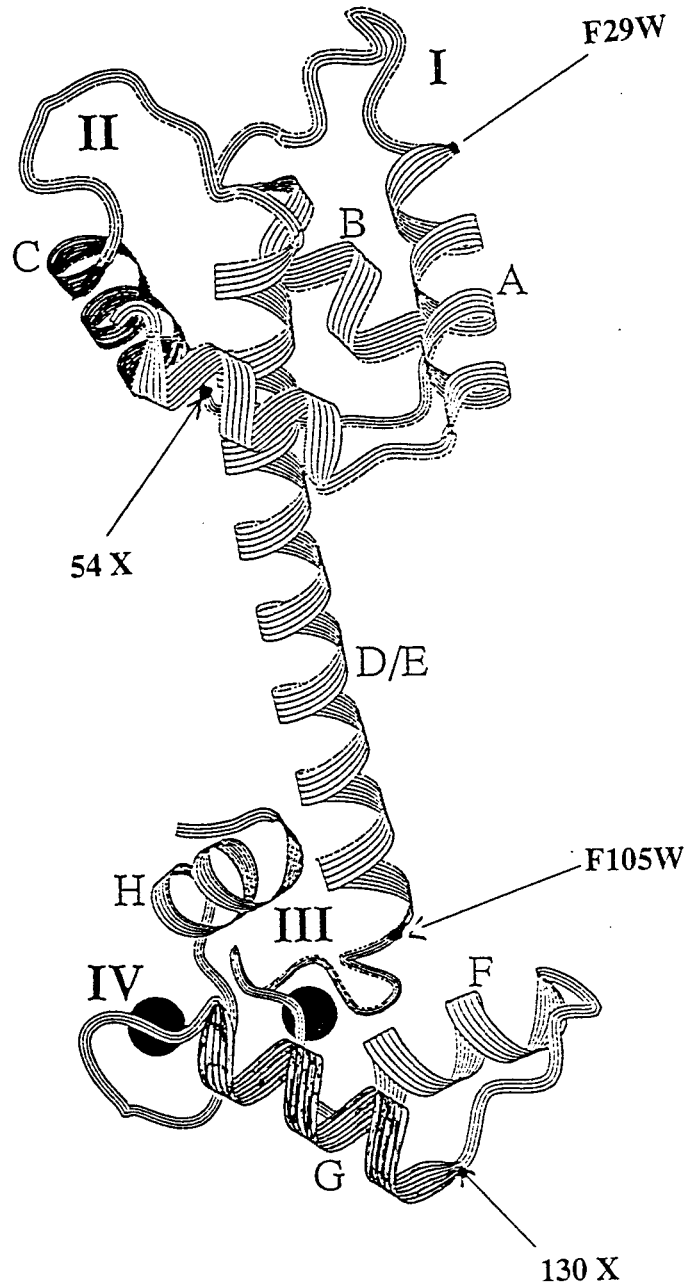


Figure 1.5. Ribbon Diagram of Troponin C.

The diagram is based on the crystal structure of the protein with two calcium ions bound. The positions of the tryptophan probes are indicated. These probes were used individually to monitor events in each domain separately. The sites for mutation in each domain are also identified.

relationship between the affinity for calcium to the sequence of residues within the loops (Shaw et al, 1991, Krudy et al, 1992, Procyshyn et al, 1994). Mutagenesis of the nine residues which comprise the calcium-binding loops of various calcium-binding proteins have been studied. These residues account for a wide range of calcium affinities. The highest affinity sequence for a calcium-binding loop is reported as Asp, Asn and Asp in positions 1,3 and 5 respectively which is found in all known sequences for high-affinity sites III and IV of TnC but not for the low-affinity sites (Shaw et al, 1991). Interestingly, the calcium affinity of the loops was not only attenuated by the residues coordinated to the calcium ion but also by the non-coordinating residues of the loop. An example of decreased affinity occurred when the lysine residue at position 2 of binding loop III was replaced by a glutamic acid residue as is found in loop II. The higher affinity of loop III may be the result of a stabilizing interaction between the positively charged residue and the partial negative charge of the helix dipole, (Creighton, 1987) at the C-terminal end of the helix. This stabilizing interaction could not occur in loop II. Another example of modified calcium-binding occurred with the replacement of the aspartic acid residue at position 5 of loop III with a serine residue as is found at position 5 of loop II. With the serine residue there appears to be a loss of some preformed structure in the loop III, needed for high calcium-binding-affinity (Procyshyn et al, 1992). In other studies relating to the binding loops, the use of synthetic peptides demonstrated that the calcium-affinity of binding loop III was related to the formation of the N-terminal end of the helix for that helix-loop-helix structure (Reid, 1981). Using ^1H NMR, the apo-peptide was observed to have little regular structure but in the presence of calcium ions the peptide organized itself into a helix-loop-helix structure (Figure 1.6). Calcium-affinity was found to increase as the length of the peptide being used was increased suggesting that the induction of the E-helix of TnC, by

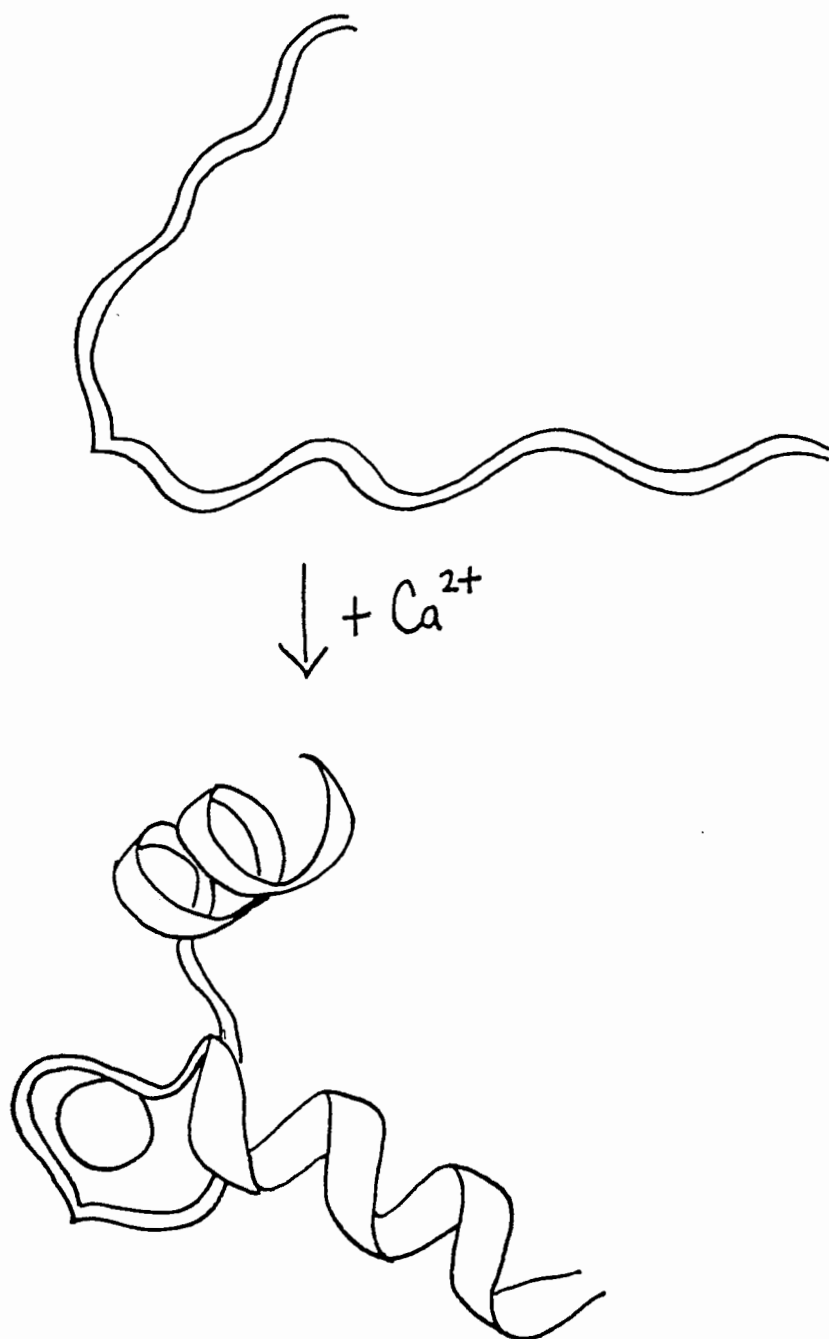


Figure 1.6. Ribbon Diagram Showing the Formation of the Helix-Loop-Helix Motif in the Presence of Calcium.

In the absence of calcium the peptide has no defined 2^o structure . In the presence of calcium the peptide is organized into a helix-loop-helix structure.

calcium-binding, was a requirement of tight calcium-binding. A recent study using chicken skeletal TnC (Trigo-Gonzalez et al, 1993) demonstrated that the calcium ion affinity of the fourth calcium-binding loop could be tailored by varying the amino acid at position 130, N-cap residue of the G-helix. This is the N-terminal helix for binding loop IV.

1.2.3. The α -Helix and the N-cap Residue

In an α -helix, hydrogen bonding occurs between an NH donor and a CO acceptor located 4 residues away. Residues participating in an α -helix have backbone dihedral angles of -57° (ϕ) and -47° (ψ). The 4 residues at either end of the helix are unable to participate in both intrahelical interactions. In 1988, it was hypothesized that helix formation required the presence of residues flanking the helix termini whose side chains could form hydrogen bonds with the initial 4 helix NH groups and the final 4 helix CO groups (Presta and Rose, 1988). The helices and their flanking residues were labelled in the following manner:



where N1, N2, N3,C3, C2, and C1 have the characteristic helix backbone dihedral angles while N and C are residues which participate in the hydrogen bonding network of the helix but do not have helical dihedral angles. The primed residues do not participate in hydrogen bonding to the helix backbone. The residue labelled as N is termed the N-cap of the helix. The N-cap residue forms a hydrogen bond with the backbone NH of N3 and the side chain of N3 forms a hydrogen bond with the backbone NH of the N-cap residue whenever possible. In the sequence for TnC shown in Figure 1.4, the N-cap residue for the C-helix is a threonine residue at position 54 while N3 is a glutamic acid residue.

The N-cap of the G-helix located at position 130 is a threonine residue in the wild-type sequence with an aspartic acid residue at N3. Since the first four residues in the helix cannot be stabilized by backbone interactions, side chain interactions with this N-cap residue provide this hydrogen bond stabilization. In this way two of the initial four backbone NH donors of the helix are enclosed in a "capping box" (Harper and Rose, 1988). Statistical evaluations of the best N-cap residues have been compiled (Richardson and Richardson, 1988, Presta and Rose, 1988, Harper and Rose et al, 1993) by comparing a number of protein sequences. The most frequent N-cap/N3 pair was found to be Ser/Glu. The most common residues at the N-cap are reported to be Ser > Asn > Gly > Asp > Thr. Several research groups have designed helical peptides with different N-cap residues and measured their propensity to form a stable helix (Lyu et al, 1992, Zhou et al, 1993, Forood et al, 1993, Chakrabartty et al, 1993a, Chakrabartty et al, 1993b, Zhou et al, 1994). Zhou confirmed the reciprocal hydrogen bonding pattern using NMR NOESY spectra. Lyu and Zhou agreed that the stability of peptides studied increased from Ser > Asn > Gly > Ala with an increase in the mean residue ellipticity. They concluded that the N-cap interaction affects σ , the nucleation constant, exerting a strong influence on the nucleation of the helix and folding of the N-terminus rather than "s", the helix propagation constant. The work of Forood's group showed a change in the ordering of the N-cap residues from most to least stable, as follows: Asp > Asn > Ser > Glu > Gln > Ala. Chakrabartty (1993) examined the effect of several hydrophobic residues and found that the burial of hydrophobic surfaces may contribute to stability since the overall arrangement of residues, in decreasing order of stability, was Asn > (Ser, Gly) > (Thr, Leu, Ile) > (Pro, Met) > Val > Ala > Gln. Many others have used site-directed mutagenesis to vary the residue at the N-cap position of a helix within their protein of choice (Serrano et al, 1989, Bell et al, 1992, Chakrabartty et

al, 1993, Harpaz et al, 1993). The N-cap residue was found to stabilize a protein by up to 2.5 kcal/mol with a negative charge on the N-cap adding up to 1.6 kcal/mol of additional stabilizing energy. However, the choice of residue reflects the overall 3^o structure as evidenced by the variability in the instability an alanine residue incurs as the N-cap of different helices within the same protein (Bell, 1992).

With this in mind, the substitutions at the N-cap position of the C-helix were selected to overlap those previously made for the N-cap of the G-helix. Site-directed mutagenesis was successfully used to substitute threonine (Thr or T) with alanine (Ala or A), glycine (Gly or G), serine (Ser or S) and valine (Val or V). The isolation of the aspartic acid (Asp or D), isoleucine (Ile or I) and asparagine (Asn or N) were unsuccessful as will be explained later. The purpose of these substitutions was twofold. Firstly, would the same amino acid substitution at the N-cap of two topologically equivalent helices result in the same change in stability of the protein? Secondly, would the substitutions, made at the N-cap position of 2 separate helices in the two domains of TnC, have the same effect on the ion-binding-affinity of each pair of calcium binding sites. Since a tryptophan reporter group was available for use in each domain, the mutant proteins of the low-affinity domain are identified as F29W/54X, where X= A, G, T, S, or V while the mutant proteins of the high-affinity domain are identified as F105W/130X, where X= D, G, I, N, S, T, or V. The valine residue at position 130 was available but not previously studied. It was added to the list for study when a valine was isolated at the N-cap position of the C-helix (position 54). If the same residues at both N-cap positions within chicken skeletal TnC attenuate the calcium-binding affinity to the same extent, that is, if this is a general feature of paired calcium-binding sites, then other calcium-binding

proteins could be modified in a similar way to optimize their calcium-binding properties.

1.2.4. The Calcium Induced Folding of Troponin C

Over 10 years ago, Tsalkova and Privalov studied whole TnC and its proteolytic fragments to decipher the organization of the two domains and the effect of calcium-binding (Tsalkova et al, 1985). Their study was centered around the idea of a cooperative folding process communicated between the two domains of TnC and the effect of metal ion binding on this cooperativity. Thermodynamic studies showed a lack of stable secondary structure associated with loop III of the C-terminal domain in the absence of calcium or magnesium. The N-terminal domain however, had a more stable structure as determined by microcalorimetry. These studies indicated a multistage unfolding of whole TnC with the N-terminal fragments undergoing a single unfolding transition. The C-terminal domain showed two transitions in the presence of metal ions. Binding loop III was identified as unfolding before loop IV but differences in the unfolding transition temperatures of the two loops decreased as the calcium ion concentration was increased. At calcium concentrations above 10^{-4}M , simultaneous melting of both loops III and IV was observed indicating a cooperative interaction between loops. The unfolding transition for the N-terminal fragment (loops I and II) was unaffected by the addition of magnesium. It is interesting to note that while the stability of loops I and II increased in the intact protein over that observed for the proteolytic fragment, a decrease in the stability of loops III and IV was observed (melted at a lower temperature) in the whole protein indicating a negative interaction between the N- and C-terminal domains of TnC. The removal of metal ions from a solution of low ionic strength resulted in the complete unfolding of loops III and IV at room temperature so

that titration with calcium produced a large change in the folding of the C-terminal domain. The compact structure of domain IV was observed simply by increasing the ionic strength of the buffer while loop III was only observed in the presence of calcium or magnesium. And so it was first speculated that binding loop III might play a role in the regulation of muscle contraction.

In vivo, TnC does not exist without sites III and IV having a metal ion bound. It binds either calcium or magnesium immediately upon synthesis (Zot & Potter, 1982). However, the calcium dissociation rates for loops III and IV are too slow for the 50ms time scale on which muscle contraction occurs. The ability to bind and release calcium ions rapidly in the physiological concentration range of 0.1 to 10 mM is observed at the N-terminal sites. Loops I and II are therefore more likely to be involved in the regulation of muscle contraction and relaxation (Sorenson et al, 1995).

1.2.5. Interactions of Troponin C Within the Thin Filament of Muscle Fibers

Recently, mutants were created to selectively inactivate each binding loop of chicken skeletal muscle TnC by substituting the aspartic acid residue at the first calcium coordinating position with an alanine residue (Sorenson et al, 1995). The mutants of sites I and II bound to the troponin complex but could not regulate muscle tension or acto-myosin ATPase activity. Mutants of the C-terminal domain (sites III and IV) regulated activity but were unable to remain bound to the thin filament in the absence of calcium. Unlike the wild-type protein, the mutants were also unable to remain bound to the thin filament in the presence of magnesium ions. A recent study (Szczesna et al, 1996) demonstrated that mutants containing either an inactive loop I or II could be displaced from a muscle fiber by the wild-type protein. This suggested an interaction between the two domains of TnC and that inactivation of the N-terminal domain affected the

structure and function of the C-terminal domain by lowering the calcium affinity of sites III and IV. The authors found that the ability of TnC to bind to the fibers depended on which loop was inactivated. If loop III was active this was sufficient for binding of TnC to the thin filament even in absence of calcium (ie. in the presence of magnesium ions).

All of the foregoing studies focused on the interaction of TnC with the thin filament and the regulation of muscle tension development after inactivation of one or more calcium-binding loops. We do know that the calcium affinity of binding loop IV can be modified (Trigo-Gonzalez, 1992). However, in the presence of calcium and under physiological conditions, even a four-fold decrease in calcium affinity has no observable effect on the force/tension development produced in muscle fibers stripped of native TnC and reconstituted with mutant protein (Dr. B. Bressler, Pers. Com). Initial studies with a valine N-cap mutant suggested a decrease in the co-operativity of binding in the low-affinity domain (ie. regulatory domain) of TnC. If the cooperative nature of muscle contraction is initiated at the level of calcium-binding to TnC, the change may be translated down the length of a muscle fiber. If so, variation in calcium affinity of this loop may translate into an observable difference in the process of muscle contraction and shed some light on the mechanism of regulation by the N-terminal domain. Cardiac TnC (cTnC), an isoform of skeletal TnC, does not have a functional calcium-binding loop I and yet the protein is still fully functional. Since loop II is the only functional loop in cTnC, it is possible that this loop is critical in the regulation of muscle contraction. The idea of loop II controlling the regulatory domain was explored as a possible mechanism in the regulation of contraction of skeletal muscle. For this reason it was decided to make substitutions which would affect the formation of the C-helix and the binding of calcium at loop II. The C-helix of TnC is also predicted to play an

important role in muscle contraction since this highly negatively charged helix interacts with the basic inhibitory component of TnI in response to increased cellular calcium levels (Wang et al, 1990, Grabarek et al, 1981, Kobayashi et al, 1991). Helices A, B and D form a hydrophobic core to which helix C does not associate closely. The helix face closest to this core which consists of a few hydrophobic residues (Leu 58, Ile 61, Ile 62, and Val 65) has been proposed to remain mobile to form important contacts with other regulatory proteins (Findlay et al, 1994). Mutation at the N-cap position may affect the formation and stability of the C-helix and not only attenuate the calcium-binding affinity of loop II, but may also interfere with the interaction of TnC with the other proteins of the troponin complex.

1.3. Analyzing the Folded States of Troponin C

To study the effects of the N-cap mutations on the structure and affinity of the calcium-binding loops, the folding pathway of skeletal TnC was viewed as a stepwise process as shown below:



where "U" is the unfolded state, F-Ca is the folded form of the protein without calcium and F+Ca is the fully-folded form with each of the four binding sites occupied by a calcium ion. By dividing the process into these three steps, it is possible to measure whether a mutation has destabilized the unfolded state or stabilized one or both of the folded states.

The tryptophan probe was excited at 278nm and the fluorescence emission monitored at 335nm. The fluorescence intensity of the probe in the low-affinity domain increased in the presence of calcium but decreased as the protein

unfolded. In the high-affinity domain, the tryptophan at position 130 responded differently to a change in its environment; the fluorescence intensity decreased in both experiments. To simplify the calculations, the equilibrium between the "U" and "F-Ca" state was studied by urea denaturation and the equilibrium between the calcium free and calcium saturated folded state was studied by titrating the apoprotein with calcium. The unfolding of the apoprotein by urea was monitored using steady state fluorescence emission spectroscopy and Far UV Circular Dichroism (CD) spectroscopy. The calcium titration of each mutant protein was monitored by fluorescence spectroscopy. Analysis of the denaturation data provided the equilibrium constant for the "U" to F-Ca step from which the ΔG value was calculated. The calcium titration data was used to calculate the free energy change from the F-Ca folded state to the F+Ca folded state.

1.4 Methods of Study

1.4.1. Far UV Circular Dichroism

Circular dichroism is an absorption phenomenon whereby the left- and right-circularly polarized components of circularly polarized light are absorbed to different extents by an optically active substance. Circular dichroism is defined as the difference in extinction coefficients for the absorption of left or right circularly polarized light. ie. $\Delta\epsilon = \epsilon_L - \epsilon_R$. Molar ellipticity, $[\theta]$, is proportional to $\epsilon_L - \epsilon_R$ as follows: $[\theta] = 3300\Delta\epsilon$. The units of $[\theta]$ used in this thesis are $10^{-3} \text{ deg.cm}^2. \text{ dmole}^{-1}$. All of the amino acid residues, with the exception of glycine, are asymmetric residues and therefore optically active. However, the polypeptide backbone also has an optical activity which in its various conformational states dominates the CD spectrum (Van Holde, 1985). Secondary structural units such as the α -helix, β -sheet and random coil produce

distinctive CD spectra which can be used to analyze changes in the 2^o structure of the whole protein. The amide bond itself has two electronic absorptions: an electric dipole π to π^* transition around 190nm and a magnetic dipole n to π^* transition at about 222nm in which the non-bonding electrons of the carbonyl oxygen are promoted to an antibonding π orbital (Drake, 1994). This is a weaker transition but it plays a major role in the CD spectrum of TnC which is 66% helical. In the denaturation of TnC with urea, the CD spectra can be recorded over a wavelength range of 200-350nm since no absorptions in the CD spectrum of the 8M urea stock solution are observed in this range (Mathews & Crisanti, 1981). The interference in the signal at a wavelength of 190nm with increasing concentrations of urea only allows the transition at 222nm to be observed as the protein unfolds. The purpose of this method is not to determine absolute values for helical content but rather to compare the signals for the mutant proteins with the wild-type protein, which differ by a single amino acid residue. This N-cap residue is reported to play a crucial role in helix stability. Molar ellipticity values, $[\theta]_{222\text{nm}}$, are expected to be a reflection of the effect of mutation on the overall secondary structure of the protein. Different conformations of the amide-amide orientation are expected to produce different CD spectra. Even though the changing states are not completely defined, CD provides a way to follow changes in secondary structure as the protein is unfolded. This spectral feature identifies the urea concentration at which the unfolded conformation is achieved.

1.4.2. Fluorescence Spectroscopy

Fluorescence spectroscopy was used to measure the calcium affinity of the F29W/54X mutant proteins as well as the F105W/130V protein. The calcium titration curves for the remaining F105W mutant proteins are reported elsewhere

(Trigo-Gonzalez, 1993). Steady state fluorescence was also used to follow the unfolding of TnC in the presence of urea.

When a molecule which contains a fluorophore is excited from its ground state to a higher energy level by the absorption of light, part of that energy can be reemitted as radiation of a longer wavelength. This is a process known as fluorescence. In proteins, those amino acids whose structure contain delocalized electrons present in conjugated double bonds exhibit fluorescence.

Chicken skeletal TnC has no tyrosine or tryptophan residues in its sequence. A tryptophan residue was previously engineered into the sequence in the low-affinity (Pearlstone et al, 1992) and then in the high-affinity domain (Trigo-Gonzalez et al, 1992). In this study, the probes were used separately to measure the change in stability and the change in calcium affinity as a result of mutation at the N-cap residue. Changes in the environment of the tryptophan affect both the wavelength of the emission maximum and the intensity of the fluorescence. The fluorescence of the tryptophan residue is very sensitive to changes in its environment: a small change produces a large change in the fluorescence intensity. The emission maximum should be observed to decrease in wavelength as the side chain is buried more deeply within the hydrophobic core of the protein. Tryptophan which is fully accessible to water has an emission maximum of 350nm compared to an emission maximum of 310nm when it is buried (Varley, 1994). The signal can also vary depending on the proximity of the tryptophan residue to another residue which can quench the fluorescence.

Since there are no tyrosine residues in TnC, the excitation wavelength was set at 280nm, the maximum absorption wavelength of tryptophan. The fluorescence emission maximum for phenylalanine in an aqueous solution is 282nm (Lapanje,S.). Due to its low extinction coefficient in the Near UV region,

the spectrum produced by any phenylalanine residues in the sequence are not observed. Some other amino acid residues such as histidine, cysteine and methionine also absorb light in the Middle and Far UV region. The excitation wavelength was set at 278nm. At this wavelength Trp will exhibit the strongest light absorption so that any other residues will not be observed in the fluorescence emission spectrum.

1.4.3. Urea Denaturation

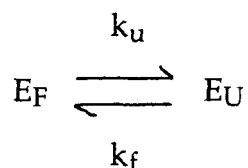
The denaturation of a protein is a process whereby the conformation is changed from a folded state to that of a random coil while keeping the 1^o structure intact, i.e. no covalent bonds are broken. To compare the stability of the mutant proteins to the wild type by denaturation, the process must be reversible to allow the application of the thermodynamics of reversible processes for the analysis. The native conformation of the protein along with its functional properties must be restored upon removal of the denaturant. Urea was the logical choice of denaturant for this protein since 8M urea is used in the purification of TnC. After the urea was removed from the protein solution on a desalting column, the protein refolded and could be titrated reproducibly with calcium. Experiments performed in a collaboration with the University of British Columbia with cloned protein samples purified by column chromatography were tested for their ability to function in muscle fibers which had been stripped of their native TnC. These fibers were tested for muscle tension development, stripped of the cloned TnC, and reconstituted once again with native TnC. In all cases, there was virtually no difference in the levels of tension development in the fiber (Dr. B. Bressler, Personal Communication). This study demonstrated that the protein was fully functional upon removal of the urea used in the purification of the cloned protein samples. In a study of the α -subunit of

tryptophan synthase , Mathews and Crisanti (1981) did not observe any absorption in the CD spectrum of their 8M urea stock solution between 205 and 260nm. This was verified by scanning the buffer solutions for this study. There was no contribution to the Far UV CD spectra of stock solutions from 0.1M to 8M urea.

If the protein undergoes reversible denaturation in a two-state process, then the free energy of unfolding can be calculated as follows:

$$\Delta G = - RT \ln K_{eq} \quad (1)$$

From thermodynamic theory, a protein folds when the free energy of the unfolded state G_U is greater than the free energy of the folded state G_F . This difference is measured for both the native protein and the mutated protein. The change in energy associated with the mutation is then be calculated.



$$K_{eq} = [E_U]/[E_F] = (k_u/k_f) \quad (2)$$

The equilibrium constant, K_{eq} was measured at different concentrations of urea. At each urea concentration the change in steady state fluorescence of the protein and the change in molar ellipticity, $[\theta]_{222nm}$, was followed. Measurements were taken after the reaction had reached equilibrium .

The method of analysis selected to calculate the ΔG of unfolding was the linear extrapolation model (LEM). This method assumes a two-state transition for the unfolding of the protein and that the change in ΔG is a linear function of

urea. A plot of ΔG versus urea concentration can be extrapolated to 0M urea to give a measure of the change in free energy between the folded and unfolded protein in the absence of urea. The value $\Delta G_{\text{unf}}(\text{H}_2\text{O})$ should be a property only of the protein and since LEM is the method which most often gives denaturant-independent values of $\Delta G_{\text{unf}}(\text{H}_2\text{O})$ it has become the method of choice (Santoro & Bolen, 1992). A recent study (Yao & Bolen, 1995) found good agreement between the predicted free energy change for RNase A and the value obtained by the LEM method. The agreement between these values demonstrated that LEM is a function of state, having the properties of additivity and independence of pathway that are required of an authentic free energy quantity. The ability to obtain $\Delta G_{\text{unf}}(\text{H}_2\text{O})$ values which were in agreement with predicted values was also independent of the length of the linear extrapolation.

A two-state mechanism was assumed for the unfolding of calcium free TnC, allowing ΔG to be calculated as a function of urea concentration from the points in the transition region of the unfolding curve.

$$\Delta G_{\text{unf}} = -RT \ln K_{\text{eq}} = -RT \ln (F_N - F) / (F - F_D) \quad (3)$$

where F is the observed fluorescence or molar ellipticity and F_N and F_D are the values for the native and denatured states of the protein respectively. It was shown (Pace, 1986) that the free energy of unfolding in the presence of urea is linearly related to the urea concentration as follows

$$\Delta G_{\text{unf}} = \Delta G_{\text{unf}}^{\text{H}_2\text{O}} - m [\text{urea}] \quad (4)$$

where $\Delta G_{\text{unf}}^{\text{H}_2\text{O}}$ is the free energy of unfolding in water and "m" is the slope of the line of a plot of ΔG_{unf} versus urea concentration. The value of "m" is a

measure of the dependence of ΔG on urea concentration. When working with urea concentrations between 0 and 6.5M urea ΔG_{unf} could be calculated by combining equations 3 and 4 to give

$$F = \frac{F_N + (F_N - F_D) \exp\{(m[\text{urea}] - \Delta G_{\text{unf}} \text{H}_2\text{O})/RT\}}{1 + \exp\{(m[\text{urea}] - \Delta G_{\text{unf}} \text{H}_2\text{O})/RT\}} \quad (5)$$

This equation assumes that the fluorescence and molar ellipticity of the protein in the folded state and denatured state are independent of the urea concentration. In denaturation studies of the enzyme barnase, this has been shown not to be the case (Horovitz, Mathews and Fersht, 1992). F_N and F_D were found to be linearly dependent on urea concentration and so equation 5 was re-written to include the slopes observed in the regions in which the protein is assumed to be fully-folded or fully unfolded.

$$F = \frac{(\alpha_N + \beta_N[\text{urea}]) + (\alpha_D + \beta_D[\text{urea}]) \times \exp\{(m[\text{urea}] - \Delta G_{\text{unf}} \text{H}_2\text{O})/RT\}}{1 + \exp\{(m[\text{urea}] - \Delta G_{\text{unf}} \text{H}_2\text{O})/RT\}} \quad (6)$$

where α_N and α_D are the intercepts, and β_N and β_D are the slopes of the baselines at the low(N) and high(D) urea concentrations. The same analysis was required for TnC. Whereas the fluorescence of the F29W mutant proteins decreased as the protein unfolded, at high urea concentrations, fluorescence intensity began to increase while Far UV CD values identified the protein samples as unfolded.

Because of the long extrapolation to estimate the value of $\Delta G_{\text{unf}}(\text{H}_2\text{O})$, small errors in the value of "m" can lead to large errors in the value of ΔG .

Using equation 4, $[\text{urea}]_{50\%}$, the concentration of urea at which 50% of the protein is denatured, can be determined. Since ΔG_{unf} is zero at $[\text{urea}]_{50\%}$ the equation reduces to:

$$\Delta G_{\text{unf}}^{\text{H}_2\text{O}} = m [\text{urea}]_{50\%}. \quad (7)$$

Values of $[\text{urea}]_{50\%}$ are reproducible and the free energy difference between two mutant proteins can be determined from information obtained in the transition region of the curve (Horowitz et al, 1992). From equation 7, a mutant protein can be compared to the wild-type protein as follows:

$$\Delta \Delta G_{\text{unf}}^{\text{H}_2\text{O}} ([\text{urea}]_{50\%}) = \langle m \rangle \Delta [\text{urea}]_{50\%} \quad (8)$$

where $\Delta [\text{urea}]_{50\%}$ is the difference in the $[\text{urea}]_{50\%}$ of the two proteins being compared and $\langle m \rangle$ is the average value of m . A change in "m" on mutation is considered diagnostic of significant changes in the structure of the folded or unfolded state or both (Serrano & Fersht, 1989).

1.4.3. Flow Dialysis

Fluorescence and CD spectroscopy were used to study the calcium affinity as well as the stability of the mutant proteins but these techniques did not provide information on the integrity of the calcium-binding sites. Initial calculations of the Hill coefficients for the valine mutant of the low-affinity domain showed a decrease in the Hill coefficient for the mutant. The two possible reasons to explain this observation were 1) the loss in cooperativity of calcium-binding to the 2 sites or 2) the loss of function of one of the binding sites. To verify that the mutants had four functional calcium-binding sites, the method

of flow dialysis was selected. This is reported to be a very sensitive method of detection for complexes which have a dissociation constant in the range of 10^{-3} to 10^{-6} M (Colowick and Womack, 1969). The calcium-binding sites of the low-affinity-binding domain of TnC have a dissociation constant of 10^{-5} M.

The flow dialysis method is more accurate than conventional equilibrium dialysis techniques since all samples are obtained from the same dialysis cell rather than from a large number of cells. Its only requirements are a sensitive detection system and binding must occur rapidly. Radiolabelled calcium (^{45}Ca) was selected for this series of experiments.

The flow dialysis apparatus (Figure 2.4) consists of two chambers separated by a dialysis membrane (Colowick and Womack, 1973, Feldmann, 1978). The sample for study is placed in the upper chamber while buffer is pumped through the lower chamber. Before an experiment is conducted with a sample, the maximal rate of dialysis of the ligand, across the dialysis membrane, is measured. A sample of radiolabelled calcium diluted in buffer is added to the upper chamber while buffer is pumped through the lower chamber with a peristaltic pump. The rate of dialysis of radiolabelled calcium from the upper chamber is simply measured as the counts per minute in the effluent collected from the lower chamber and used as a measure of labelled calcium in the upper chamber. Aliquots of unlabelled calcium are then added to the upper chamber, in regularly scheduled pulses, and the counts per minute in the effluent measured after each pulse. The concentration of isotope in the collected samples should only depend on the fraction of radiolabelled calcium in the upper chamber and not on the total calcium concentration. When working with charged ligands such as calcium, charge balancing across the membrane can result in an increase in labelled ligand in the effluent which is dependent on total

calcium concentration. This is known as the Donan effect and is prevented by the use of buffers which are at least 40mM Tris (Porumb, 1994).

On adding protein to the upper chamber, if the ligand binds to the protein, then the rate of dialysis should decrease with an observable decrease in the counts per minute recorded in the effluent. For each experiment, a protein sample with radiolabelled calcium is added to the upper chamber. When the system is at steady state, the rate of isotope entering the lower chamber by diffusion and leaving in the effluent are equal. The counts per minute recorded in the effluent reflect the concentration of labelled ligand in the effluent which, as indicated above, is a measure of the concentration of labelled calcium in the upper chamber (Colowich and Womack, 1969). The addition of measured pulses of unlabelled calcium to the upper chamber results in an increase in the amount of labelled calcium free in solution in the upper chamber since the unlabelled calcium displaces radiolabelled calcium from the protein. This results in an increase in the concentration of labelled calcium in the effluent. The final pulse of unlabelled calcium results in an excess over the labelled calcium so that there is essentially no radiolabelled calcium is bound to the protein. The accuracy of the binding measurements requires that there be little loss of isotope from the upper chamber over the time course of the experiment. Hence the requirement for rapid equilibration across the membrane. The assumption is made that the concentration in the upper chamber is the same both at the beginning and at the end of the experiment. The final pulse with unlabelled calcium produces a maximal rate of dialysis of the radiolabelled calcium across the membrane which is related to the concentration which was initially added to the upper chamber. The addition of an excess of unlabelled ligand at the conclusion of the experiment also shows that the rate change is due to substrate binding and not

the overall calcium concentration. The data was processed according to equation 7 (section 2.14.1.3).

By withdrawing equal aliquots of sample from the upper chamber both before pulsing with unlabelled calcium and at the end of the experiment, (being sure to include the dilution factor), loss of radioisotope due to diffusion can be calculated for the determination of calcium affinities using this method.

1.4.4. Stopped Flow Measurement of the Off-Rates for Calcium-binding

The experiments up to this point were designed to show whether the ion affinity of the N-terminal domain of TnC could also be tailored by substitutions of the N-cap residue, as observed for the high-affinity domain (Trigo-Gonzalez et al, 1992). The calcium titration of each domain provided a measure for the degree of cooperativity between the calcium-binding sites. However it was not known whether the change in affinity was due to a change in the rate of calcium dissociation from the protein or a change in the rate of binding to the protein. In other words has the "off-rate" or the "on-rate" been affected by the mutation? A large change in fluorescence was observed for the dissociation of calcium from the F29W/54X mutant proteins. With the exception of the F105W/130V mutant protein, the mutant proteins of the high-affinity domain could not be studied by this method since the change in fluorescence associated with calcium removal was too small to distinguish two separate rates.

2. MATERIALS AND METHODS

2.1 Buffers and Solutions

Buffer A:	50mM Tris HCl, pH 8.0 1mM EGTA 25% sucrose 0.5mM PMSF
Buffer B:	50mM Tris, pH 8.0 8M Urea 2mM MgCl ₂ 1mM DTT 85mM KCl (low salt) or 1mM KCl (high salt)
Buffer C:	50mM Tris-HCl, pH 8.0 2mM DTT 1mM CaCl ₂ 0.1mM PMSF 200mM NaCl (low salt) or 1M NaCl (high salt)
Chelex buffer:	50mM MOPS, pH 6.95 150mM KCl 1mM DTT (added just before use)
TE pH 8.0:	10mM Tris-HCl 1mM EDTA
1x TAE:	0.04M Tris-acetate 1mM EDTA
Solution I:	50mM glucose 10mM EDTA 25mM Tris-HCl, pH 8.0 4 mg/mL lysozyme
Solution II:	0.2N NaOH 1% SDS
Solution III:	60mL of 5M potassium acetate 11.5mL of glacial acetic acid 28.5mL ddH ₂ O

Phenol Solution: DNA extractions were performed using phenol prepared from pure liquified phenol equilibrated to a pH>7.8 as described in Sambrook et al, 1989.

TfBIBuffer: 30mM CH₃COOK
50mM MnCl₂
100mM KCL
10mM CaCl₂
15% glycerol
pH should be close to 7.0. Filter sterilize.

TfBII Buffer: 10mM Na-MOPS, pH 7.0
75mM CaCl₂
10mM KCL
15% glycerol
Filter sterilize

10x TBS: 90.0 g NaCl
24.2g Tris-HCl, pH 7.4
Bring volume to 1L

1X PBS: 8g NaCl
0.2g KCl
1.44g Na₂HPO₄
0.24g KH₂PO₄
Dissolve in 800mL ddH₂O, adjust pH to 7.4 with HCl
Add ddH₂O to 1L. Autoclave to sterilize.

BLOTTO: 1x TBS
0.05% TWEEN 20
5% Skim milk powder

Transfer Buffer: 39mM glycine
48mM Tris
0.0375% SDS

IgG Low salt: 20mM Tris, pH 8.0
20mM NaCl

IgG High Salt: 20mM Tris, pH 8.0
1M NaCl

SAS: 450g ammonium sulfate
H₂O to 500mL
Heat. Filter hot and store over crystals of ammonium sulfate.

33% SAS: 33mL SAS
67mL IgG low salt buffer

Separating Buffer: 0.75M Tris, pH 8.8
0.2% SDS

Stacking Buffer: 0.1458M Tris, pH 6.8
0.117% SDS

Running Buffer: 0.025M Tris, pH 8.3
0.1% SDS
0.192M glycine

Laemli Buffer (5X): 0.0625M Tris, pH 6.8
2% SDS
10% glycerol
5% b-mercaptoethanol
0.001% Bromophenol Blue
Each made as a 5x stock and added together in equal volumes.

Staining Solution: 0.3% Coomassie Blue
Made up in a 500:100:400 solution of Methanol/glacial acetic acid/H₂O

APS: 10% ammonium persulfate

Slow Destain solution: 90% H₂O
10% glacial acetic acid

Fast Destain solution: 50% H₂O
40% methanol
10% glacial acetic acid

Anticoagulant : 0.12M Sodium citrate
0.05M Benzamidine-HCl pH 6.9
50,000 units Heparin
500 mg trypsin inhibitor

Barium citrate buffer: 0.15M sodium chloride
5mM benzamidine-HCl saturated with barium citrate

Sodium citrate buffer: 20mM Sodium citrate
1mM Benzamidine-HCl pH 6.9

DEAE buffer A: 100mM Sodium citrate
1mM Benzamidine-HCl pH 6.9
0.1mM PMSF

DEAE buffer B: 600mM Sodium citrate
1mM Benzamidine-HCl pH 6.9
0.1mM PMSF

Assay buffer: 50mM Tris-HCl, pH 8.0
100mM NaCl.

Factor X_a Buffer: 50mM Tris-HCl pH 8.0
0.1M NaCl
2mM CaCl₂

2.2 Bacterial Strains

2.2.1 *Escherichia coli* Strain QY13

Genotype: F⁻lac_{am}trp_{am}B B[']bio-256 N⁺ cI857 TS Sm^r recA

Growth conditions: On TY-Amp (200µg/mL) plates incubated for 36 hours at 30°C. In 2xTy-Amp (100µg/mL) broth incubated for 12 hours at 30°C with constant shaking. Culture is grown at 37°C following induction of recombinant gene expression. A recombinant derivative of pLcII-FX containing the mutated gene of troponin-C was used to transform competent QY13 cells. The expression of the gene is regulated by the temperature sensitive repressor cI857.

2.2.2 *Escherichia coli* Strain K12cI

Growth conditions: On TY-Amp 200 plates incubated for 12 hours at 37°C.
In 2xTY-Amp 100 broth incubated for 8 hours at 37°C with

constant shaking. This strain constitutively expresses the lambda cII repressor protein. This strain is used when induction of the recombinant gene is undesirable upon transformation with plasmid DNA. This strain was used for all routine transformations of plasmids and ligation mixtures for the replication of large quantities of DNA for transformation of the QY13 strain.

2.2.3 *Escheichia coli* Strain DH5 α

Genotype: supE44 Δ lacU169 (f80 lacZ Δ M15) hsdR17 recA endA1
gyrA96 thi-1 relA1.

Growth conditions: On TY-Amp 200 plates incubated for 12 hours at 37°C.
In 2XTY-Amp 100 broth incubated for 8 hours at 37°C with constant shaking.

2.3 MEDIA

TY-Amp plate: TY plate with 200 μ g/mL of ampicillin (Sigma)

2xTY broth: 1.6% tryptone, 1.0% yeast extract, 0.5% NaCl

2xTY-Amp broth: 2xTY broth with 100 μ g/mL of ampicillin (Sigma)

TY/Mg broth: 2% tryptone, 0.5% yeast extract, 0.5% NaCl, 10mM MgSO₄
The MgSO₄ is added from a 1M filter sterilized stock.

S.O.B. media: 2% tryptone, 0.5% yeast extract, 0.05% NaCl; add 10 mL of a 250mM solution of KCl; adjust to pH 7.0 with 5N NaOH

and then adjust volume to 1L with ddH₂O. Autoclave 20'.
Before use add 0.5 μL/mL of sterile 2M MgCl₂ and
10μL/mL of 20% glucose.

2.4 Preparation of Competent *Escherichia coli* Cells

2.4.1 QY13 Strain

A 1mL aliquot of TY/Mg broth was inoculated with a fresh *E. coli* colony and incubated overnight at 30°C. This culture was used to inoculate 20mL of prewarmed TY/Mg broth and incubated at 30°C to an O.D.₆₀₀=0.5. Similarly, 200mL was inoculated with the 20mL culture and incubated at 30°C to an O.D.₆₀₀=0.6. The cell culture was cooled on ice, then centrifuged at 4,500 rpm for 15 minutes at 4°C. The cell pellet was resuspended in 40mL of cold filter sterilized, TfBI buffer and centrifuged again. The cell pellet was resuspended in 8mL of cold, filter sterilized TfBII buffer. Aliquots of 200μL were dispensed into sterile centrifuge tubes, flash frozen and stored at -70°C.

2.4.2 K12 Strain

A 1mL aliquot of TY/Mg broth was inoculated with a fresh *E. coli* colony and incubated overnight at 37°C. This culture was used to inoculate 20mL of prewarmed TY/Mg broth and incubated at 37°C to an O.D.₆₀₀=0.5. Similarly, 200mL was inoculated with the 20mL culture and incubated at 37°C to an O.D.₆₀₀=0.6. The cell culture was cooled on ice and centrifuged at 4,500 rpm for 15 minutes at 4°C. The cell pellet was resuspended in 40mL of cold, filter sterilized TfBI buffer and centrifuged again. The cell pellet was resuspended in 8mL of cold, filter sterilized TfBII buffer. Aliquots of 300μL were dispensed into sterile centrifuge tubes, flash frozen and stored at -70°C.

2.4.3. DH5 α Strain

Competent cells were prepared as for the K12 strain.

2.4.4 Preparation of Electrocompetent Cells

A TY plate was streaked with a stock of competent cells of the desired type and incubated at 37°C for 12 hours. A single colony was selected to inoculate 4.5mL of 2xTY liquid broth and incubated overnight at 37°C with continuous shaking. This culture was used to inoculate 350mL of 2xTY liquid broth. The culture was grown with vigorous aerations to an O.D.₆₀₀ of 0.6. The culture was chilled on ice for 15 minutes. From this point all work was carried out in a cold room (at 4°C). The culture was poured into a sterilized, pre-chilled 500mL centrifuge bottle and centrifuged for 15 minutes at 4,500 rpm at 4°C. The broth was poured off and the cells resuspended by shaking vigorously with 350mL of pre-chilled, autoclaved ddH₂O. The cells were centrifuged as before. This process was repeated two more times. The cell pellet was resuspended in approximately 350mL of pre-chilled, autoclaved ddH₂O to a final volume of 800 μ L. The cells were dispensed in 100 μ L aliquots in pre-chilled 1.7mL centrifuge tubes and stored on ice until ready to use or flash frozen and stored at -70°C until ready to use.

2.5 Transformation of Competent *Escherichia coli* Cells

2.5.1 Transformation of *E. coli* Strain QY13

To a 50 μ L aliquot of competent cells, thawed on ice, 1mL of plasmid DNA was added. The cells were incubated on ice for 30 minutes, heat shocked by incubating in a 30°C water bath for 2.5 minutes, and then placed on ice for another minute. The cells were then added to 2mL of 2xTY broth and incubated for 2 hours at 30°C in a shaker incubator. Aliquots of the transformed cells were

spread-plated on TY-Amp 200 plates and incubated for 36 hours at 30°C. Single colonies were then selected to inoculate 2mL 2xTY A100 broth culture tubes to perform protein expression tests.

2.5.2 Transformation of *E. coli* Strain K12

An aliquot of competent cells was thawed on ice. To a 150 µL of cells, 1mL of plasmid DNA was added. The cells were incubated on ice for 30 minutes, heat shocked in a 37°C water bath for 2.5 minutes, and then placed on ice for another minute. The cells were then added to 2mL of 2xTY broth and incubated for 2 hours at 37°C in a shaker incubator. Aliquots of the transformed cells were spread-plated on TY-Amp 200 plates and incubated for 12 hours at 37°C. Single colonies were then selected to inoculate 2mL 2xTY A100 broth culture tubes .

2.5.3 Transformation of *E.coli* Strain DH5α

Transformation was carried out as per *E. coli* strain K12.

2.5.4 Electroporation of Electrocompetent Cells

DNA was prepared for electroporation directly from a ligation mixture. To a 10µL ligation mixture 40mL of ddH₂O was added, followed by 1µL of a 10µg/mL solution of tRNA and 150µL of 95% ethanol. The mixture was left overnight at -20°C, then centrifuged at maximum speed. The supernatant was decanted. The DNA pellet was dried and then resuspended in 10µL of ddH₂O. The electroporator (Model) was set to 2500 volts, 25mfd and 200 ohms. One half of the resuspended DNA (5ng) was mixed with 100µL of electrocompetent cells and gently mixed. The sample was transferred to a pre-chilled electroporation cuvette (Biorad) and placed in the cuvette holder. The power cycle was initiated. Immediately after completion of the power cycle, 1mL of S.O.B. media was

added to the cuvette and drawn back for transfer to a 15mL culture tube. The culture was incubated at 37°C with shaking for 1 hour and then spread plated in aliquots onto several 2xTY A200 plates. The plates were incubated overnight at 37°C. Individual colonies were selected to inoculate 2mL of 2xTy A100 broth.

2.6 PLASMIDS

2.6.1. pLcII-Fx-TnC

The pLcII-Fx-TnC vector (Figure 1.3) is a fusion expression vector driven by a leftward promoter (P_L) of the bacteriophage λ . The recombinant genes for the various mutants were expressed as fusion proteins with a 31 amino acid portion of the λ cII protein connected to the recombinant protein through the Factor X_a tetrapeptide recognition sequence Ile-Glu-Gly-Arg.

2.6.2. pUC 18

The plasmid pUC18 is an *Escherichia coli* cloning vector which includes the ampicillin resistance gene and the origin of replication from pBR322. It also contains the multiple cloning site of one of the M13mp sequencing vectors. In pUC18, the HindIII site is closest to the pUC forward sequencing primer binding site.

2.6.3. Preparation of Plasmid DNA

Test tubes containing 2mL of sterile 2X TY media and ampicillin were inoculated with a single bacterial colony. In the case of QY13, the tubes were incubated at 30°C with shaking, for 24 hours. If K12 was the inoculum, the tubes were incubated at 37°C with shaking for 7 hours. After the required incubation time the cultures were poured into sterile 1.7mL eppendorf tubes and centrifuged at full speed for 2 minutes. The supernatant was decanted and the

cell pellet resuspended in 100 μ L of solution I. The tube was stored at room temperature for 10 minutes at which time 200 μ L of freshly prepared Solution II was added. The tube contents were mixed by inverting and then stored at room temperature for 5 minutes. To the cleared solution, 150 μ L of solution III was added. Mixing was achieved by inverting and the tube was stored for 5 minutes at room temperature. The tube was centrifuged at full speed for 5 minutes and the supernatant transferred to a fresh tube. To the supernatant, 200 μ L of phenol and 100 μ L of chloroform were added. The tube was vortexed and then centrifuged for 2 minutes. The top layer containing the plasmid DNA was transferred to a fresh tube. Two volumes of 95% ethanol were added, mixed by inverting and allowed to stand at room temperature for at least 5 minutes. The tube was centrifuged at maximum speed for a minimum of 10 minutes. The supernatant was drawn off carefully, leaving the DNA pellet which was dried and then resuspended in autoclaved ddH₂O. DNase-free pancreatic RNase A and T1 were added and incubated at 37°C for one hour to remove any contaminating RNA.

2.6.4. Purification of Plasmid DNA for Sequencing

The DNA isolated as per 2.6.2 required further purification for sequencing. To 30 μ L of DNA, 90 μ L of ddH₂O, 40 μ L of 10M NH₄OAc and 250mL of 95% alcohol were added. After a 5 minute incubation at room temperature, the mixture was centrifuged at maximum speed for 5 minutes. The pellet was dried briefly and then resuspended in 25 μ L of 0.4M NaOH. The solution was gently mixed and stored at room temperature for 10 minutes. To precipitate the DNA, 7.5 μ L of 3M NaOAc, pH 5.6, and 150 μ L of 95% ethanol were added. The mixture was stored at -70°C for 15 minutes followed by centrifugation at maximum speed for 10 minutes at room temperature. The supernatant was

carefully decanted and the DNA pellet immediately washed with 100 μ L of cold 70% ethanol. A salt-free DNA pellet was obtained by centrifugation at maximum speed for 10 minutes. The pellet was dried and resuspended in 7 μ L of ddH₂O for sequencing.

2.6.5. Sequencing of Plasmid DNA

Plasmid DNA isolated from the QY13 strain of *Escherichia coli* was sequenced by means of the chain-termination DNA sequencing method using the Sequenase Version 2.0 DNA sequencing kit from USB.

2.7 Cloning Procedures

2.7.1 Purification of DNA for Cloning

DNA required for cloning work was isolated by electrophoresing the sample on a 1% agarose gel. The gel was viewed under low intensity U.V. light to identify the location of the desired band of DNA. The band was cut out of the gel using a clean scalpel and placed in a spin column. The column was centrifuged at 6,000 r.p.m. for 10 minutes. The agarose was trapped in the column while the DNA, suspended in TAE buffer used to prepare the gel, passed through the column into a centrifuge tube. To the DNA suspension, 0.1 volumes of 3M sodium acetate, pH 5.6 and 2X volume of 95% ethanol were added. The mixture was incubated at room temperature for 30 minutes then centrifuged at maximum speed for 1 hour. The supernatant was decanted and the DNA pellet briefly vacuum dried. The pellet was resuspended in 5 to 10 μ L of ddH₂O.

2.7.2 Restriction Digests of Constructs

The pLcII-Fx-TnC vector with a tryptophan residue at position 105 was digested with NdeI (NEB) and XbaI (NEB) using the NEB2 buffer . The vector

pUC18 was also digested with the same two restriction enzymes. The double digest were performed at 37⁰C for 1 hour. The 2 fragments from the digest of the pLcII vector were isolated as per 2.7.1.

2.7.3 Ligation of pLcIIFx-TnC DNA Fragments into pUC 18

Equal volumes of vector and insert were ligated overnight, at room temperature, using T₄ DNA ligase (BRL). The ligation mixtures were diluted 5 fold with ddH₂O. Competent cells were transformed as per section 2.5.2. Plasmid DNA was prepared from cultures grown from each ligation mixture. Restriction digests with BamH1 and EcoR1 (BRL), in React 3 buffer, identified the fragment ligated into pUC18 which carried the gene for TnC.

2.8 Site-directed Mutagenesis

2.8.1 Primer Extension

2.8.1.1 Primers Selected for PCR Mutagenesis

A stock of cII forward primer was diluted to 300ng/mL for use as the forward primer in the extension step.

cII Primer: 5' GCTTGGAACTGAGAAG 3'

The sequence of the pLcII vector beyond the insertion point of the gene for TnC was not available. Insertion of the gene for TnC into pUC18 using directional cloning ensured the orientation of the gene so that the reverse primer of pUC 18 could be used in conjunction with the cII primer for PCR site directed mutagenesis.

The underlined triplet in the sequence below is the codon for the amino acid threonine at position 54 in the sequence of TnC.

Wild-type: 5' C CAG AAC CCC ACC AAA GAG GAG C 3'

Initially, two mutant primers were designed. By substituting a single base (designated X) in each primer with each of the four possible bases, a total of 8 different amino acids could be obtained upon translation.

AXC primer: 5' C CAG AAC CCC AXC AAA GAG GAG C 3'

GXC primer: 5' C CAG AAC CCC GXC AAA GAG GAG C 3'

Table 2.1 Mutagenic Possibilities from the Two Oligonucleotides

CODON	AMINO ACID
ACC	THR
AGC	SER
ATC	ILE
AAC	ASN
GCC	ALA
GGC	GLY
GTC	VAL
GAC	ASP

After isolating four of the eight possible amino acids at position 54, two new primers were designed to generate the remaining four possible mutants.

AXC2 primer 5' C CAG AAC CCC AA^A/TC AAA GAG GAG C 3'

GXC2 primer

5' C CAG AAC CCC G^A/T C AAA GAG GAG C 3'

2.8.1.2 Preparation of Mutant DNA Using the Polymerase Chain Reaction

The pUC18/TnC construct was linearized with the restriction enzyme Ssp1 for use as the template in the Polymerase Chain Reaction (PCR). A 1mL aliquot was added to the reaction mixture which consisted of 38.5µL ddH₂O, 1µL dNTPs (25mM) (Pharmacia), 2µL reverse primer (300ng/mL), 2µL forward primer (300ng/mL), 5µL reaction buffer (USB) and 0.5µL VENT DNA polymerase (USB). The PCR reaction was carried out in two steps (Figure 2.1). First, each mutant primer was used in combination with the pUC reverse primer to synthesize a mutated piece of DNA, 580 base pairs in length, extending from position 267 in nucleotide sequence (Figure 2.2) of TnC to the polylinker in pUC 18. This fragment of DNA was gel purified as outlined in section 2.7.1.

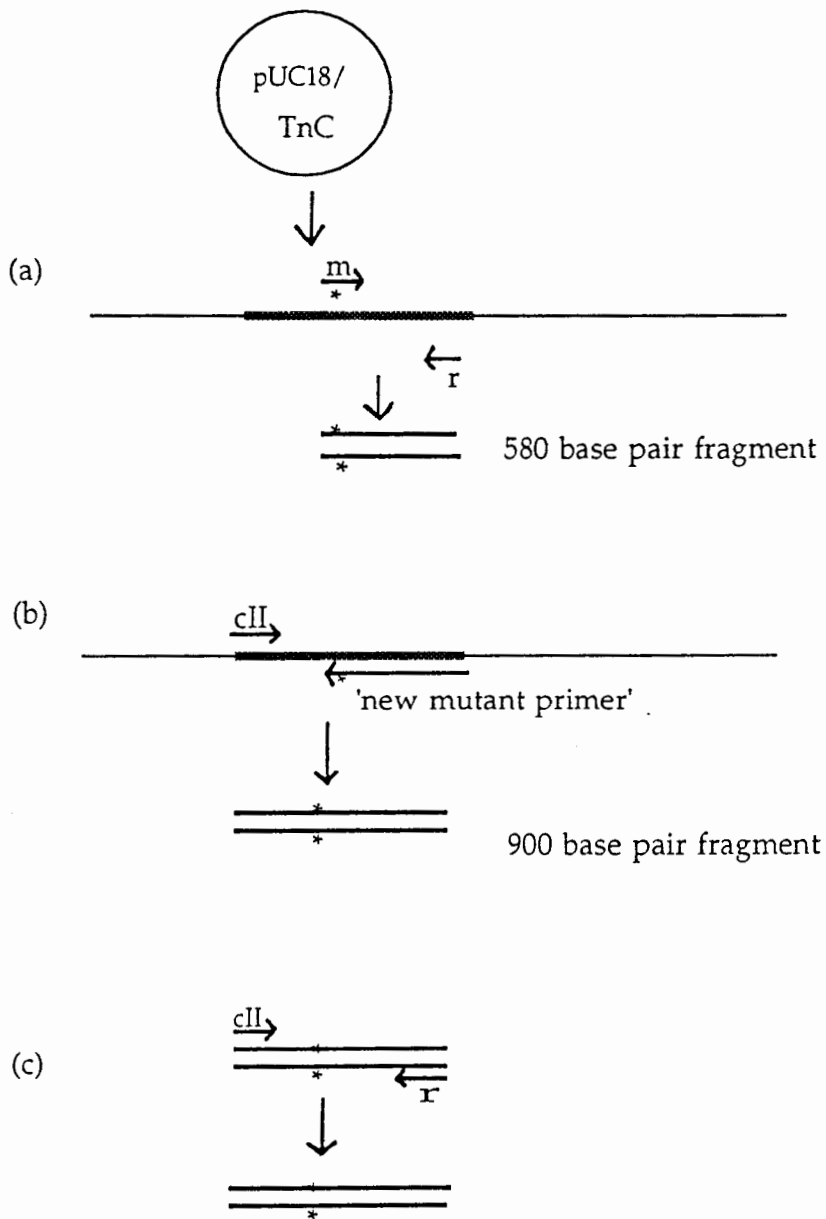
The second step used the same template as above. The mutated piece of DNA obtained from step 1 was used as the reverse primer and the cII primer was used as the forward primer to synthesize the full length gene. The product was electrophoresed on a 1% agarose gel and the 900 base pair product purified as per section 2.7.1.. The full length gene obtained from the second PCR step was amplified using the cII forward primer and the pUC 18 reverse primer. The product was gel purified.

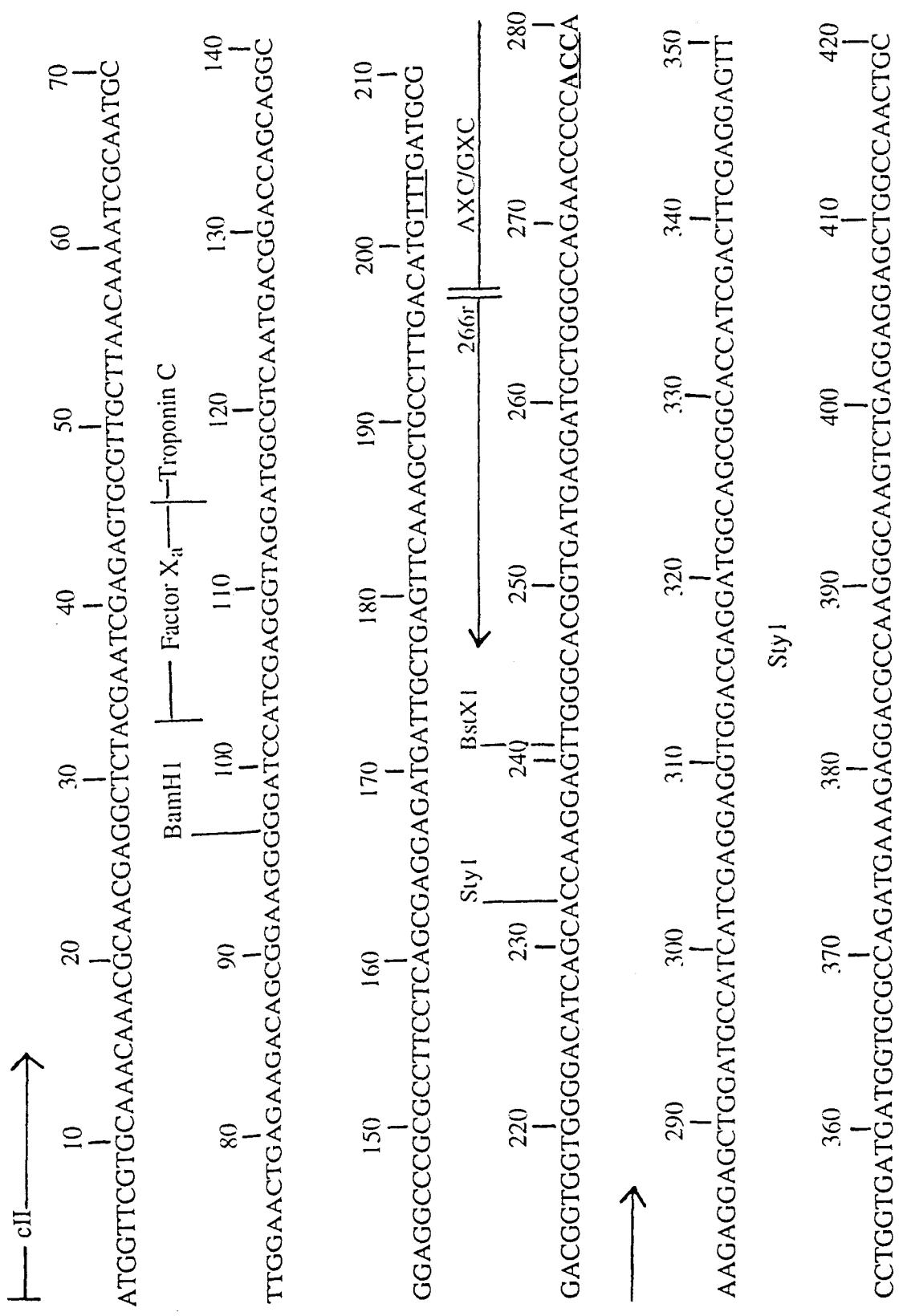
2.8.1.3 Ligation of PCR Products Into pLcIIFx-TnC

The full length gene generated by PCR was digested in a double digest with the restriction enzymes BamH1(BRL) and Xba1(NEB) using NEB4. The resulting 750 base pair fragment of DNA was purified as per section 2.7.1. This gene fragment was ligated into pLcIIFx-TnC, previously digested with the same two enzymes and purified as per section 2.7.1. The ligation mixture was used to

FIGURE 2.1. Primer Extension PCR Mutagenesis

- a) The pUC18/TnC vector was first linearized. The thickened line represents the gene for the cII-Fusion TnC. Using the AXC or GXC mutant primer with the pUC18 reverse primer, a 580 base pair fragment of DNA was synthesized with a mutation, designated by an asterisk.
- b) The 580 base pair fragment was gel purified and used in conjunction with the cII forward primer to synthesize the entire gene for TnC while incorporating the mutation into the sequence.
- c) To have a large enough quantity of the gene to work with, the 900 base pair fragment from part (b) was amplified by PCR using the cII forward primer and the pUC18 reverse primer.





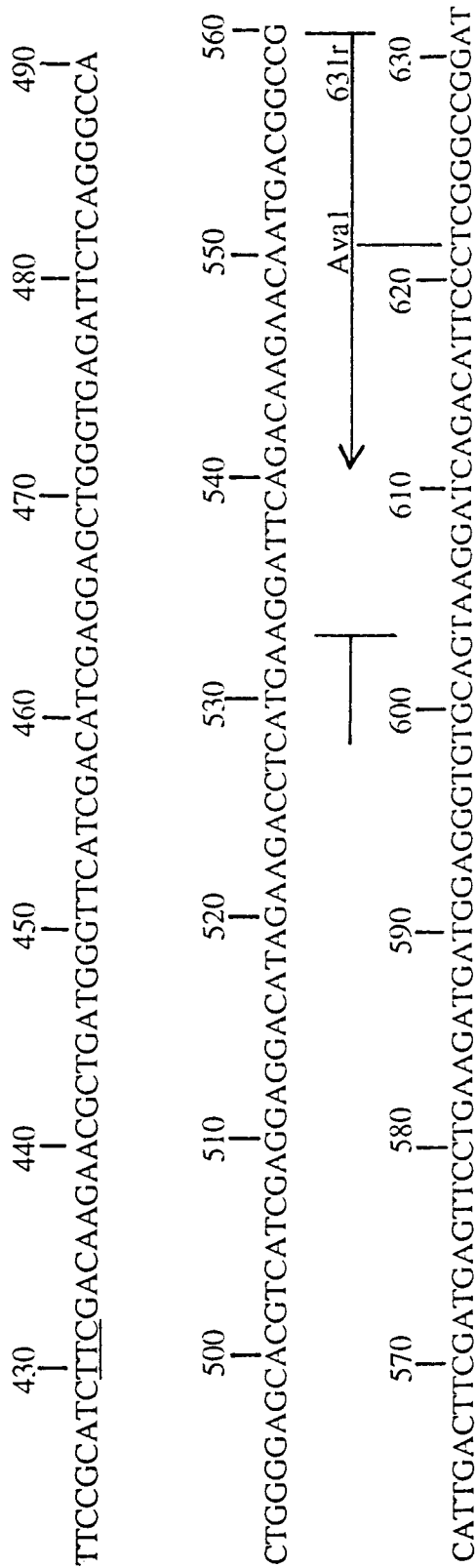


FIGURE 2.2. DNA Sequence of cIIFX-TnC

The nucleotide sequence is abbreviated to the one letter code representing each deoxyribonucleotide base. Numbering of the sequence begins with the cII fusion sequence. The location of the tryptophan substitutions are underlined. The site of mutation for the 54X mutants is in underlined bold typeface. The enzyme restriction sites used for cloning are identified above the sequence as are the primer sequences. The arrows associated with the primer names indicate the direction in which primer extension occurred in the PCR reactions.

transform *E. coli* K12 competent cells. A control sample containing vector only was prepared simultaneously to ensure that a ligation mixture without the insert could not transform competent cells. The plasmid DNA isolated from the K12 cultures was digested with the enzymes EcoR1 and BamH1 to confirm the insertion of the gene into the pLcII vector. If a 750 base pair fragment of DNA, was visible upon electrophoresis, the plasmid DNA was used to transform *E. coli* QY13 competent cells to test for protein expression.

2.8.2 Triple Ligation of PCR Products Into pLcII Vector

2.8.2.1 Selection of PCR Primers

Due to the difficulty in successfully carrying out primer extension with this gene, an alternate method of generating the mutants was devised. The second set of mutant primers (AXC2 and GXC2) were designed at this point along with two new reverse primers (266r and 631r). Both of these reverse primers are located within the sequence of the fusion gene for TnC.

266r primer: 5' CCC AGC ATC CTC ATC ACC 3'

631r primer: 5' TCC GGCCCG AGG AAT GTC 3'

2.8.2.2 Preparation of the DNA Fragments for Ligation

The pLcII-Fx-TnC vector, with a tryptophan residue at position 29 in the amino acid sequence of the gene, was linearized with the restriction endonuclease Nde1 for use as the template in the following PCR reactions.

The cII forward primer was used in combination with the 266r reverse primer. The 197 base pair fragment generated was electrophoresed using a 1% agarose gel and purified as per section 2.7.1. The fragment was then digested

with the restriction endonuclease BamH1. The resulting 169 base pair fragment was gel purified as above.

Initially the AXC2 and GXC2 mutant primers, and later the AAC, ATC and GAC mutant primers, were used in turn with the 631r reverse primer to generate a 365 base pair fragment which were electrophoresed in a 1% agarose gel and purified as per section 2.7.1. The fragments were each digested with the restriction endonuclease Ava1(NEB). The resulting 355 base pair fragments were gel purified as above.

The pLcII-Fx-TnC vector F29W was prepared for cloning using a double digest with the restriction endonucleases Ava1 and BamH1. The vector was electrophoresed on a 0.8% agarose gel and purified as per section 2.7.1.

2.8.2.3 Triple Ligation

In separate tubes, an aliquot of each digested mutant DNA fragment was added to an aliquot of the digested cII primer product. A 0.5 μ L aliquot of the prepared pLcII-Fx-TnC vector was added along with ligase buffer and T₄ DNA ligase (BRL). This ligation is directional for the ends of the vector and one end of each fragment, plus a blunt end ligation of the two PCR products (Figure 2.3). The samples were left overnight at room temperature. The ligation mixtures were then prepared for electroporation into electrocompetent *E. coli* K12 cells as per section 2.5.4.

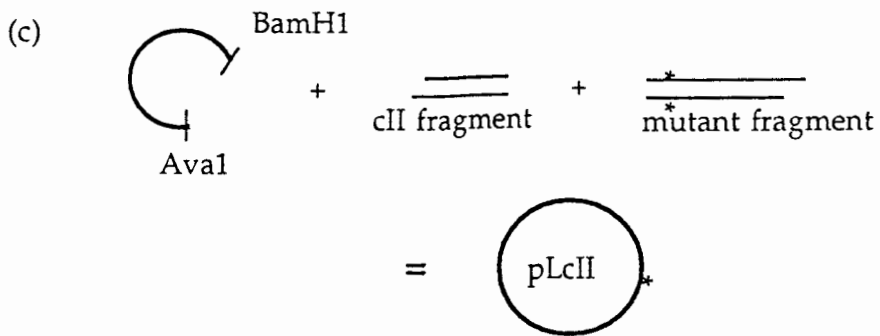
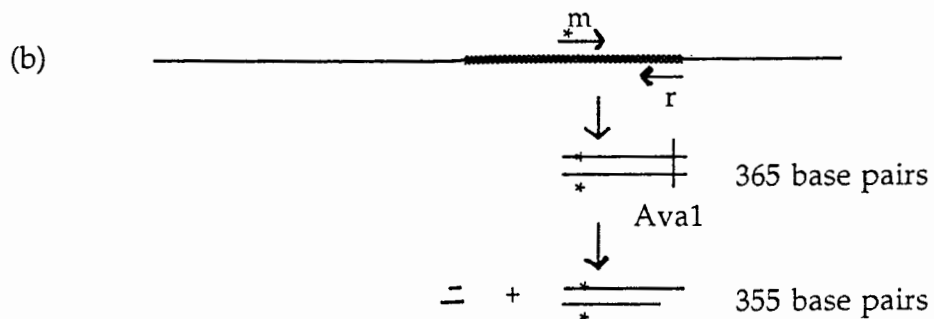
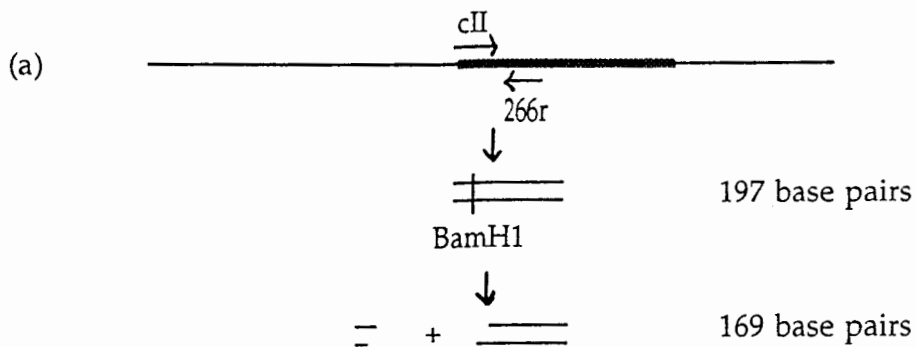
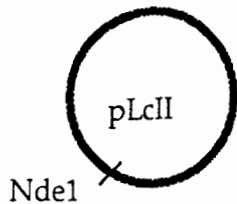
2.8.2.4 Identification of Mutant Clones From Triple Ligation Into pLcII Vector

Each colony obtained from the electroporation method was used to inoculate individual 2mL culture tubes of 2x TY A100 broth and incubated for 8 hours at 37°C. The cell pellets were collected to prepare plasmid DNA. Each potential mutant clone was digested with the restriction endonucleases BamH1

FIGURE 2.3. Triple Ligation Protocol of PCR Fragments into the pLcII Vector.

The pLcII-Fx-TnC vector was first linearized.

- a) Using the cII forward primer and the 266r revers primer, a 197 base pair fragment was synthesized. The fragment was digested with BamH1 to give a 169 base pair fragment.
- b) A second DNA fragment was synthesized with a mutant forward primer and the 631r reverse primer. The 365 base pair fragment was digested with Ava1 to remove a 10 base pair fragment.
- c) A fresh sample of the pLcII-Fx-TnC vector digested with BamH1 and Ava1 is ready to be ligated with both fragments from (a) and (b). The two fragments each have a matching end with the vector while the fragments themselves can join in a blunt end ligation to "reseat" the vector which can be used to transform competent cells.



and *Ava*1 in a double digest. Successful insertion of both fragments produced a 524 base pair fragment upon digestion of the DNA which was visualized by electrophoresis on a 1% agarose gel. Those potentially positive clones were sequenced as per section 2.6.3 and 2.6.4.

2.8.2.5 PCR Amplification of Triple Ligation Mixture

A 1mL aliquot of the triple ligation mixture from 2.8.2.3 was used as a template for PCR reactions using the *cII* forward primer and the reverse primer 631r. The triple ligation mixture was not treated with a restriction endonuclease to linearize the vector prior to amplification. Annealing temperatures of 45°C and 47°C were successful in amplifying a DNA fragment of approximately 562 base pairs. The electrophoresed fragment was gel extracted and prepared with a double digest using the restriction enzymes *Bam*H1 and *Ava*1, for ligation into pLcII-Fx-TnC prepared with the same enzymes. The ligation mixture was used to transform electrocompetent *E. coli* K12 cells.

2.8.2.6 PCR Amplification of Blunt End Ligation

The two PCR fragments obtained as per 2.8.2.2 were ligated in a blunt end ligation. Instead of digesting the PCR fragments for a triple ligation, the two fragments alone were ligated. A 1mL aliquot of a 1/50 dilution of the ligation mixture was used as a template in a PCR mixture which was electrophoresed on a 1% agarose gel. The DNA fragments were extracted from the gel and ethanol precipitated to concentrate the DNA for a restriction digest with *Bam*H1 and *Ava*1. The fragments were ligated into the vector pLcII-Fx-TnC which was previously treated with the same restriction enzymes and gel purified. The ligation mixture was used to transform electrocompetent *E. coli* K12 cells.

2.8.3 Triple Ligation of PCR Products Into pUC18

Primers selected for the PCR reactions were as described in 2.8.2.1. The pUC18 vector was linearized with SmaI, a blunt end cutting restriction endonuclease. The vector was then treated with calf alkaline phosphatase to prevent closure of the vector in a ligation reaction. The DNA fragments generated by PCR as per section 2.8.2.2 were not digested prior to ligation into pUC18.

In separate tubes, an aliquot of each mutant DNA fragment was added to an aliquot of the prepared pUC18 vector. In a separate control sample, no PCR fragments were added to the vector. A 1 μ L aliquot of ligation mixture was used to transform competent DH5 α cells.

2.8.3.1 Identification of Mutant Clones From pUC18

Colonies obtained from the transformation were randomly selected to inoculate 2mL culture tubes of 2xTY A100 broth and incubated for 8 hours at 37°C. The cell pellets were collected to prepare plasmid DNA. Each sample of plasmid DNA was digested with the two restriction endonucleases BamHI and AvaI. StyI. A fragment of 560 base pairs was expected upon electrophoresis of the digest mixture if two different fragments were correctly ligated into pUC18 regardless of their overall orientation upon insertion into the vector. If only one fragment was ligated into the vector the latter was only linearized. Any other orientation of any number of fragments produced different sized fragments upon digestion with StyI.

Clones identified to carry the full gene for TnC were digested with BamHI and AvaI for ligation into pLcII-Fx-TnC (F29W) prepared with the same enzymes. This ligation mixture was then used to transform competent *E. coli* K12 cells. Plasmid DNA isolated from each clone was used to transform

competent *E. coli* QY13 cells for protein expression tests. The plasmid DNA of clones which tested positive for protein expression was then purified for sequencing.

2.9. Expression Vector Constructs

Once the sequence of a mutant was confirmed in the pLcII-Fx-Tnc (F105W/T54X) vector (obtained from the primer extension method outlined in section 2.8.1), a fragment of the gene, located between the two possible tryptophan sites (position 29 or position 105 in the amino acid sequence) was isolated using the restriction endonuclease Sty1 (NEB) using the NEB3 buffer. For the Alanine, Glycine and Serine mutants at position 54, the resulting 155 base pair fragment excluded the tryptophan at position 105. This fragment was then ligated into the pLcII-Fx-TnC vector which included a tryptophan at position 29 instead of position 105..

2.9.1 Preparation of pLcII-Fx-Tnc (F29W) Expression Vector

A 10 μ L volume of the pLcII-Fx-TnC (F29W) vector was digested (total volume of 50 μ L) with the restriction endonuclease Sty1 at 37°C for 1.5 hours. The DNA was extracted from the reaction mixture by adding a 60:40 mixture of phenol/chloroform, followed by a 100 μ L chloroform extract. The DNA was precipitated from the second extract by adding 0.1 volumes of 3M sodium acetate, pH 5.6, and 2x volume of 95% ethanol. The mixture was incubated for 1 hour followed by centrifugation at maximum speed for a minimum of 30 minutes. To prevent the vector from simply closing on itself in the next ligation step, the free ends of the vector DNA were dephosphorylated using the following procedure. The DNA pellet was dried briefly and resuspended in 25.5 μ L of ddH₂O. A 3 μ L aliquot of enzyme buffer plus 1.5 μ L of calf intestinal

phosphatase (Boehringer Mannheim) were added. The mixture was incubated at 50°C for a total of 2 hours with a second aliquot of enzyme added after 1 hour. The mixture was electrophoresed on a 1% agarose gel and the vector fragment gel extracted without further purification.

The 155 base pair Sty1 fragments isolated from each of the mutants listed above were then ligated into the prepared F29W vector. The ligation mixture was left overnight at room temperature. The ligation mixture was then precipitated as per section 2.5.4. and used to transform *E. coli* K12 electrocompetent cells.

2.9.2 Verification of Fragment Insertion Into the Expression Vector

A total of 24 colonies were selected to inoculate individual tubes of 2x TY A100 broth. Cultures were incubated at 37⁰ C for 7 hours after which time the cell pellets were collected by centrifugation. The plasmid DNA isolated from each cell pellet was treated with the restriction endonucleases BamH1 and Ava1 to verify the insertion of the Sty1 fragment. Correct insertion of the fragment was verified by visualization of a 524 base pair fragment on a 1% agarose gel.

Clones which carried an insert of the correct size were used to transform competent *E. coli* QY13 cells. While the above digest confirms insertion of the fragment it gives no information as to the orientation of the fragment. Cultures of each clone were grown and tested for protein expression. If the clone tested positive then the DNA for that clone was sequenced to verify the identity of the mutant and the integrity of the DNA sequence.

2.10 Protein Expression From the pLcII-Fx-TnC Mutants

2.10.1 Test for Expression

A 2mL culture was grown by inoculation with a single colony from a 36 hour plate of QY13 transformed with the plasmid DNA to be studied. After a 12 hour incubation at 30°C, a 1mL aliquot was drawn from the culture and heat shocked in a 42°C water bath for 10 minutes followed by a 2 hour incubation at 37°C in a shaker incubator. The cells were then harvested by centrifugation at 15,000 rpm for 10 minutes and resuspended in 50µL of TE buffer, pH 8.0, with 1 µL of 0.5mM PMSF. The cells were lysed by three cycles of freezing and thawing and then sonicated for 10 minutes in a bath sonicator (Branson Model B-32, SmithKline Co.). The suspension was centrifuged at 15,000 rpm for 12 minutes. Expression of fusion TnC was determined by sodium dodecyl sulfate polyacrylamide gel electrophoresis (SDS PAGE) of the cell supernatant fractions using laboratory stocks of Fusion TnC, prepared by G. Trigo-Gonzalez, as a standard.

2.10.2 Preparation of Large Scale Cultures

The remaining 1mL of culture not used for the test expression was used to inoculate 200 mL of 2xTY-Amp broth. This culture was incubated at 30°C to an O.D.₆₀₀ of 0.5 and used to inoculate 15L of 2xTY A100 broth in a Chemap 3000, 20L fermenter. The culture was incubated overnight with constant agitation and aeration until an O.D.₆₀₀ of 0.8 was reached. The temperature of the fermenter was raised to 42°C over a time period of 5 minutes and maintained for 10 minutes to induce expression of the cII-Fx-TnC gene. The temperature was then lowered to 37°C and incubated for a further 4 hours after which time the culture was cooled to 16°C. The cells were concentrated to a volume of 1 litre by means of a tangential flow filtration system fitted with three 0.45micron Pellicon cassette

filters (Millipore). A cell pellet was obtained by centrifugation at 4,500 rpm for 30 minutes at 4°C.

2.11 Purification of the Recombinant Proteins

2.11.1 Release of Fusion Troponin-C by Cell Lysis

The cell pellets collected from the fermenter were resuspended in 440mL of Buffer A. The addition of 15 μ L of a 100mM stock of Phenyl Methyl Sulfonyl Fluoride (PMSF) inhibited proteolysis. Lysozyme was used to lyse the cell wall; 960mg dissolved in 40 mL ddH₂O. The homogenate was incubated on ice for 30 minutes. A further 30 minute incubation on ice followed the addition of 4.8mL of a 1 mg/mL solution of DNase 1, 9.6mL of a 1.0M solution of MgCl₂, and 480mL of a 1.0M solution of MnCl₂. Following the addition of 2.4mL of 100mM PMSF, the homogenate was sonicated with three 20 second bursts at maximum power from a probe sonicator fitted with a medium sized probe (Fisher Sonic-Dismembrator, Model 300). The homogenate was stored on ice between exposures. The homogenate was centrifuged at 18,000 rpm for 30 minutes, at 4°C, in a Sorvall SS34 rotor to remove cell debris. The supernatant was stored at -70°C until ready for use.

2.11.2 Purification by Ion Exchange Chromatography

To one half of the supernatant obtained from the release of fusion troponin-C by cell lysis, 180 grams of urea (reagent grade) was added along with 375mL of Tris-HCl, 1M, pH7.5. The supernatant was placed in a 37°C water bath and stirred continuously until the urea dissolved. The container was removed from the water bath and 58.125mg of DTT (Sigma) was added.

Since troponin-C is an acidic protein, an anion exchange column was selected to purify the fusion protein. A 2.6 cm x 40 cm chromatography column

packed with 180mL of Q-Sepharose Fast Flow media (Pharmacia) was pre-washed with 500mL of degassed low salt Buffer B (85mM KCl). Once a baseline reading was achieved, the protein homogenate was loaded onto the column at a rate of 200mL per hour. Low salt Buffer B was used to wash the column until a baseline was observed. The fusion troponin-C was eluted with Buffer B using a salt gradient from 85mM to 1M KCl and monitored using a single path monitor, UV1, optical unit and control unit connected to a chart recorder (Pharmacia). Fractions corresponding to the peaks were tested for the presence of fusion troponin-C using SDS-Page. These fractions were pooled for further purification.

2.11.3 De-salting by Gel Filtration

To remove the urea from the protein, the pooled fractions were loaded on a 2.6 cm x 90 cm chromatography column packed with 500mL of G-25 Sephadex (Pharmacia) and pre-equilibrated with 0.1% TFA (in ddH₂O) at a flow rate of 85mL per hour. The column was then washed with 0.1% TFA to elute the protein which was collected in 10mL fractions. Protein fractions were confirmed by SDS PAGE. The fractions were pooled, lyophilized and stored at -20°C.

2.12 Preparation of Factor X_a

2.12.1. Isolation and Purification of Factor X

To 50L of fresh bovine blood 5L of anticoagulant solution was added. The mixture was centrifuged at 4,200 rpm for 15 minutes at 4°C using a GS3 Sorvall rotor to separate the plasma from the red blood cells. The plasma was centrifuged a second time for a better separation. To the isolated plasma, a 1M BaCl₂ solution was added. A volume equivalent to 0.087X the volume of plasma was sufficient to co-precipitate the vitamin K-dependent plasma proteins with the barium citrate produced on mixing. A 270mL aliquot of 100mM PMSF was

added. The mixture was centrifuged at 4,000 rpm for 15 minute at 4°C. The resulting protein pellet was washed several times with a barium citrate buffer to remove any red blood cells still present. The pellet was resuspended in 500mL of sodium citrate buffer. The slow addition of 2.2L of 1M sodium sulfate released the proteins by reprecipitating the barium ions as the less soluble barium sulfate. The solution was centrifuged at 4,200 rpm for 15 minutes. The supernatant was concentrated to 50 mL using a Minitan P-10 membrane. After dialyzing against ddH₂O overnight at 4°C, one half of the concentrate was loaded onto a 1.0cm x 50cm DEAE 6B CL Sepharose column (Pharmacia) with the DEAE buffer A. The second half was stored at -20°C until ready to use. Factor X was eluted with a 100mM to 600mM gradient of sodium citrate (DEAE buffers A and B).

SDS PAGE was used to identify the fractions containing Factor X. These fractions were pooled and concentrated to 50 mL using a Minitan apparatus (Millipore). A 2.5cm x 100cm G-50 Sephadex column was used at a flow rate of 50 mL/hr, to exchange the citrate buffer with 50mM Tris-HCl, pH 8.0.

2.12.2. Preparation of CNBr-Sepharose 4B Column

To prepare the CNBr Sepharose 4B column, 4g of resin (Pharmacia) was weighed out. It was washed with 1mM HCl, and then swelled in a fresh solution of 1mM HCL for 30 minutes. The resin was then washed with ddH₂O until the pH was approximately 5.5 and then swelled in 0.1M NaHCO₃ pH 8.3 for 30 minutes.

Approximately 40mg of Russel's viper venom (Sigma) was dissolved in 20mL of 0.1M NaHCO₃, pH 8.3. The washed and swelled CNBr Sepharose 4B resin was added and left to mix, very gently, overnight at 4°C. A solution of 0.2M Tris-HCl, pH 8.6, was used to block excess reactive groups. After washing the resin with 50mM Tris-HCl, pH 8.0 a 1.0cm x 10cm column was packed.

2.12.3 Activation of Factor X

The protein obtained from the G-50 column was concentrated to 15mL using an Amicon filtration apparatus. The concentrate was then circulated through the CNBr column for 22 hours at room temperature to obtain the active form of the enzyme. Factor X_a was eluted from the column using 50mM Tris-HCl, pH 8.0.

2.12.4 Assay of Factor X_a

A 3mM solution of substrate (N-benzoyl-Ile-Glu-Gly-Arg-p-nitro-anilide, acetate salt) (Sigma) was prepared by dissolving 5 mg in 2.5mL of ddH₂O. An absorbance of $E_{316nm}^{mM} = 13$ in H₂O was used to calculate an accurate concentration and diluted to 3mM. The solution was kept frozen at -20°C until ready to use. The level of activity of Factor X_a was measured by mixing 2.5 μ L of Factor X_a from the column and 100mL substrate with 400mL of Assay buffer. The O.D.₄₀₅ was followed for approx. 10 minutes. All spectra were recorded on a Beckman Du-600 spectrophotometer.

2.13 Preparation of Recombinant Proteins for Spectroscopic Analysis

2.13.1 Factor X_a Digestion of Fusion Troponin-C

The conditions for the digestion of each preparation of fusion protein by Factor X_a were determined empirically. In general, a 50mg sample of fusion TnC was resuspended in 10mL of Factor X_a buffer. The troponin-C fusion protein was digested by incubating the protein with Factor X_a for 12 hours at room temperature, using a 1000:1 weight ratio (cII-TnC:Factor X_a). Complete digestion was confirmed by SDS PAGE.

2.13.2 Purification of Digested Proteins by FPLC

Troponin-C was purified after digestion with Factor X_a by anion exchange chromatography on a Pharmacia FPLC system equipped with a Waters Protein-Pak™ Q 8HR column (Millipore). Troponin-C was eluted in a 40 minute linear gradient with Buffer C using a salt gradient from 200mM to 1M NaCl. Pure fractions of TnC were identified by SDS PAGE and pooled for dialysis.

2.13.3 Dialysis of Proteins

Pure TnC fractions of each mutant protein were dialyzed against four 1 litre changes of Chelex buffer with 1mM EGTA added. Proteins to be used for flow dialysis studies were dialyzed against a further four 1litre changes of Chelex buffer without EGTA. In each case, all proteins to be studied by a common method were dialyzed together.

2.13.4 Quantitation of Proteins

Protein concentrations of the dialyzed proteins were measured using the Lowry method of protein determination. Proteins were diluted with the appropriate Chelex buffer to obtain a final concentration of 45μM.

2.14 Metal Binding Properties of Proteins

2.14.1 Spectroscopic Analysis of Purified Proteins

2.14.1.1 Fluorescence Spectroscopy

Fluorescence spectra of calcium titrations were recorded using a 4800 SLM Aminco Fluorometer equipped with a thermostated cell assembly interfaced with an IBM P.C.. Titrations were performed at 21+/- 1°C in a 1 cm square quartz cuvette (O.D.280 < 0.05). Protein stock solutions were diluted to 5μm with Chelex buffer with 1mM EGTA. A volume of 1,800 μΛ of each protein solution

was equilibrated to 21°C with constant stirring until a steady voltage reading was obtained. The excitation wavelength was set at 278nm for all titrations. Emission spectra were recorded from 300nm to 420nm. The fluorescence was titrated by the addition of Ca²⁺ stock solutions in 1mL increments using a 10mL Hamilton syringe.

2.14.1.2 Circular Dichroism Spectroscopy

Circular Dichroism (CD) spectra of the calcium free and the calcium saturated proteins were recorded on a Jasco J700 spectropolarimeter equipped with a thermostated cell assembly interfaced with an IBM P.C.. Spectra were obtained in a quartz cuvette with a 1.0mm path length. Ellipticities were measured at a 10nm/min scan speed, 1.0nm band width, with a 4 second response time and a 0.1 nm step resolution. Protein solutions were all diluted to 5mM in a final volume of 1.8mL and equilibrated to 21°C prior to scanning. Two scans were taken for each measurement.

2.14.1.3 Flow Dialysis

Flow dialysis was used to confirm the presence of four functional binding sites in the valine mutants of TnC. The apparatus design was adapted from Colowick and Womack and manufactured by in-house machine shop staff. The unit consisted of two chambers (Figure 2.4) separated by a dialysis membrane disc with a molecular weight cutoff of 6-8,000 (Spectra/Por), making it permeable to calcium but impermeable to TnC. The upper chamber held 500µL of a 28µM solution (determined by the Lowry Method) of the calcium free protein to be studied. The lower chamber volume was 150µL. The buffer flowing through the lower chamber was the same as that in the upper chamber minus the protein. The minimum buffer flow rate was set at 4x the lower

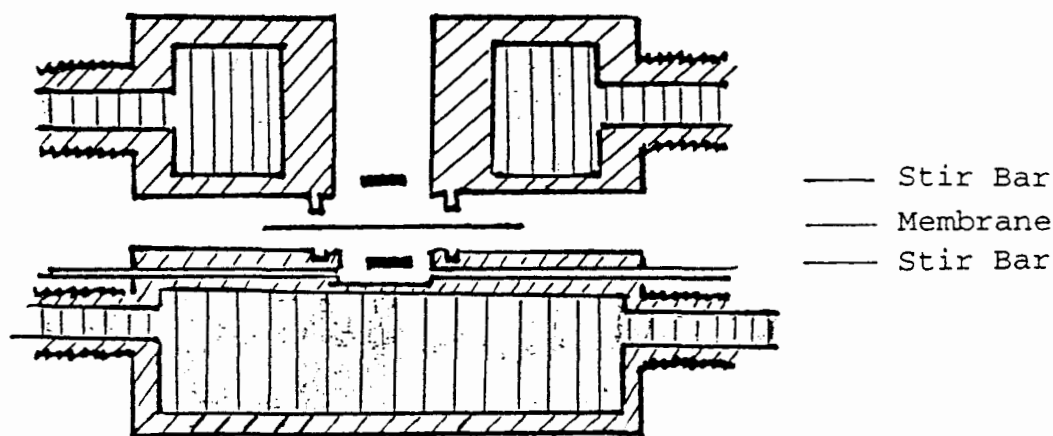




FIGURE 2.4. Flow Dialysis Apparatus

The flow dialysis apparatus was adapted from diagrams of a similar unit designed by Colowick and Womack. The unit was made of plexiglass () and included a water jacket surrounding the sample chamber and buffer chamber (). The upper chamber is 8mm in diameter with a volume capacity of 650 μ L. The lower chamber is a well, instead of a spiral groove, which is 8mm in diameter by 3mm in height. Magnetic stir bars, 2mm in length, were sealed in glass to minimize the damage to the dialysis membrane held taught between the two chambers by means of a groove. The two halves of the apparatus are held together by four stainless steel screws enabling easy decontamination of the two wells after each experiment. Removable stainless steel needles project into the the sides of the lower chamber for continuous flow of buffer through the chamber. A peristaltic pump was used to maintain a constant flow rate.

chamber volume (600 μ L) to achieve rapid equilibration to a steady state flow of calcium from the upper chamber to the lower chamber. At this flow rate steady state was achieved within 2 minutes of pulsing the system with calcium.

Initially, the rate of dialysis of $^{45}\text{Ca}^{2+}$ across the dialysis membrane in the absence of protein was measured to show that the change in rate of dialysis was not due to a change in viscosity on adding unlabelled calcium nor due to an increase in pore size due to stretching. Unlabelled Ca^{2+} was added to the upper chamber in measured aliquots. The isotope concentration in the effluent was measured to confirm that there was no change in the rate of dialysis of the labelled calcium.

For each experiment a 500 μ L aliquot of the protein to be studied was added to the upper chamber. Prior to adding the radiolabelled calcium to the upper chamber, the calcium free buffer was pumped through the lower chamber for one half hour. A sample of the effluent was collected to measure the background cpm value on a scintillation counter (Beckman). A 5mL aliquot of the radiolabelled calcium (0.121 $\mu\text{g}/\mu\text{L}$) (Amersham) was added to the upper chamber. After mixing for 2 minutes, a 5 μ L aliquot of the protein solution was drawn off to obtain an initial value of the counts per minute for the total amount of radiolabel added. In the presence of protein, the binding of the radiolabelled calcium reduced the steady-state value of $^{45}\text{Ca}^{2+}$ in the effluent compared to the value obtained without protein present in the upper chamber. The steady state concentration of labelled calcium in the effluent was measured with a scintillation counter and taken as a measure of the fraction of free calcium in the upper chamber. The system was pulsed with 3 μ L of unlabelled calcium at 4 minute intervals. Fractions were collected every 2 minutes. Unlabelled calcium was added to the system to titrate from .4x to 1.2x the concentration of available binding sites assuming 4 moles/mole of protein. An excess of unlabelled

calcium was added in a final pulse of 10 μ L of 1M calcium to obtain a maximum value for the rate of dialysis. This excess ensured that there was essentially no labelled calcium-bound to the protein. Data was processed according to Porumb (1994), where:

$$[\text{Ca}^{2+}]_{\text{free}} = [\text{Ca}^{2+}]_{\text{total}} \times \text{cpm}_i / \text{cpm}_{\text{final}} \times \text{Final vol.} / \text{Vol}_i \quad (9)$$

The total calcium in the above equation includes both labelled and unlabelled calcium corrected for dilution with each additional aliquot. The counts per minute were corrected for volume effects by taking the ratio of the volumes. Calcium-bound was easily calculated since the total calcium is known. The total calcium bound was then divided by the protein concentration to give the number of binding sites.

2.14.1.4 Stopped Flow Fluorescence Spectroscopy

The rates at which calcium is released from loops I and II were measured for the 54X mutant proteins using the method of stopped-flow with a single mixing. Emission spectra were recorded at 335nm on a Sequential Stopped-Flow Spectrofluorimeter from Applied Photophysics, equipped with a thermostated cell assembly interfaced to an Acorn 5000 with a RISC Operating System. Protein samples were diluted to 5 μ M and equilibrated to 21 $^{\circ}$ C +/- .1 $^{\circ}$ C prior to scanning. Excitation wavelength was set at 278nm. Initial scans were carried out at 5 μ M protein, 1mM [Ca²⁺] and 10mM EGTA. To verify that the rates were not dependent of the concentration of one of the starting materials, the calcium ion concentration was decreased to 0.5mM followed by a decrease in the EGTA concentration to 5mM. A last set of measurements were made at 2.5 μ M protein.

2.15 Unfolding of Proteins Using Urea as the Denaturant

2.15.1 Steady State Fluorescence Spectroscopy

Urea denaturation of the F105W/130X proteins (where X= D, G, I, N, S, T, or V) and F29W/54X proteins (where X= A, G, S, T or V) was monitored using steady state fluorescence spectroscopy. The excitation wavelength was set at 278nm with emission data recorded at 335nm for F29W proteins and 355nm for F105W proteins. Fluorescence spectra were recorded using a 4800 SLM Aminco Fluorometer equipped with a thermostated cell assembly interfaced with an IBM P.C.. Protein solutions were dialyzed against 4 changes of a calcium-free MOPS buffer which had been passed over a Chelex column. All proteins were dialyzed in the same buffer solution to standardize starting calcium concentrations. Protein concentrations were measured after dialysis using the Lowry method of protein determination.

2.15.1.1 Preparation of Urea Stock Solutions

Ultrapure urea (BRL) was used to prepare a series of 57 urea solutions ranging from 0.1M to 8M in concentration. A total volume of 100mL of each was prepared, divided into 10mL aliquots and flash frozen. The solutions were stored at -20°C to minimize the formation of ammonium cyanate. Chelex was added to each 10 mL fraction of urea before withdrawing an aliquot for addition to the protein solutions.

2.15.1.2 Procedure for Denaturation of Proteins

Fifty seven 200µL aliquots of protein, were dispensed into 2mL centrifuge tubes which were acid washed and well rinsed with ddH₂O. To each sample, 1,600µL of a stock urea solution was added. Before the fluorescence was recorded, the samples were left at 21°C for 1 hour allowing the reaction to reach

equilibrium. Prior to measuring the fluorescence, each sample was sparged with helium for 20 seconds. Each recorded measurement was the average of 50 readings.

2.15.2 Circular Dichroism Spectroscopy

Circular Dichroism (CD) spectra of the protein/urea solutions were recorded on a Jasco J700 spectropolarimeter equipped with a thermostated cell assembly interfaced with an IBM P.C.. Spectra were obtained in a quartz cuvette with a 1.0mm path length. Ellipticities were measured at a 10nm/min scan speed, 1.0nm band width, with a 4 second response time and a 0.1 nm step resolution. Protein/urea solutions were scanned immediately after fluorescence data was recorded. All solutions equilibrated to 21°C prior to scanning. Samples were re-scanned 24 hours later to verify that equilibrium had been reached prior to the first scan. Two additional mutant proteins, F105W/54G and F105W/54V, were studied by CD to determine the effect of the placement of the tryptophan probe on the secondary structure as the protein unfolded.

2.16 Preparation of Antibodies and Immunoblotting of Troponin C

2.16.1 Immunization of Rabbits

Antibodies were raised against cII-F_x-troponin-C by subcutaneously injecting a rabbit with a 1mg/mL sample of F105W/ I130 fusion troponin-C purified on an FPLC column. The purified fusion protein appeared as a single band on an SDS PAGE stained with Coomassie Blue. The purified fusion protein was combined with Freund's incomplete adjuvant to aid in triggering an immune response to the antigen. Injections were carried out bi-weekly over a period of 3 months. Approximately 120 mL of blood was collected from each of two rabbits over the same period of time.

2.16.2 Isolation of Rabbit Anti-cII-TnC Immunoglobulin G

The blood from each rabbit was incubated at 37°C for 1 hour and then centrifuged at 10,000 rpm for 15 minutes. To 120mL of antiserum, 60mL of saturated ammonium sulfate (SAS) was added dropwise with constant mixing at 4°C. The precipitate was allowed to form over 6 hours. The pellet was centrifuged for 12,000rpm for 20 minutes. The pellet was washed by vortexing in 120mL of cold 33% SAS solution and centrifuged again. The wash procedure was repeated. The pellet was dissolved in 10mL of IgG low salt buffer and dialyzed over 48 hours at 4°C using a membrane (Spectra/Por) with a molecular weight cutoff of 12,000 to 14,000. To fully remove the ammonium sulfate, three-4 liter changes of buffer were used. The dialysate was loaded onto a 10cm, Waters Protein-Pak 8HR Q AP-1, column which was prewashed with IgG low salt buffer. After loading, the column was washed with IgG low salt buffer until a baseline was achieved. The IgG was eluted using a step-wise gradient from 20mM NaCl to 1M NaCl. The IgG proteins eluted between 10% and 20% IgG high salt buffer at a flow rate of 2 mL min⁻¹.

2.16.3 SDS PAGE Identification of IgG Fraction

Fractions were identified by SDS PAGE. The IgG heavy and light chains will run separately with molecular weights of 50,000 and 25,000 respectively.

2.16.4 Enzyme Linked Immunosorbant Assay of FPLC Fractions

Purified fusion troponin-C, chicken skeletal TnC and rabbit TnC were used to coat ELISA plates. Each well of the plate was loaded with 100µL of one of the stock protein solutions diluted in PBS buffer. The plates were incubated overnight at 4°C. Excess protein was then removed by washing the plates with distilled water. The uncoated regions of the plate were blocked with 200µL of

PBS/TWEEN buffer containing 1% (w/v) ovalbumin. The plates were incubated at 37°C for 1 hour and then washed with distilled water. The purified IgG fraction was diluted 1/500, 1/1000 and 1/3000 with PBS/TWEEN/0.5% (w/v) ovalbumin. The plates were incubated for a further 2 hours at 37°C. Following a thorough wash with distilled water, 100µL of goat anti-rabbit serum conjugated to horseradish peroxidase diluted by 1/4000 in PBS/TWEEN/0.5%(w/v) ovalbumin, was added to each well. Following a 2 hour incubation at 37°C and a wash with distilled water, the antibodies were detected by colour development. The substrate consisted of 10mL of 0.1M sodium acetate to which 10mg of O-phenylenediamine and 10µL of 30% H₂O₂ were added. Aliquots of 100µL were added to each well. The colour was allowed to develop for 10 to 30 minutes and stopped by the addition of 50µL of 1M H₂SO₄. The plates were read at A_{490nm} on a EL321e Bio-Kinetics Microplate reader (Bio-Tek Instruments, Inc.).

2.16.5 Immunoblotting of Proteins

The protein samples were electrophoresed on SDS denaturing gels composed of 12% polyacrylamide. Proteins were blotted onto an Immobilon-P filter (polyvinylidene fluoride) washed with methanol, rinsed with ddH₂O and soaked in transfer buffer prior to use. Electoblotting was performed using a (Model) transfer apparatus. The transfer was achieved at 1.2mA cm⁻² for 2 hours. The filters were blocked with BLOTTO either overnight at 4°C or for 2 hours at room temperature on a shaker table. The filters were transferred to 30mL of fresh BLOTTO to which 40µL of purified IgG was added. After an hour, a 15 minute wash with TBS/TWEEN was performed followed by two-5 minute washes. The remaining steps were performed in hybridization bottles to reduce the volumes of 2°antibody required. To each bottle 10mL of TBS/TWEEN was added with 10µL of goat anti-rabbit IgG, conjugated to horseradish peroxidase.

The mixture was placed in a hybridization chamber set at room temperature for 1 hour. The filters were then repeatedly washed with TBS/TWEEN before developing using the ECL kit by Amersham. This system uses the HRP/hydrogen peroxide catalyzed oxidation of luminol in alkaline conditions. The maximum light emission is at a wavelength of 428nm which can be detected by a short exposure to blue-light sensitive autoradiography film (Hyperfilm ECL - Amersham).

3. RESULTS

3.1 Cloning of the Troponin C Gene into pUC18

In order to prepare N-cap mutants of the low affinity domain, it was necessary to subclone the gene for TnC into pUC18, a vector for which there already existed a reverse primer for PCR mutagenesis.

The restriction digest of the pLcII-Fx-TnC (F105W) vector with the enzymes Nde1 and Xba1 produced two DNA fragments: one of 900 base pairs and the other 2450 base pairs in length. A digest of the two fragments with BamH1 identified the fragment carrying the gene for TnC as the larger of the two. The fragment carrying the gene for TnC was ligated into pUC18 (Figure 3.1). Two strains of *E. coli*, K12 and DH5 α , were transformed with an aliquot of the ligation mixture. Plasmid DNA was isolated from each of the two strains. The restriction enzyme BamH1 was used to determine if the gene for TnC was present on the plasmid. The plasmid DNA from K12 consistently generated a gene fragment of the correct size and a remaining vector fragment of the same size. The vector fragments and the DNA fragments from the DH5 α strain were of various sizes (Figure 3.2).

3.2 PCR Mutagenesis

3.2.1 Primer Extension

The gene for fusion TnC inserted in pUC18 was amplified with 30 cycles of the polymerase chain reaction using the cII forward primer and the pUC18 reverse primer and an annealing temperature of 48°C. The reaction mixture was electrophoresed on a 1% agarose gel revealing a single band of approximately 900 base pairs in length. Annealing temperatures of 51°C and 53°C gave no product.

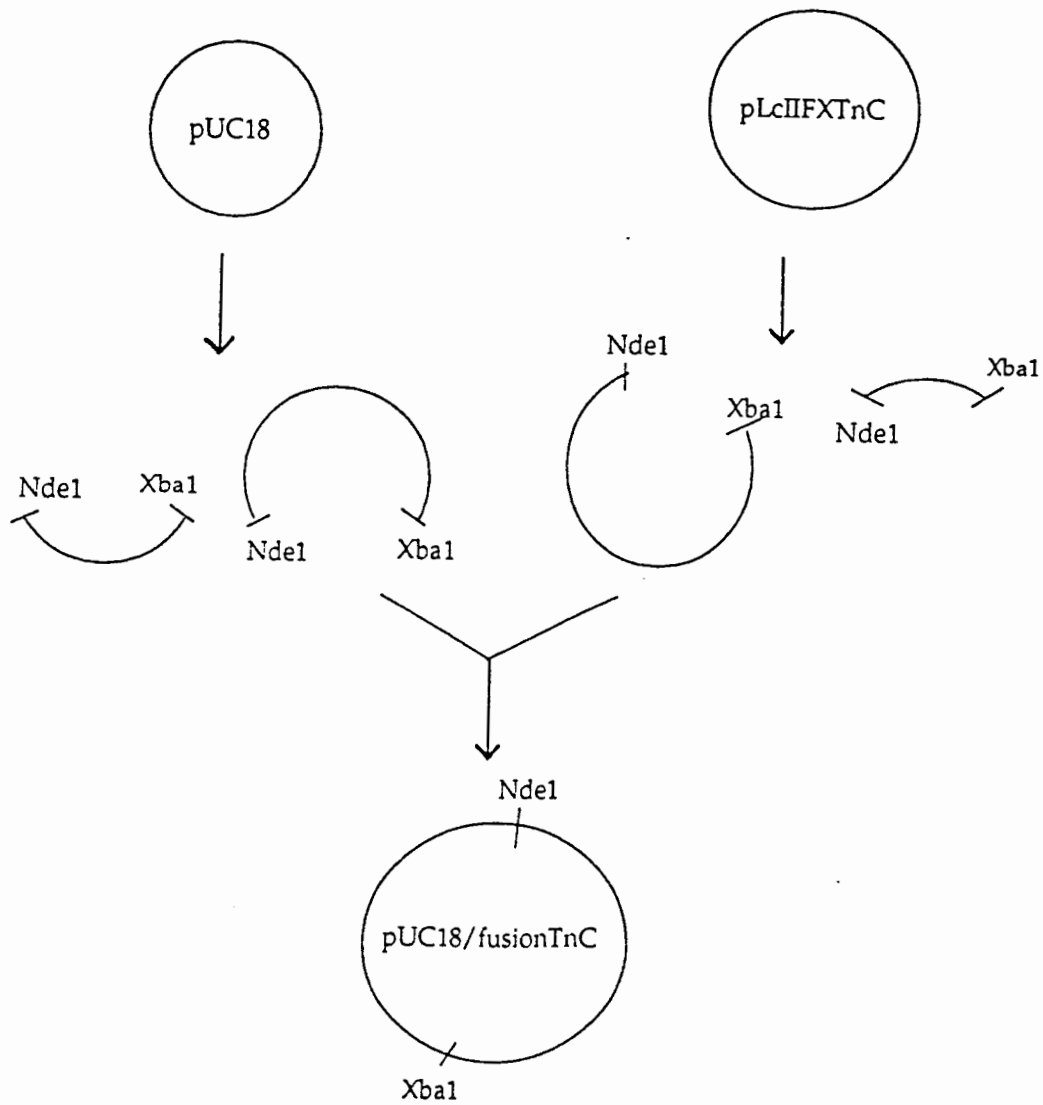


FIGURE 3.1. Cloning the Gene for Troponin C From the pLcII Vector Into the pUC18 Vector.

The Figure illustrates the enzymes used to remove the fragment carrying the gene for TnC from the pLcII-Fx-TnC vector for ligation into the pUC 18 vector to create a new vector for use in PCR mutagenesis.

FIGURE 3.2. Ligation of Fusion TnC Gene into pUC18

A restriction digest with BamH1 resulted in a DNA fragment 800bp in size, if the gene for fusion TnC was successfully ligated into pUC18. The digested DNA was electrophoresed on a 1% agarose gel. Lane 1: uncut plasmid DNA from DH5 α . Lane 2 to 6: Plasmid DNA from the ligation of the 2640 bp fragment into pUC18, isolated from DH5 α and digested with BamH1. Lane 7: 1 Kb DNA Ladder (BRL). Lane 8: uncut plasmid DNA from K12. Lane 9 to 12: Plasmid DNA from the ligation of the 2640bp fragment into pUC18 isolated from K12 and digested with BamH1. Lane 13 to 14: 2 samples of digested plasmid DNA from the ligation of the 900bp fragment (section 3.1) into pUC18.



PCR reactions with the AXC primer and pUC18 reverse primer produced a single large band of 600 base pairs in length, with an annealing temperature of 45°C. At 42°C other bands were observed while at 48°C a single but fainter band of the appropriate size was observed. PCR reactions with the GXC primer and the pUC18 reverse primer generated a single band of 600 base pairs with an annealing temperature of 45°C and 2 bands at 48°C, one of which was the appropriate size (Figure 3.3). Each 600 base pair fragment was gel extracted and labelled as the "new AXC or GXC mutant primer" for use as reverse primers in subsequent PCR reactions.

Primer extension was attempted in order to synthesize a full length gene product using the cII primer and the "new" mutant primers. The procedure was unsuccessful using the linearized construct of pUC18/fusion TnC as a template. The only DNA product obtained was 1,500 base pairs in length. When the gene for TnC, generated with the cII forward primer and the pUC18 reverse primer, was used by itself as a template, a DNA fragment of approximately 850 base pairs in length was obtained (Figure 3.3). This primer extension product was gel purified and then amplified using the cII forward primer and pUC18 reverse primer. A sample of the amplified product was digested with Xba1 and BstX1 in a double digest, and visualized on a 1% agarose gel (Figure 3.4). The expected fragment pattern for TnC was observed. An aliquot of each primer extension product was then treated with the restriction endonucleases Xba1 and BamH1 in preparation for ligation into the F105W - pLcII-Fx-TnC vector digested in the same way. Plasmid DNA isolated from *E. coli* bacteria (K12 strain) transformed with the ligation mixture was screened using restriction digests. Since the AXC primer included the wild type sequence ACC, a large number of clones were expected to be wild type. Of the 486 clones screened by restriction digest (Figure 3.5), 133 were tested for protein expression by transforming competent cells of

**FIGURE 3.3. Agarose Gel Electrophoresis of the Primer Extension PCR
Mutagenesis Products**

Gel A

Lane 1, 2 and 4: PCR product using the AXC primer and pUC18 reverse primer at 42°C, 45°C and 48°C respectively. Lane 3: 1 Kb ladder (BRL). Lane 5 to 7: PCR product using GXC primer and pUC18 reverse primer at 51°C and 54°C.

Gel B

Lane 1 and 2: Amplified "wild type" fusion TnC using the cII primer and the pUC18 reverse primer. Lane 3: 1 Kb DNA Ladder (BRL). Lane 4 and 5: "new mutant AXC primer" and cII primer were used to synthesize the full length gene for TnC at 53°C and 55°C respectively. Lane 6: Amplification of AXC mutant fusion TnC using cII primer and pUC18 reverse primer.

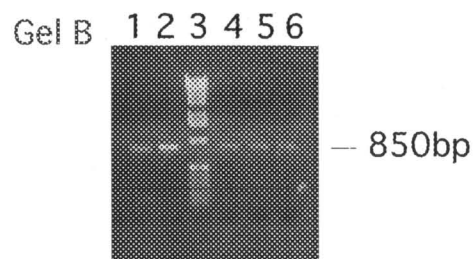
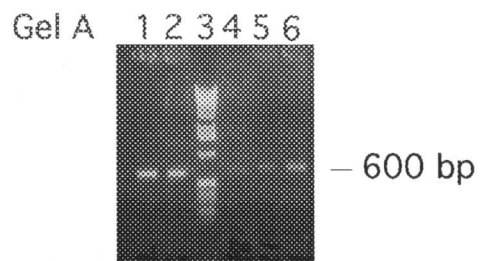


FIGURE 3.4. Agarose Gel Electrophoresis of the Restriction Digests of PCR Products.

The GXC primer extension product obtained at 48°C, shown in lane 1, was digested with Xba1 and BstX1 as shown in lane 2. Samples of the "wild-type" fusion TnC DNA before and after digestion with the same enzymes are shown for comparison in lanes 4 and 5 respectively.

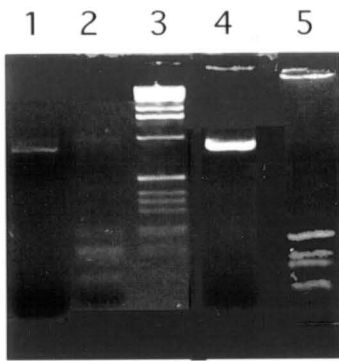
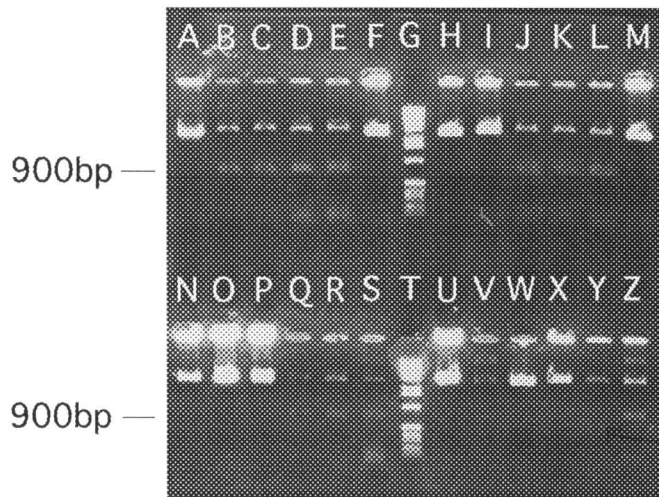


FIGURE 3.5. Identification of Potential Mutant Clones Using Restriction Digests Followed by Agarose Gel Electrophoresis.

Lanes G and T are the 1 Kb DNA Ladder (BRL). The remaining lanes are samples of plasmid DNA digested with EcoR1 and BamH1 in a double digest. Lanes B to E, J to L, Q to S, V, Y and Z show a DNA fragment of about 900bp expected when the gene for TnC is present within the plasmid. These 13 clones were tested for protein expression (Figure 3.6).



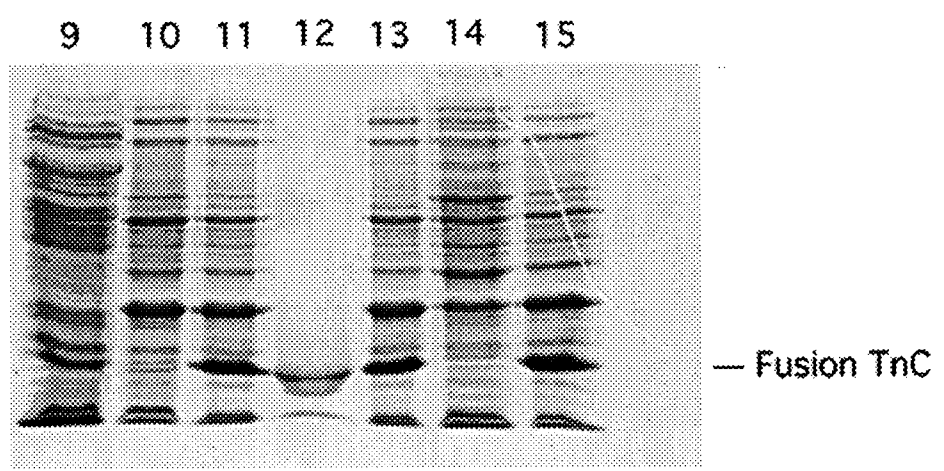
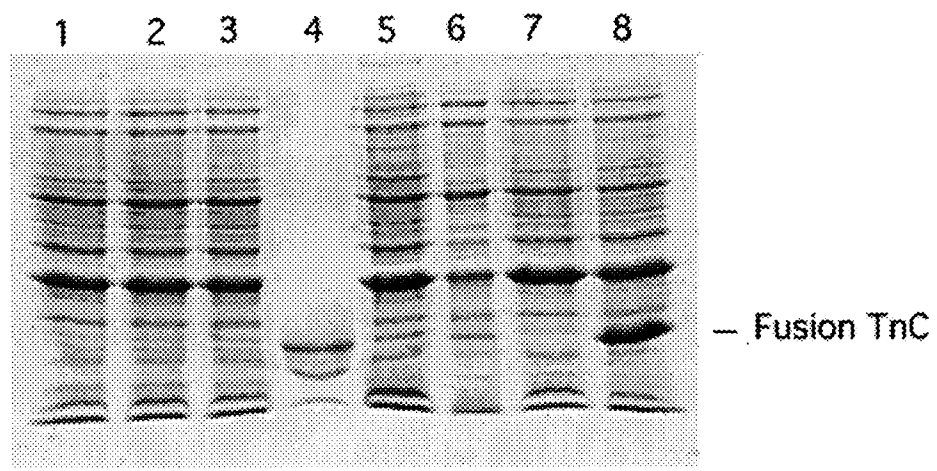
the QY13 strain of *E. coli* (Figure 3.6). A total of 130 clones over-expressed protein of the appropriate size as visualized by SDS-PAGE. The plasmid DNA from each of these clones was purified for sequencing. Only 3 of the clones were found to be mutants: 1 glycine, 1 serine and 1 alanine. Some of the clones which did not express protein were sequenced. There were 3 more alanine clones but a single base was missing at the junction between the fragment and the vector producing a frameshift in the sequence which resulted in the loss of protein expression. With the large number of wild type clones observed, it was decided to design a new AXC primer mixture which did not include the wild type (ACC) sequence. Since serine was also isolated, the AGC sequence was no longer required either. The primer was renamed AXC2. A GXC2 primer was designed which did not include the sequence for glycine or alanine in the mixture. An alternate method for obtaining mutant clones with the new primers was attempted along with primer extension. A product of 1500 base pairs in length using primer extension predominated. A restriction digest of the fragment with BamH1 showed it did not include the gene for TnC.

3.2.2 Triple Ligations

A very low rate of transformation was observed with the ligation mixture from the triple ligations of PCR products into the F29W - pLcII vector. Using all of the ligation mixture of the AXC2 and GXC2 mutant fragments, a total of 92 colonies were screened. The only mutant clone which expressed protein was sequenced and found to have a valine residue at position 54. Eleven other clones were randomly selected for sequencing as well. These clones were missing one of the two PCR fragments. Since few colonies were isolated from triple ligations, the mutant fragments generated by the GXC primer were used in separate transformation experiments in an attempt to isolate an Asp mutant.

FIGURE 3.6. SDS -PAGE of the Protein Expression Test.

The cell lysate of the transformed cultures grown to test for expression of fusion TnC were loaded onto an SDS-PAGE gel. Lanes 4 and 12 were samples of a standard of fusion TnC. Lane 8, 11, 13 and 15 show over-expression of a protein of the appropriate size. The plasmid DNA from these four clones was sequenced. The clone in lane 8 was expressing mutant TnC with a glycine residue at position 54. The other clones were expressing the wild type protein with a threonine residue at position 54.



3.2.3 Analysis of Clones From the PCR Amplification of Triple Ligations

Because of low transformation efficiencies using the CaCl₂ method of preparing competent cells, electroporation was used. Seventy two clones were randomly selected for the preparation of plasmid DNA, an aliquot of which was digested with the two restriction endonucleases BamH1 and EcoR1. There were 19 colonies which did not have an insert of the correct size. The remaining clones were tested for protein expression in the QY13 strain. Only 17 of these tested positive for protein expression. Sequencing identified these to be 2 glycine mutants and 1 alanine mutant. The rest were wild type DNA. A few non-expressing clones were also sequenced for diagnostic purposes since the insert was apparently the correct size. Four bases were found to be missing in the sequence at the junction between the two PCR fragments.

3.2.4 Analysis of Clones From the PCR Amplification of Blunt End Ligations

Transformation of electrocompetent cells was required to obtain colonies from this ligation mixture. A total of 104 colonies were obtained. Of these, 15 were discarded on the basis of restriction digests. The only mutant clones identified were three valines and a glycine. Once again there was a high background of wild type colonies.

3.2.5 Analysis of Clones From Blunt End Ligation of PCR Fragments Into pUC18

For this experiment only mutant fragments generated from the AXC2 and GXC2 primers were used. Three hundred colonies were randomly selected from which plasmid DNA was analyzed by restriction digest with BamH1 and Ava1. The double digest identified 7 clones with the cII fragment inserted in the wrong orientation relative to the mutant fragment, 5 clones with 2 cII fragments,

20 colonies with only mutant fragments and 8 colonies with both fragments in the correct orientation to give a DNA insert of 524 base pairs in length (Figure 3.7). The remaining clones were linearized due to the BamH1 site in the polylinker of pUC18. (The Ava1 site in the polylinker was destroyed by the Sma1 digest.)

The 524 base pair fragment from each of the eight clones described above was ligated into pLcII-Fx-TnC prepared with the same restriction endonucleases. Protein expression tests showed 3 clones over-expressed a protein smaller than expected. The remaining tested positive for protein expression and were sequenced. All of these clones had the wild type sequence with a threonine at position 54. The occurrence of the wild type clones even in this experiment was explained when the mutant PCR fragment was sequenced directly from the PCR reaction mixture to reveal the wild type sequence with a threonine residue at position 54 was being synthesized.

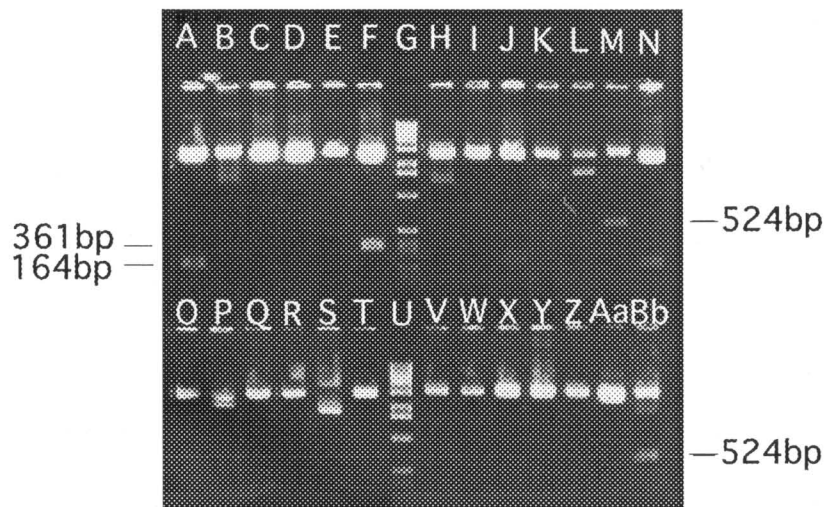
3.3 Preparation of pLcII-Fx-TnC (F29W) Expression Vector

Primer extension was unsuccessful in generating the F29W/T54X mutants. The transfer of the 155 base pair Sty1 DNA fragments from the F105W/T54A/G/S vectors to the F29W vector were all performed successfully. Sequencing of each F29W construct was performed and confirmed the integrity of the junction points.

3.4 Expression and Purification of the Fusion Mutant Proteins

The following mutant fusion proteins were successfully expressed in the *E. coli* QY13 strain: F29W/T54A, F29W/T54G, F29W/T54S, F29W/54T, F29W/T54V, F105W/130D, F105W/130G, F105W/130I, F105W/130N, F105W/130S, F105W/130T, and F105W/130V. The cell pellets collected from the

FIGURE 3.7. Analysis of the Blunt End Ligation of PCR Fragments Into pUC18
Agarose gel of 26 clones screened with an *Ava*1/*Bam*H1 double restriction digest. Lanes G and U are the 1Kb DNA Ladder (BRL). Lanes M and Bb reveal the presence of a 524 base pair fragment which can only be obtained if the two PCR fragments are ligated into pUC18 in the correct orientation. Both of these clones were sequenced and found to be the wild type sequence with a threonine residue at position 54.



15L fermenter cultures (section 2.10.2) were lysed (section 2.11.1). One quarter of the cell lysate was loaded on a Q-sepharose column as per section 2.11.2. Since TnC is negatively charged at a pH of 6.95, the protein could be purified on the anion exchange column using a salt gradient to elute the protein. An elution profile is shown in Figure 3.8. Fractions which contained TnC were identified using SDS-PAGE (Figure 3.9). Those fractions were pooled and desalted on a G-25 gel filtration column (Figure 3.10). The fractions which contained the protein were pooled and freeze-dried. An average of 200mg of fusion protein was obtained from each quarter of the cell lysate. The proteins were digested with Factor X_a (2μg/μL), using a 800:1 (w:w) ratio of TnC to Factor X_a, before being purified any further.

3.5 Preparation of Factor X_a

3.5.1 Isolation and Purification of Factor X_a

The vitamin K-dependent plasma proteins were successfully precipitated and loaded onto a DEAE Sepharose CL-6B column (section 2.12.2). Factor X was purified from the mixture of plasma proteins by eluting with a salt gradient of sodium citrate. Figure 3.11 shows the chromatogram of the fractions eluted from the column. The fractions which contained Factor X were identified by SDS-PAGE (Figure 3.12). Disulfide bridges which covalently link the 2 chains of Factor X were reduced by the β-mercaptoethanol in the Laemmli loading buffer. This produced two bands, representing the 2 chains, in each lane containing Factor X: one of 16,900D and one of 42,100D. Fractions 87 to 101 were pooled and passed through a G-50 Sephadex column to exchange the citrate buffer with Tris buffer (pH 8.0). Figure 3.13 is a chromatogram from the gel filtration column and shows that Factor X eluted as a single peak.

3.5.2 Activation of Factor X_a

The Factor X obtained from the G-50 column was successfully activated by circulating it through the CNBr Sepharose 4B -activated Russel viper venom column for 22 hours. A 500 μ L aliquot was withdrawn and the protein concentration was measured spectrophotometrically. An aliquot of this sample was diluted with 50mM Tris-HCl, pH 8.0, to obtain a 1mg/mL solution of Factor X_a. The specific activity was calculated to be 1.3 Δ O.D.₄₀₅/min/mg F_{xa}. The remaining Factor X_a was eluted from the column and stored at -20°C until ready to use.

3.6 Preparation and Purification of the Troponin C Mutant Proteins

Fusion TnC proteins were digested with Factor X_a as per section 2.13.1 to obtain the TnC mutant proteins used in all subsequent studies. Completion of digestion by Factor X_a was confirmed by SDS-PAGE (Figure 3.14). The pre-digested sample was seen to migrate with a purified sample of fusion TnC obtained from G. Trigo. The digested sample was seen to migrate with a stock sample of pure TnC. After digestion of the fusion mutant proteins with Factor X_a, the TnC mutant proteins were purified by FPLC. TnC eluted as a single peak at a NaCl concentration between 0.40M and 0.44M (Figure 3.15). Pure fractions of troponin C were identified by SDS-PAGE (Figure 3.16). In samples where digestion was not complete it was observed that the undigested fusion protein eluted before TnC which can be attributed to an additional 5 positively charged residues associated with the fusion portion of the protein.

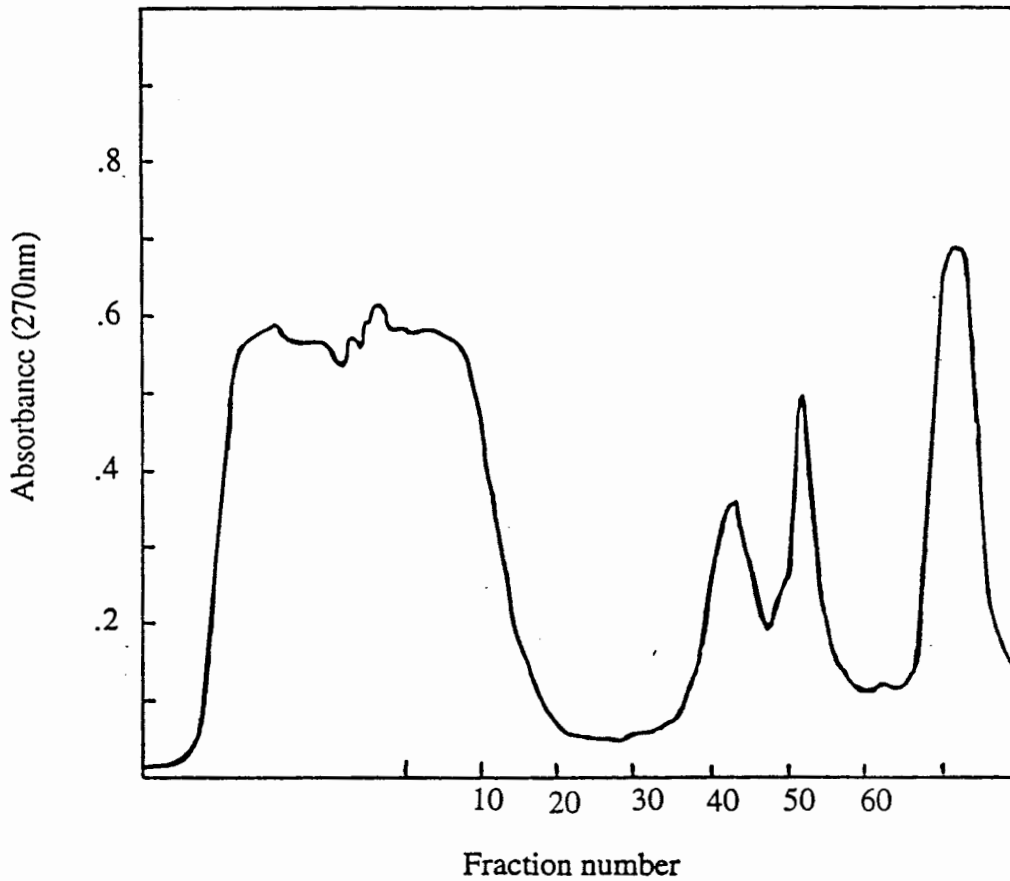


FIGURE 3.8. Anion Exchange Chromatography of Cell Lysate

The Figure represents a chromatogram of a sample of cell lysate eluted from a Q-Sepharose anion exchange column using a KCl gradient from 200mM to 1M. Fusion TnC was eluted in fractions 49 to 55 as identified by SDS-PAGE (Figure 3. 9).

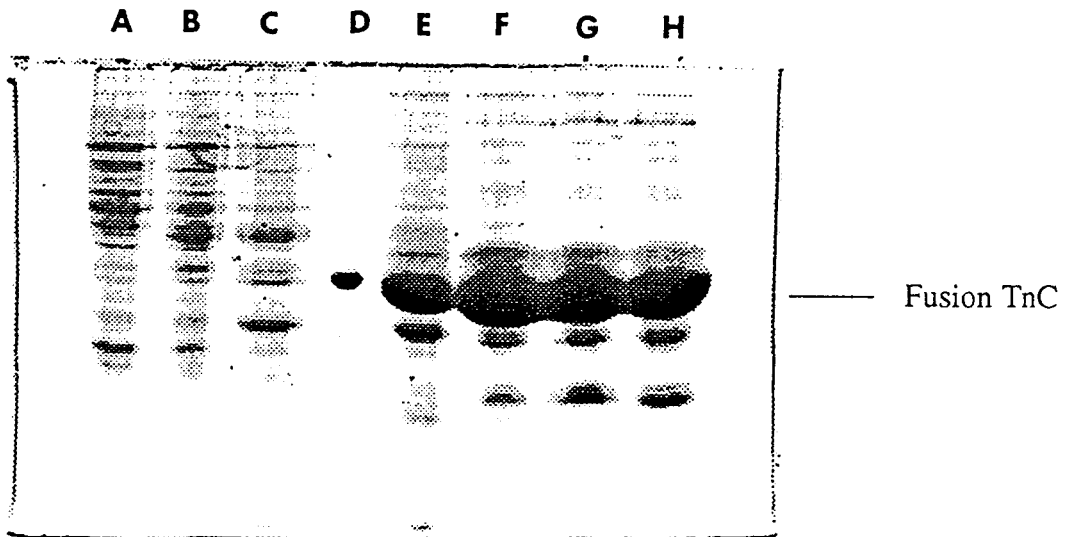


FIGURE 3.9. SDS Polyacrylamide Gel Electrophoresis of Fusion TnC

SDS PAGE of Lane A to C: fractions 44, 45 and 47. Lane D: Fusion protein standard.

Lane E to H: Fractions 49, 51, 53 and 55.

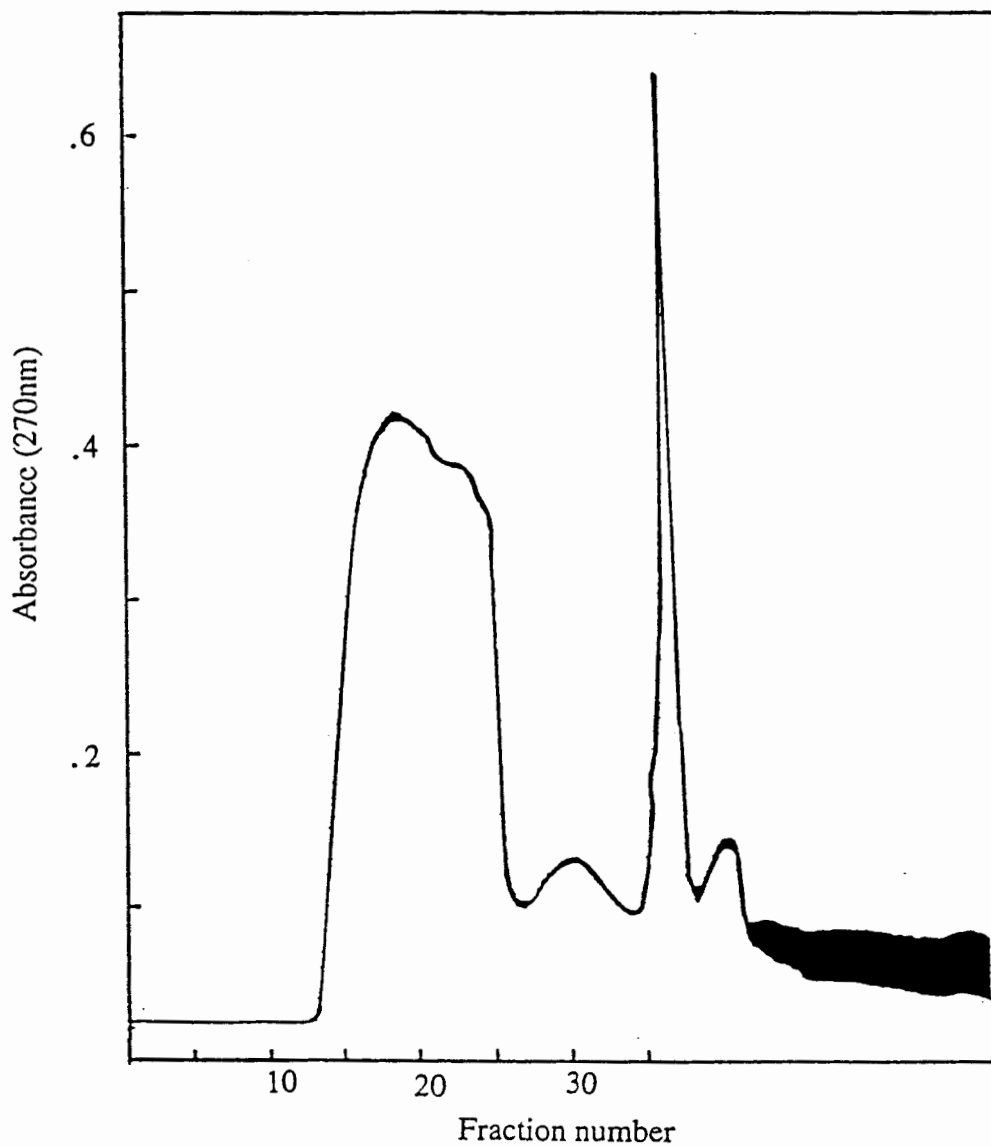


FIGURE 3.10. Gel Filtration Chromatography of Fusion protein

The figure represents the elution profile of a sample of mutant fusion protein being desalted on a G-25 gel filtration column as per section 2.11.3. Fusion TnC was eluted in fractions 12 to 21 which were lyophilized and freeze dried.

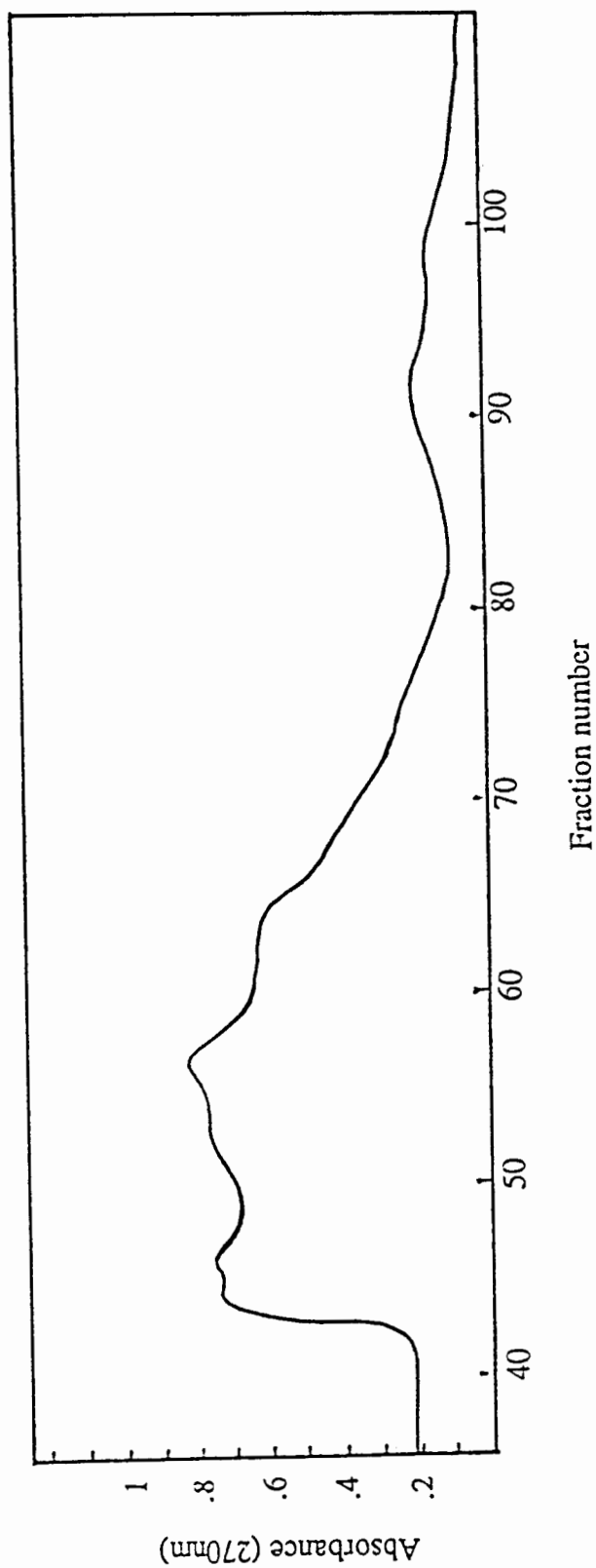


FIGURE 3.11 Anion Exchange Chromatography of Bovine Blood Extract

The figure corresponds to a chromatogram of a plasma protein extract eluted from a DEAE Sepharose CL-6B column (section 2.12.2). Factor X was identified in fraction 87 to 101 as determined by SDS Polyacrylamide Gel Electrophoresis (figure 3.12).

FIGURE 3.12 SDS-PAGE Gels of Factor X eluted from DEAE Sepharose CL-6B Column.

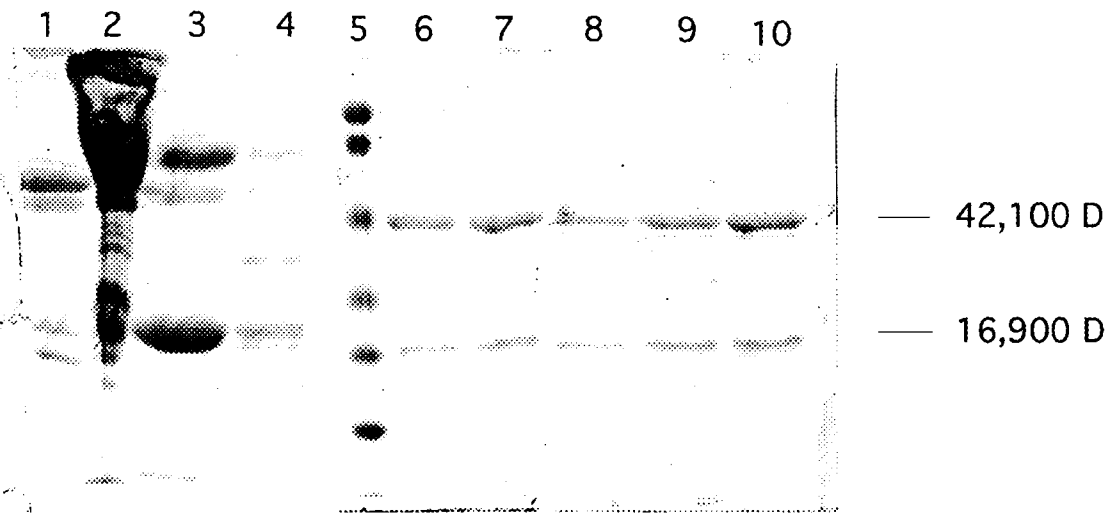
Gel A

SDS-PAGE of Lane 1: Flow through on wash with 20mM Na citrate. Lane 2: aliquot of sample to be purified. Lane 3: Fraction 39 (1st peak). Lane 4 : Fraction 64. Lane 5: Low Range Molecular Weight Markers (Biorad). Lane 6 to 7: Fractions 88 and 89. Lane 8 to 10: Fractions 94 to 96.

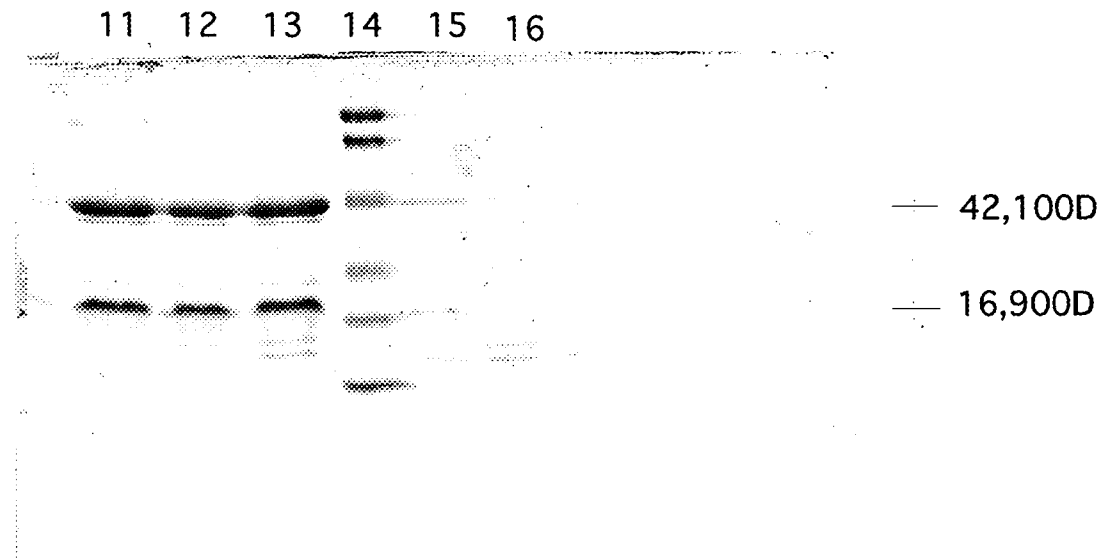
Gel B

Lane 11 to 13: Fractions 97 to 99. Lane 15: Low Range Molecular Weight Markers (Biorad). Lane 15 &16: Fractions 100 and 101.

Gel A



Gel B



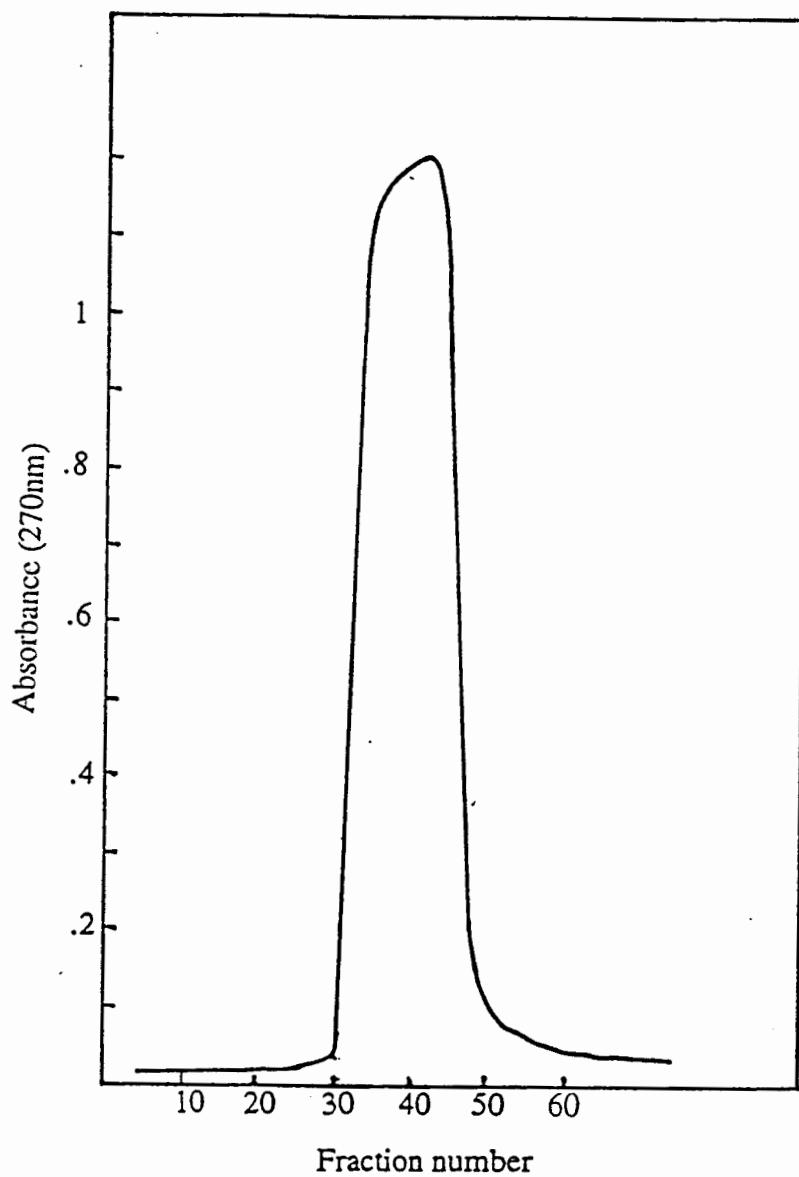
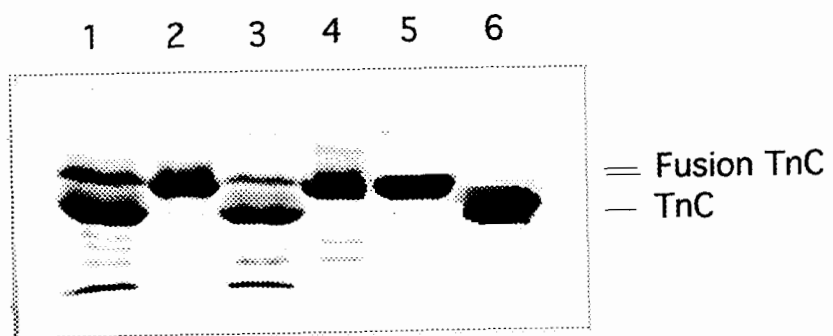


FIGURE 3.13 Gel Filtration Chromatography of Factor X

The Figure corresponds to the chromatogram of Factor X samples eluted from the G-50 gel filtration column. (section 2.12.2). Factor X was collected from fractions 30 to 48.

FIGURE 3.14. SDS-PAGE Gel of Troponin C Mutants Digested With Factor X_a
SDS-PAGE shows Lane 1 & 3: Reaction mixture of fusion proteins F29W/54T and F29W/54V respectively, with Factor X_a after 15 hours. Lane 2 and 4: Uncut samples of fusion proteins F29W/54T and F29W/54V respectively. Lane 5: Sample of a fusion proteins standard. Lane 6: Sample of chicken skeletal TnC standard.



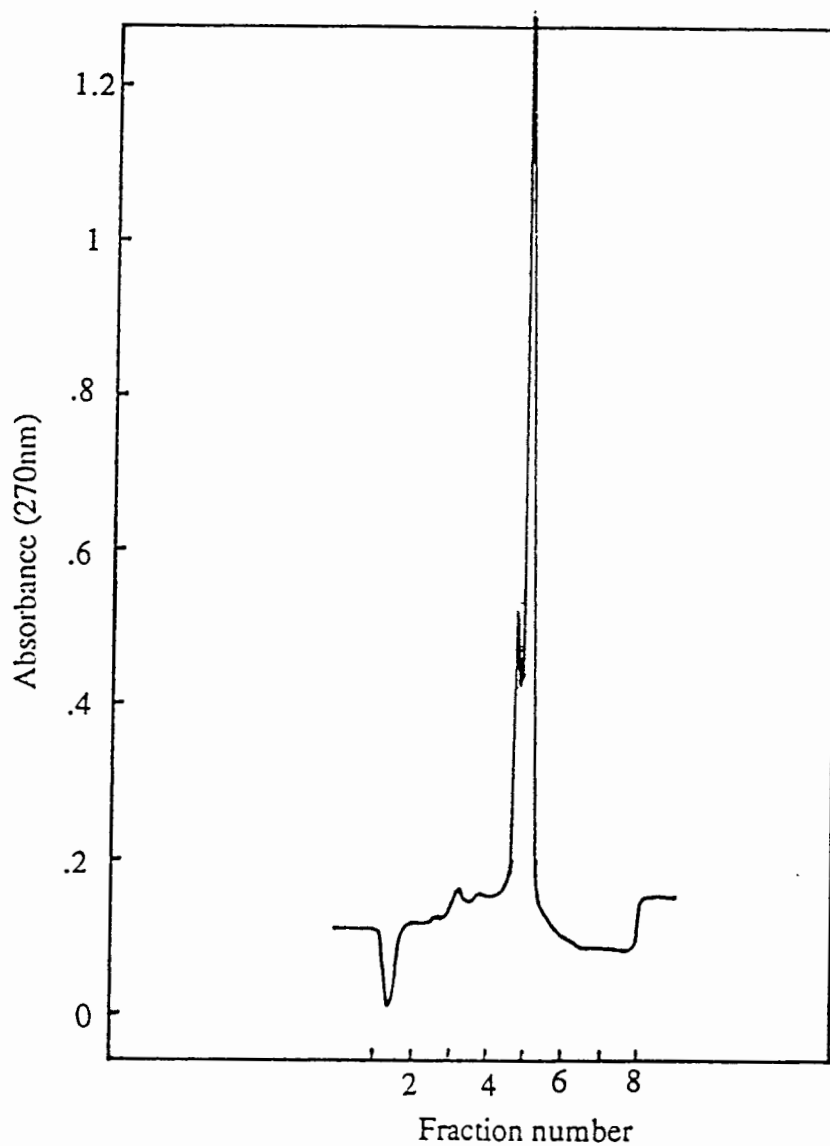


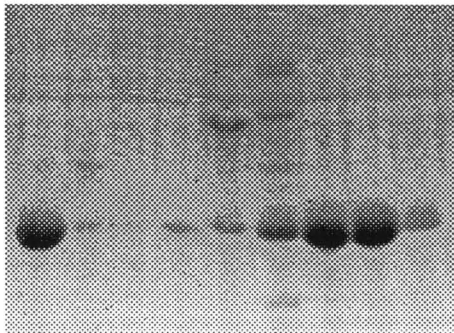
FIGURE 3.15. FPLC Chromatography of TnC Digested With Factor X_a

The Figure corresponds to a chromatogram of mutant TnC (F29W/54T) eluted from an FPLC mono-Q column as per section 2.13.2. Fractions containing pure TnC were identified by SDS-PAGE (Figure 3.16).

FIGURE 3.16. SDS-PAGE of Mutant TnC Eluted From the FPLC Mono-Q Column

Lane 1: TnC protein standard. Lane 2 to 9: Fractions of F29W/54S protein. Fractions 6 and 7 (lanes 7 and 8) were pooled and dialyzed (Section 2.13.2).

1 2 3 4 5 6 7 8 9



3.7 Metal Binding Properties of the Mutant Proteins

3.7.1 Far UV Circular Dichroism

Far UV CD spectra were collected for all mutants 1) unfolded in 8M urea, 2) folded but calcium-free and 3) fully folded and calcium-saturated. Absolute ellipticities and relative changes are reported in Table 3.1. All variant proteins showed approximately the same helical content in 8M urea represented by a large decrease in the negative ellipticity at 222nm relative to the folded protein. Figure 3.17, Panel A, shows that all variant proteins except for F105W/130D and F105W/130G have nearly identical absolute ellipticity values at 222 nm indicating that except for D and G they appear to have the same helical content in the calcium-free state. Greater variability in secondary structure was observed in the calcium-saturated state (Figure 3.18, Panel B). A serine residue at the N-cap position results in a large increase in the negative ellipticity at 222nm representing an increase in the helical content even in the absence of calcium. In the presence of calcium, all proteins showed some increase in negative ellipticity at 222nm.

The Far UV CD spectra of the F29W/54T/V and G mutant proteins are shown in Figure 3.19 in the unfolded, calcium-free and calcium-saturated states. Since the F105W/54T/G/and V clones were made as by-products of preparing the F29W mutants, the CD spectra of these clones were collected. Therefore, it was possible to examine the effect due to the position of the tryptophan probe. The F105W/54T/G/ and V proteins are shown in Figure 3.20.

3.7.2 Fluorescence

The fluorescence emission spectra of the F29W/54X proteins and the F105W 130T/V proteins were recorded under calcium-free conditions and then calcium saturating conditions. The addition of calcium to the F29W proteins

(Figure 3.21) induced an average 2.93 fold increase in fluorescence with a small blue shift from 342nm (no calcium present) to 340 nm (calcium-saturated). While a 1.07 fold reduction in fluorescence was observed for F105W/130T/G, I, N (Figure 3.22 and 3.23) with a blue shift of 10nm, a 2.6 fold increase in fluorescence was observed for F105W/130V with a blue shift of 13nm (Figure 3.23).

The fluorescence spectra for all of the calcium-free F29W /54X proteins showed the same fluorescence emission maximum as the calcium-free spectrum of the wild-type (F29W/54T). The fluorescence spectra for all the calcium-saturated mutant proteins showed the same emission maximum as the wild-type calcium-saturated protein (Figure 3.21). This verified that the protein has not undergone a drastic structural change by inserting different residues at the N-cap position of the C-helix. Therefore the reporter group, the tryptophan residue at position 29, appears to undergo the same environmental shift regardless of the residue at position 54.

The spectra for all F105W proteins except 130V overlap and so the same can be concluded about the environment of the reporter group at position 105 (Figure 3.22). In the case of the valine mutant protein, the spectrum for the calcium-saturated protein appears to overlap those of the F29W calcium-saturated proteins while the spectrum for the calcium-free protein appears to overlap those of the F105W proteins. Since the Trp probe is in a different environment for the valine mutant upon addition of calcium, when compared to the wild type protein, the valine residue may have produced a change in the structure of the protein.

Calcium titration curves for each of the F29W/54X mutants (Figure 3.24) and F105W/130T and 130V mutants (Figure 3.25) were recorded. The binding data for the six proteins is presented in Table 3.2.

The calcium titration data for the F29W proteins and the F105W/130T and 130V proteins were fit with a monophasic titration curve:

$$y = (k_1[\text{Ca}^{2+}]^h \times 100 / 1 + (k_1[\text{Ca}^{2+}]^h) \quad (10)$$

Calcium titrations of the mutant proteins showed a decrease in calcium affinity in the order Ser /Thr > Val > Ala > Gly. The free energy differences are shown in Table 3.2.

FIGURE 3.17. Far UV CD Spectra of Mutant Proteins in the Absence of Calcium.

Panel A: F105W/130X mutant proteins in the absence of calcium. Aspartic acid and glycine at position 130 produce the greatest negative ellipticity at 222nm.

Panel B: F29W/54X mutant proteins in the absence of calcium. Serine at position 54 produces a large increase in the negative ellipticity at 222nm. The remaining 54X proteins all show approximately the same negative ellipticity values at 222nm. They are also in the same range as those for the F105W mutant proteins. Since glycine and serine are different for each of the domains there must be some other structural change in the protein influencing its overall secondary structure.

0.000E+00

PANEL A

CD [mdeg]

93b

-3.000E+01

205.0

260.0

WL [nm]

- 130D
- 130G
- 130I
- 130N
- 130S
- 130T
- 130V

PANEL B

205.0

260.0

WL [nm]

- 54A
- 54G
- 54S
- 54T
- 54V

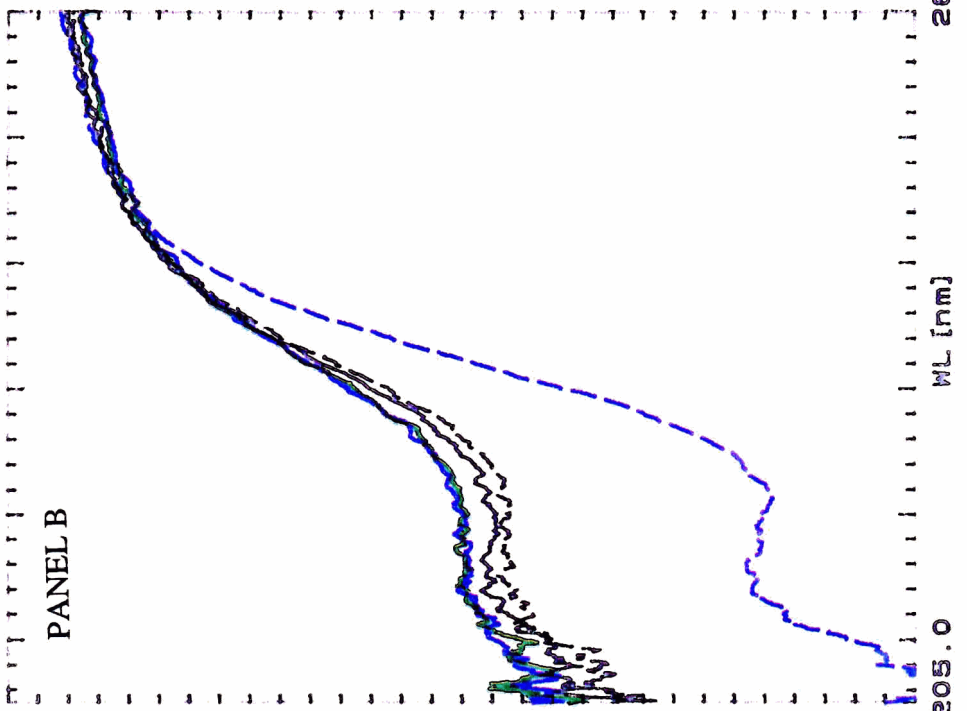
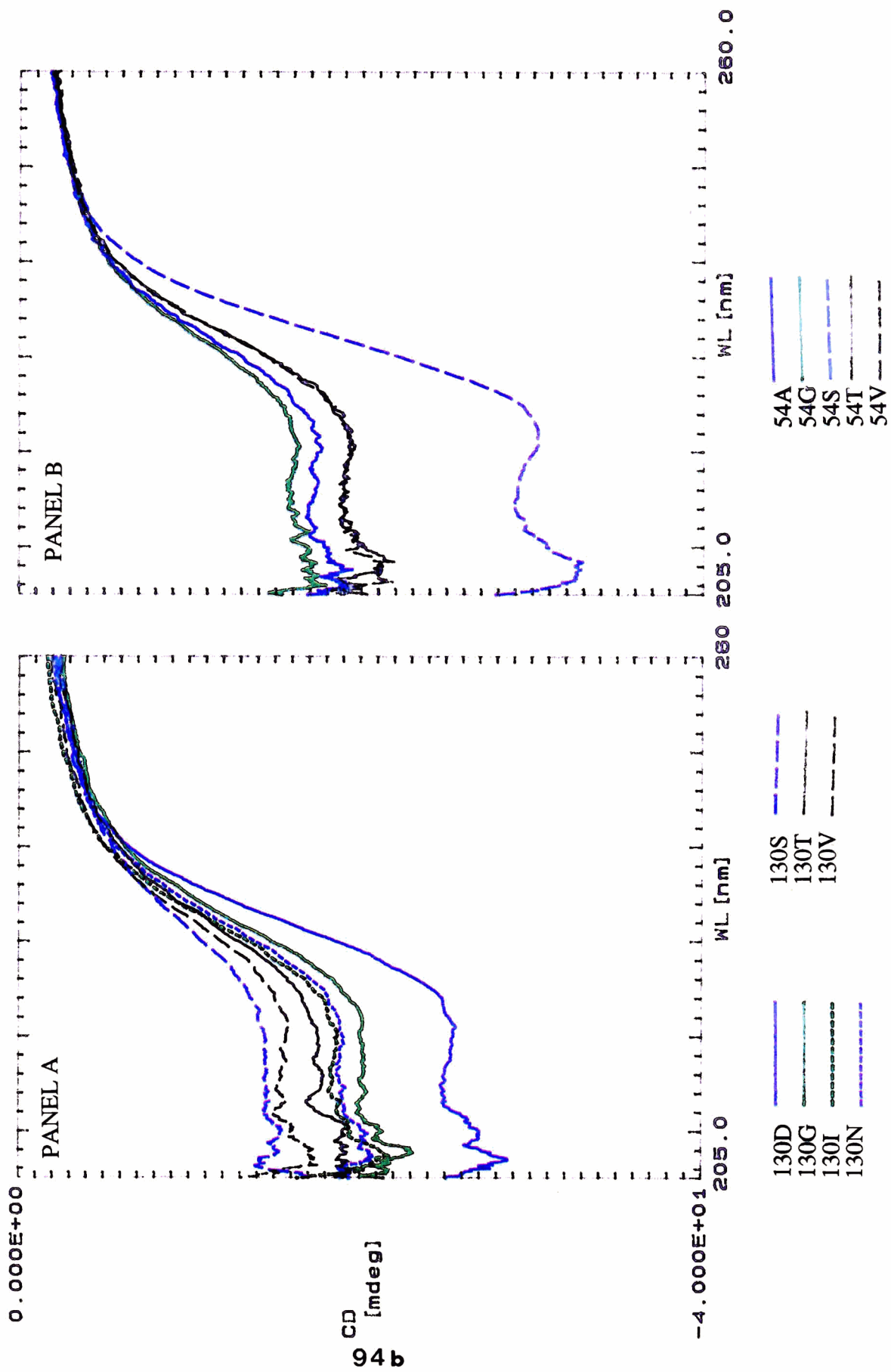


FIGURE 3.18. Far UV CD Spectra of Mutant Proteins at Saturating Calcium Concentrations .

Panel A: Calcium-saturated F105W mutant proteins. Aspartic acid at position 130 produces a large increase in the negative ellipticity value at 222nm upon addition of calcium.

Panel B: Calcium-saturated F29W mutant proteins. The serine mutant at position 54 produces a large increase in the negative ellipticity value at 222nm unlike the serine at position 130.



94b

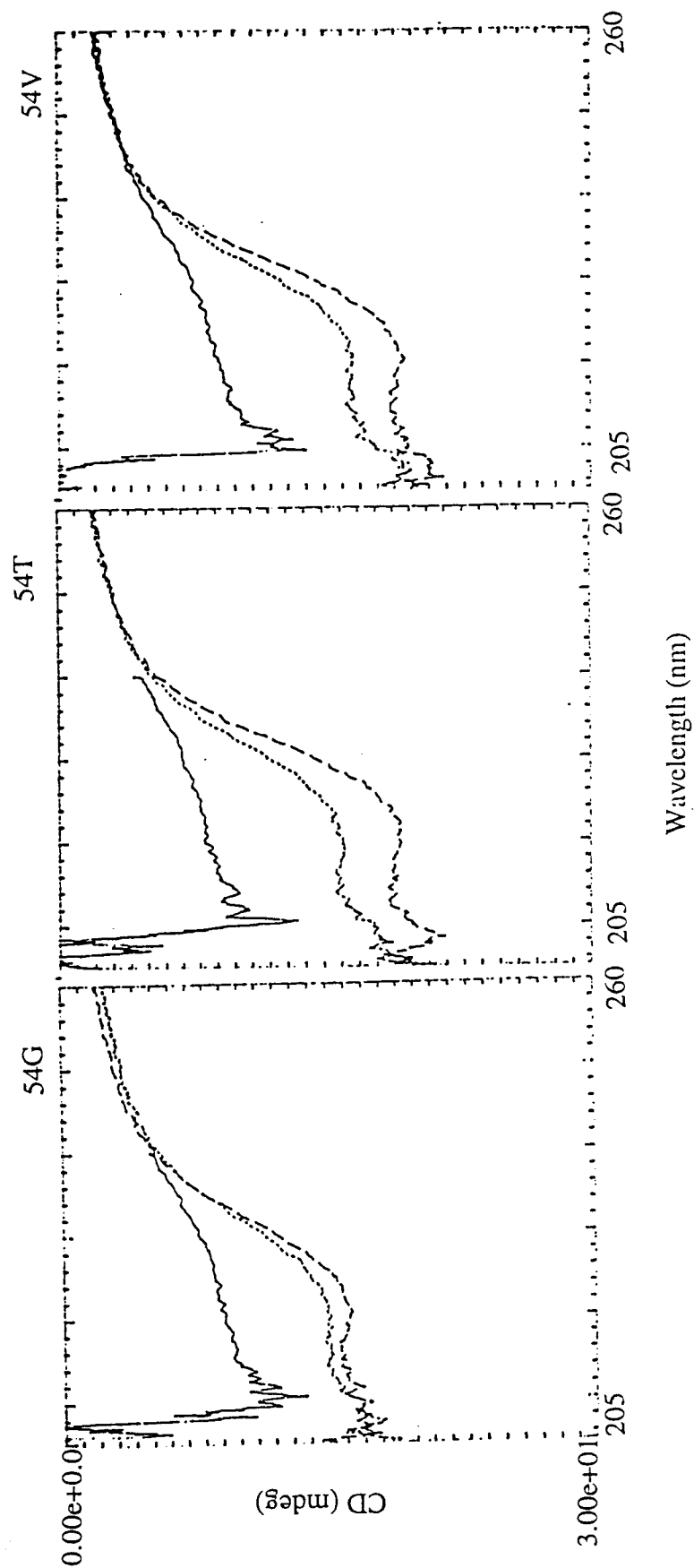


FIGURE 3.19. Far UV Circular Dichroism Spectroscopy of F29W/54X Proteins

These spectra represent the unfolded (—), folded but calcium free (- - -) and the folded, calcium saturated (- · - ·) proteins. Protein concentration was 5 μ M. Unfolded protein samples were in 8M urea.

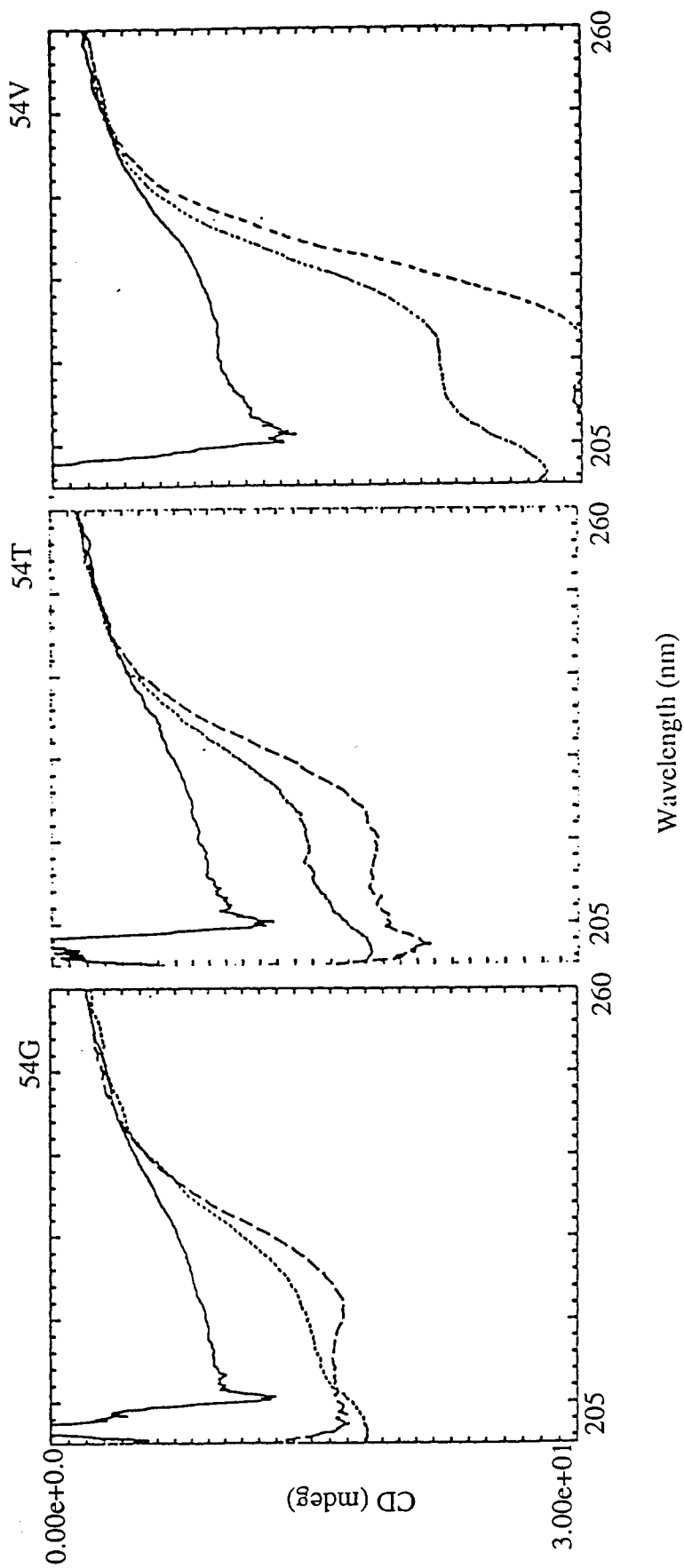


FIGURE 3.20. Far UV Circular Dichroism Spectroscopy of F105W/54X Proteins.

These spectra represent the unfolded (---), the folded, calcium free (····) and the folded, calcium saturated (—) proteins. Protein concentrations were 5 μ M. Unfolded protein samples were in 8M urea.

Table 3.1: Circular Dichroism Spectroscopy Values at 222nm as a Measure of the Helical Content for the Three Folded States of Each Mutant Protein

Protein	[θ] 222nm (mDeg)			Δ [θ] 222nm**	
	Unfolded in Urea	Calcium free	Calcium-saturated	Unf. to Ca Free	Ca free to Saturated
F29W/54A	-8.907	-14.66	-17.32	-5.75	-2.66
F29W/54G	-9.012	-14.95	-15.95	-5.94	-1.00
F29W/54S	-9.116	-25.14	-30.32	-16.02	-5.18
F29W/54T	-8.423	-15.85	-19.37	-7.43	-3.52
F29W/54V	-9.648	-16.38	-19.20	-6.73	-2.82
F105W/130D	-8.788	-18.16	-25.26	-9.37	-7.10
F105W/130G	-8.378	-18.16	-20.14	-9.78	-1.98
F105W/130I	-8.264	-14.48	-18.14	-6.22	-3.66
F105W/130N	-8.236	-15.54	-18.78	-7.30	-3.24
F105W/130S	-8.381	-10.61	-11.79	-5.56	-1.19
F105W/130T	-9.079	-15.01	-17.09	-5.93	-2.08
F105W/130V	-8.331	-13.37	-15.68	-5.04	-2.31
F105W/54G	-8.548	-14.37	-16.68	-5.82	-2.31
F105W/54T	-8.264	-14.48	-18.14	-6.216	-3.66
F105W/54V	-9.280	-22.50	-30.80	-13.22	-8.30

** Δ [θ]_{222nm} represents a 2 scan average in ellipticity at 222nm in going from the calcium-free state to the calcium-saturated state. All protein samples were diluted to 5 μ M concentration prior to measurements.

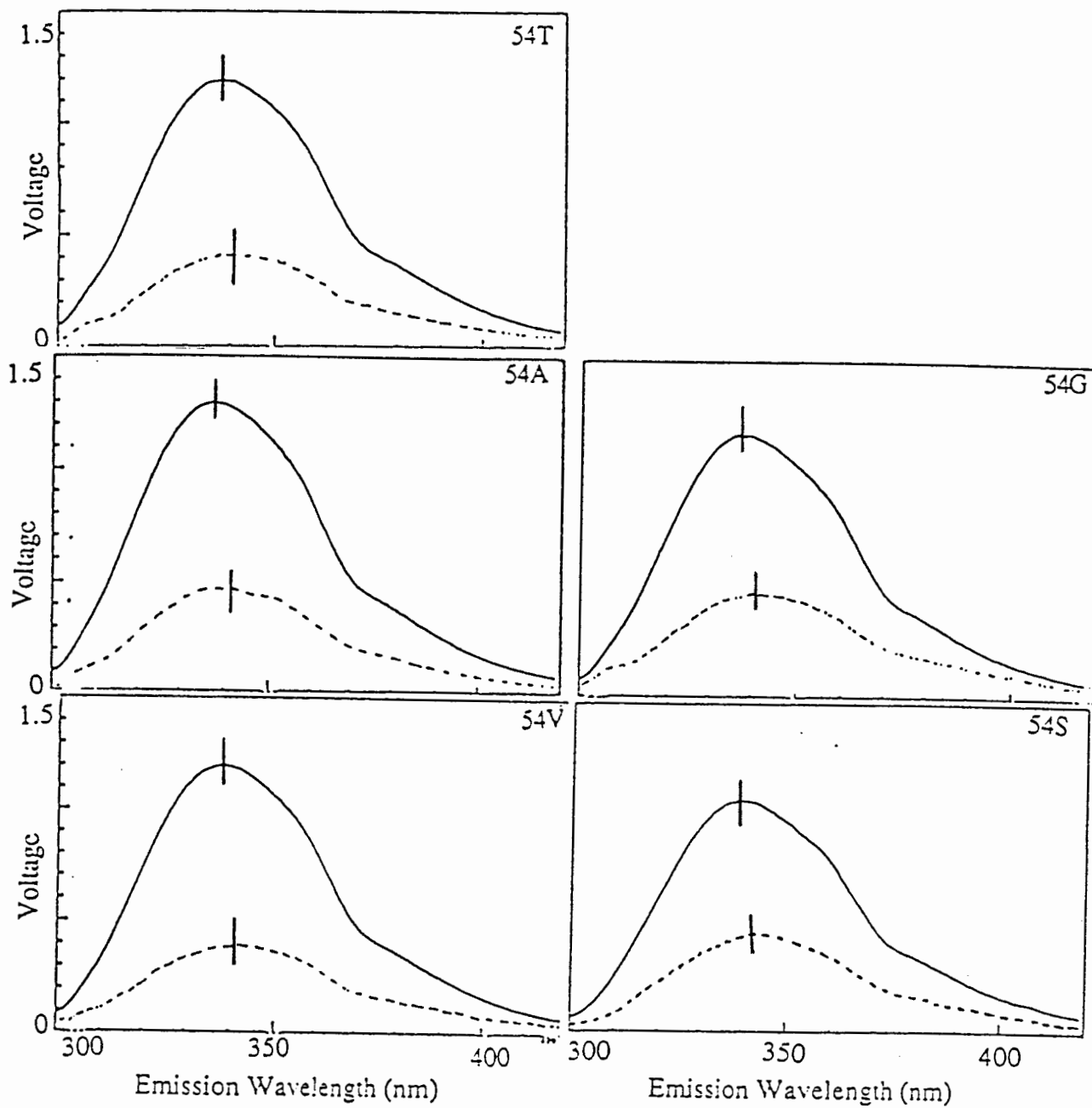


FIGURE 3.21. Fluorescence Emission Spectra of F29W/54X Mutant Proteins.
 This Figure shows the emission spectra of the calcium-free (---) and calcium-saturated (—) proteins. The excitation wavelength was set a 278nm with the emission being followed from 300nm to 420nm. The data was collected at the same voltage settings for all four proteins. The protein concentrations were 5 μ M.

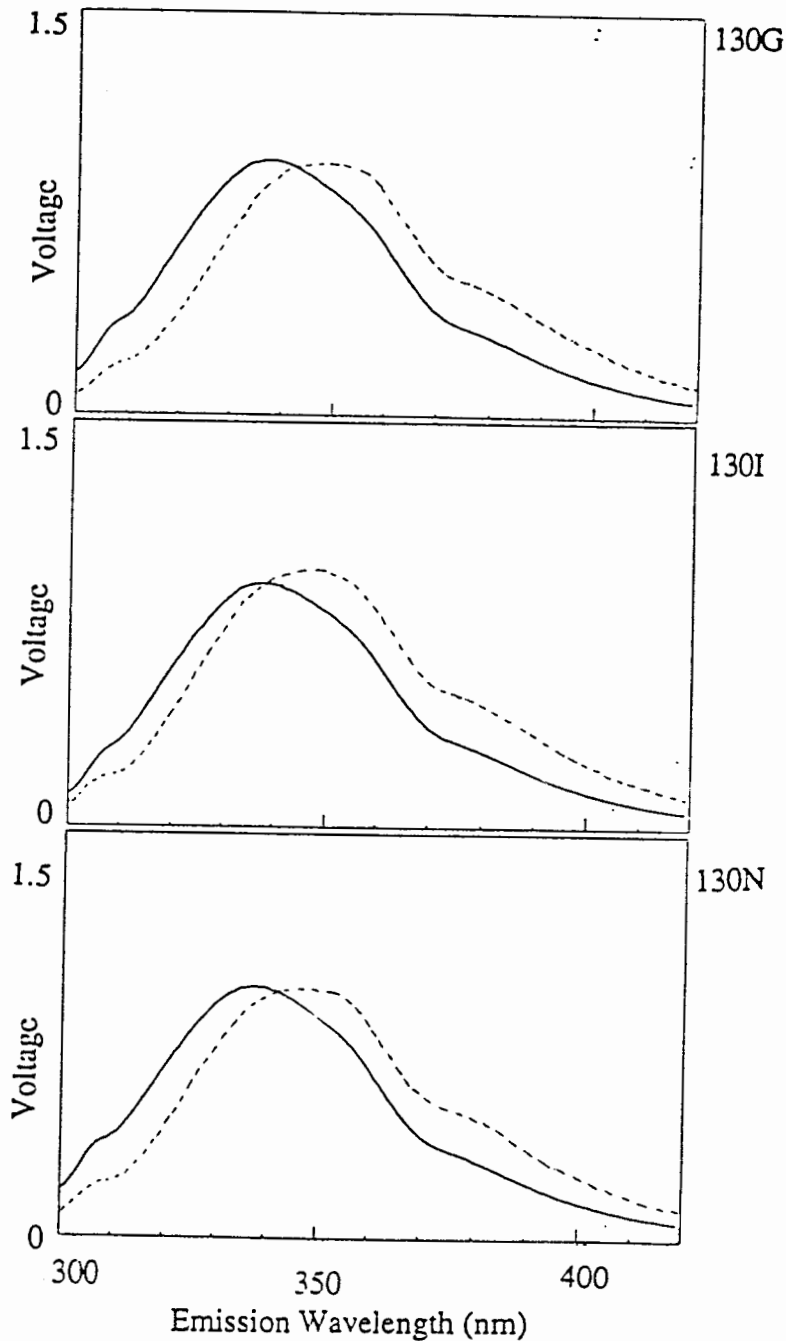


FIGURE 3.22 Fluorescence Emission Spectra of F105W/130X Mutant Proteins.

This Figure shows the emission spectra of the calcium-free (---) and calcium-saturated (—) proteins. The excitation wavelength was set a 278nm with the emission being followed from 300nm to 420nm. The data for these three proteins was collected at the same voltage settings. Protein concentrations were 5 μ m.

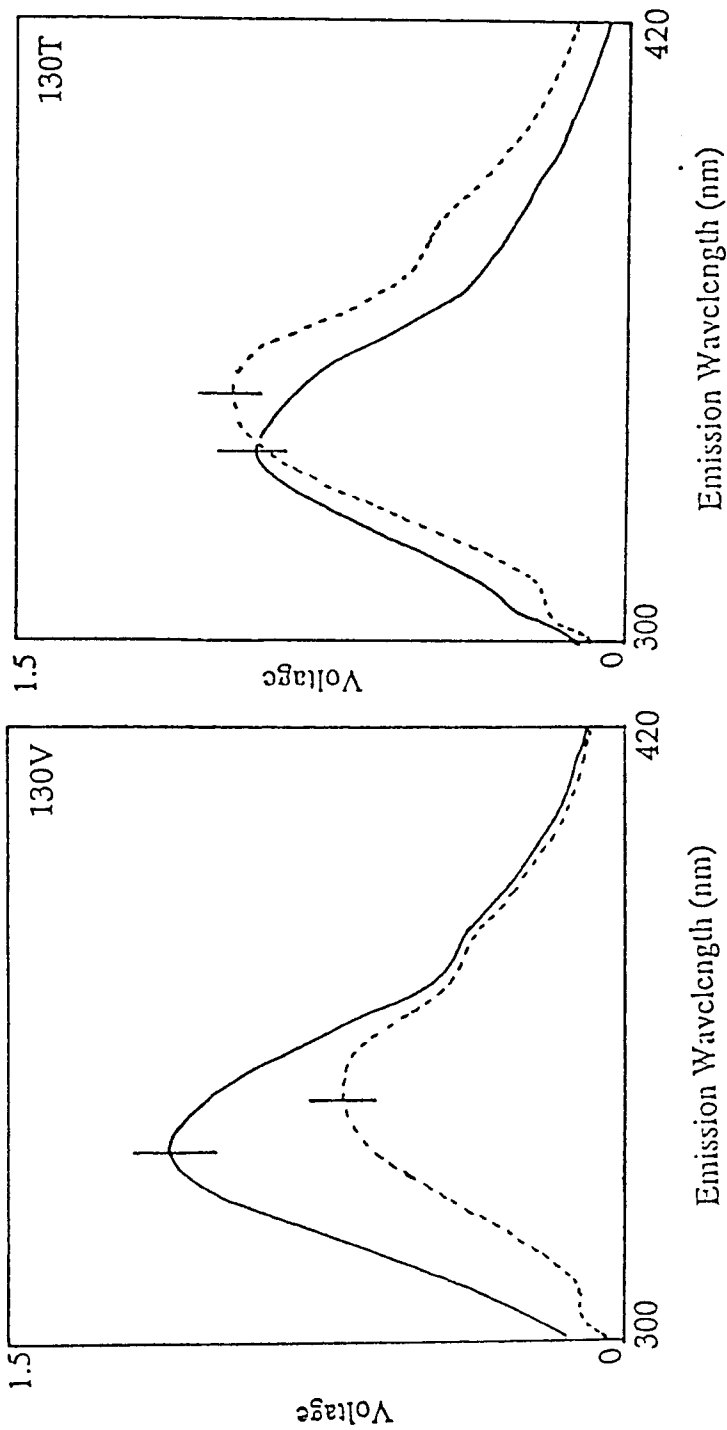


FIGURE 3.23. Fluorescence Emission Spectra of F105W/130T and F105W/130V Mutant Proteins.

This figure shows the fluorescence emission spectra of the calcium free (- - -) and calcium saturated (—) proteins. The excitation wavelength was set a 278nm with the emission being followed from 300nm to 420nm. The data for these two samples was normalized for comparison. Protein concentrations were 5µm. The calcium saturated 130V mutant protein generated a curve characteristic of the 54X mutant proteins. The calcium free 130V mutant protein produced a trace showing the same emission maximum as the calcium free 130T protein but with a decreased intensity.

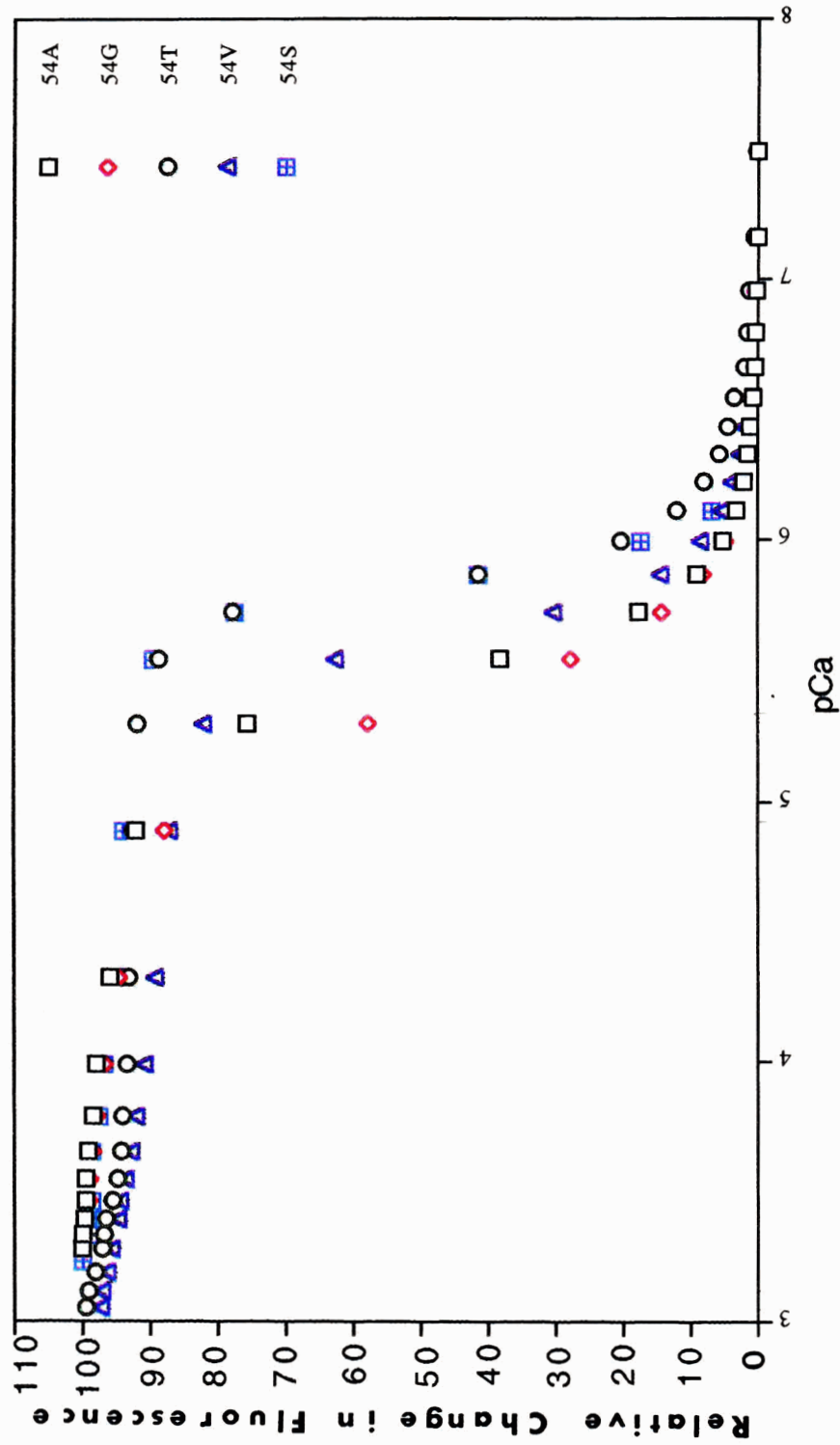


FIGURE 3.24. Calcium Titration of Tryptophan Fluorescence of F29W/54X Mutant Proteins.

Calcium titration of the 54X proteins following fluorescence emission at 335nm. Protein and EGTA concentrations were 5μM and 1mM respectively. Data points are expressed as a percentage change in fluorescence from the starting values.

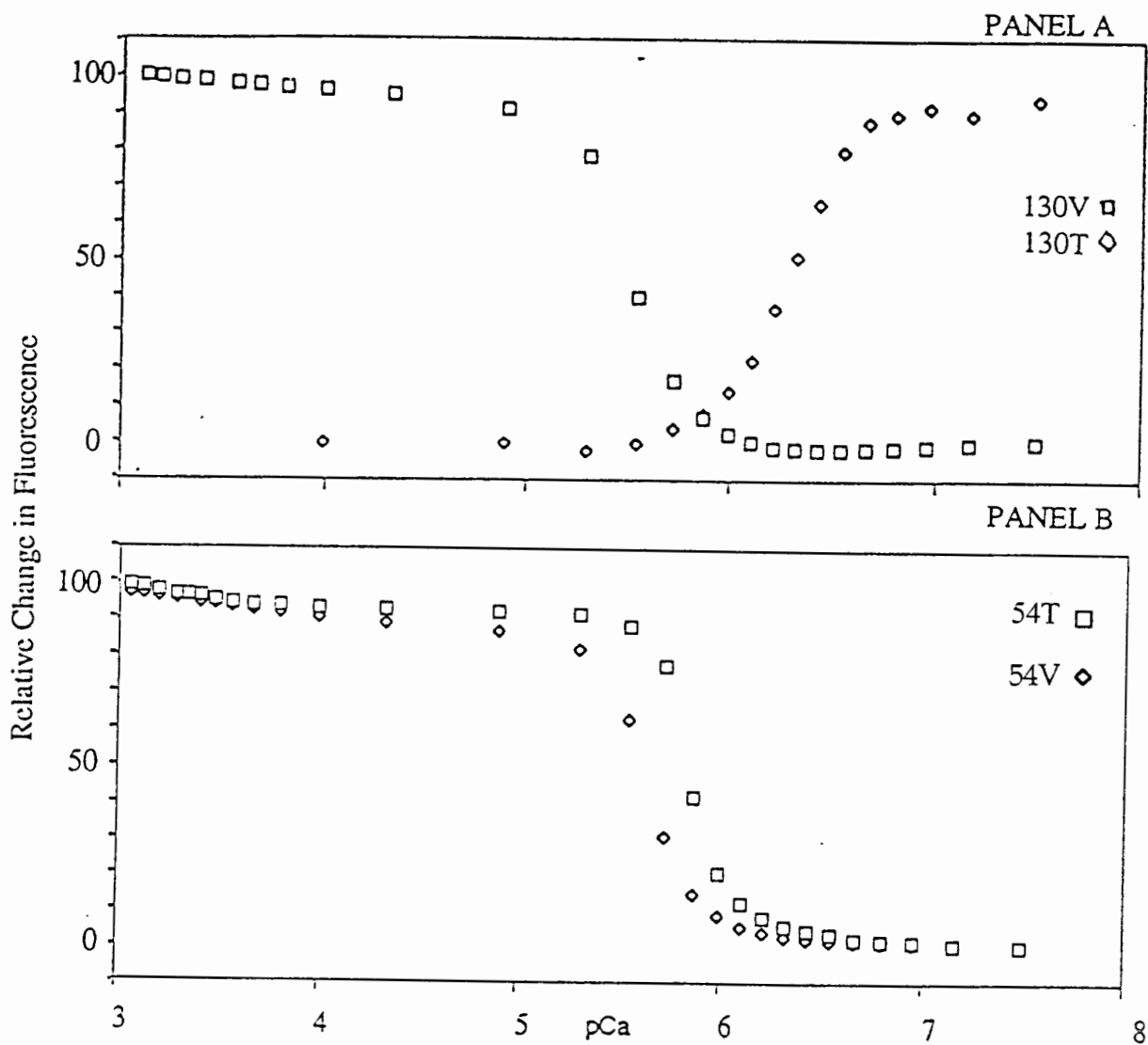


FIGURE 3.25. Calcium Titration of the Tryptophan Fluorescence of the Valine Mutant Proteins.

Panel A: Calcium titration of the F105W/130V and 130T proteins following fluorescence emission at 335 nm.

Panel B: Calcium titration of the F29W/54V and 54T proteins following fluorescence emission at 335nm.

The excitation wavelength was set at 278nm. Protein concentration was 5 μ M for all proteins. The EGTA concentration was 1mM. Data points are expressed as a percentage change in fluorescence from the starting values.

Table 3.2: Binding Parameters Determined by Calcium Titration of F29W/54X Mutant Proteins and F105W/130V Mutant Protein.

Mutant	Hill Coefficient*	$-\log K_d$ (M)	$-\Delta G$ (kcal/Mol)*	$\Delta\Delta G_{\text{Thr-Mut}}$ (kcal/Mol)
54T	3.85+/-0.26	5.86	7.90+/-0.02	0.00
54A	2.64+/- 0.08	5.48	7.38+/-0.01	.52
54G	2.12+/-0.04	5.37	7.23+/-0.01	.67
54S	3.75+/-0.24	5.87	7.91+/-0.01	-.02
54V	2.99+/-0.14	5.64	7.59+/-0.01	.30
130V	2.90+/-0.09	5.51	7.41+/-0.01	3.27#

* These values were obtained using the entire data set from the fluorescence-monitored calcium titration , fitted with the nonlinear regression analysis program GraFit by using equation 9.

The $\Delta\Delta G$ calculation is for 130T to 130V with the ΔG_{130T} taken from previous work done on the F105W mutant proteins (Trigo-Gonzalez, 1992). The value for the $-\log K_d$ for 130T was taken as 7.943+/-0.012.

3.7.3 Flow Dialysis

The stoichiometry of calcium-binding to the mutant proteins F29W/54T, F29W/54V, F105W/130T and F105W/130V was measured using flow dialysis. Fluorescence spectroscopy revealed a decrease in the Hill coefficient for the mutant proteins but provided no information about the number of functional binding sites. The results are shown graphically in Figure 3.26. The mutant proteins bound from 3.8 to 4.5 moles of calcium per mole of protein. To obtain a measurable change in the counts per minute with each aliquot of labelled ligand (^{45}Ca) added to the upper chamber, a minimum of $3\mu\text{L}$ was added for each pulse. The first addition of radiolabelled calcium was observed to saturate one of the high affinity sites. The next two pulses revealed a stepwise binding transition for the valine N-cap mutants of each domain unlike the single transition for the proteins with a threonine residue at the N-cap position. From the calcium titration data (Figure 3.22) we saw that the valine mutants in the high affinity domain showed a large decrease in calcium affinity, resembling that of loop II in the low affinity domain. The flow dialysis studies indicate that valine N-cap perturbed both domains in a similar way, with both of these mutants approaching the calcium saturation level at a different rate than the threonine N-cap proteins. The rate at which the four proteins approach saturation appears to be related to the calcium affinity observed for each mutant. Of importance to this study, the graph shows that all of the proteins are equally saturated at the end of the titration curve. The loss of radioisotope due to diffusion across the membrane was calculated to be 7.3% over the time course of the experiment. This value would have to be corrected for if these experiments were used to measure association constants and Hill coefficients. The loss of calcium would affect the values at low calcium concentrations while the steepness of the curve would be underestimated.

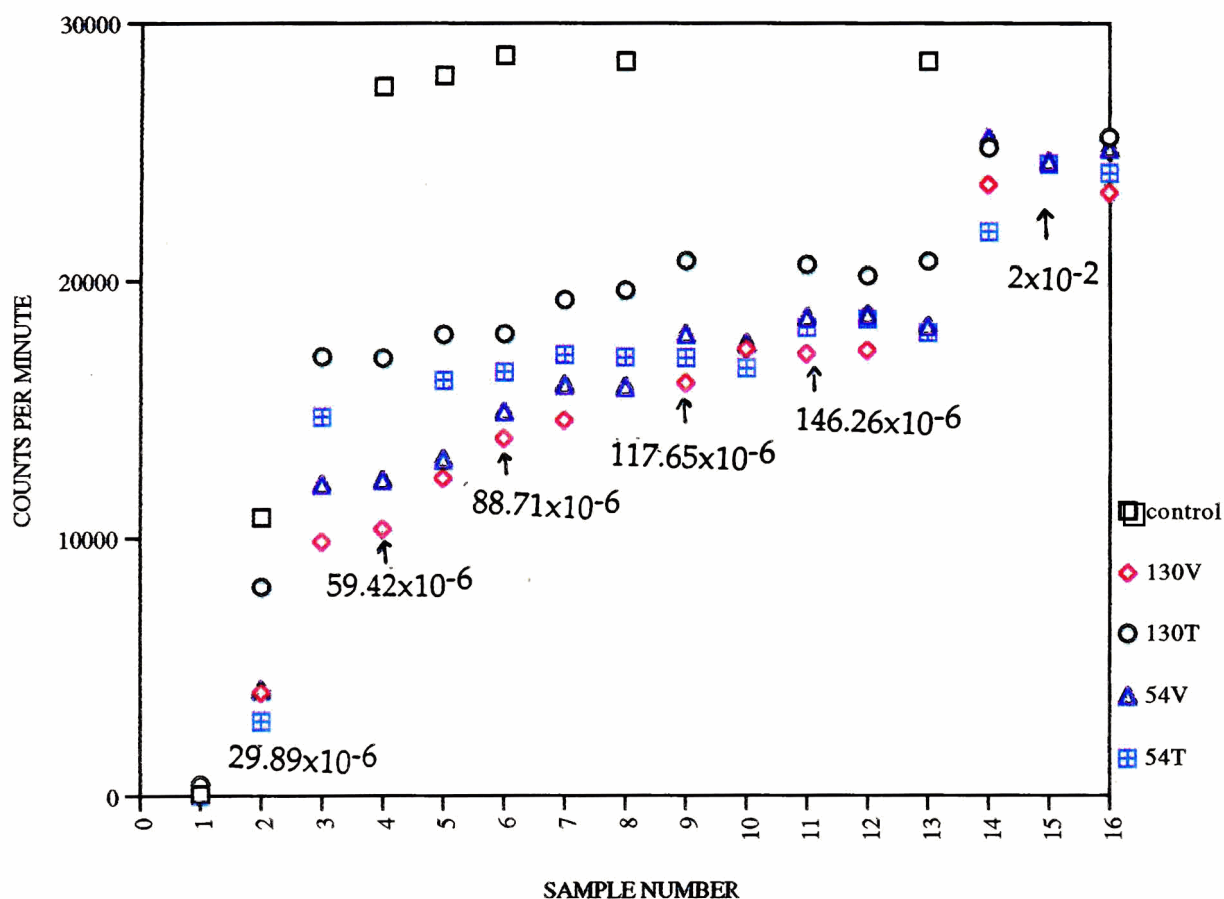


FIGURE 3.26. Measurement of Calcium-binding to Mutant Proteins.

This Figure shows the flow dialysis rates without protein (\square) and with protein (see legend). A 5mL aliquot of radiolabelled calcium was added to the upper chamber. Increments of unlabelled calcium were added to give total calcium concentrations as indicated by the arrow. The four binding curves approach the same plateau by the final addition of calcium. The two valine mutants show a stepwise binding process which is not present with a threonine as the N-cap residue. The four protein curves shown were collected within 24 hours of each other. A protein concentration of $28\mu\text{M}$ was determined using the Lowry Method of protein determination from a sample taken from the upper chamber. ^{45}Ca has a half life of 165 days but after 60 days interference was observed from the decay product (^{45}Sr).

3.7.4. Stopped Flow Analysis of Binding Sites

The F29W/54A/G/T/V and the F105W/130V mutant proteins were studied using stopped-flow fluorescence spectroscopy. The calcium dissociation rates were measured to see if a particular substitution at the N-cap affected the off-rate. The data, acquired at 21°C is summarized in Table 3.3. Prior to measuring the change in rates for all of the mutant proteins, the calcium off-rates for the 54V mutant protein were measured at different concentrations of protein, EGTA and calcium. It was necessary to verify that the rate measured was not dependent on a limiting concentration of one of these components. The concentration of protein was varied from 2.5µM to 5µM. The concentration of EGTA was varied from 5mM to 10mM while the calcium concentration was varied from 0.5mM to 1mM. The results for F29W/54V are summarized in Table 3.4. These measurements were made at 16°C. From these results it is shown that the data can be analyzed using 1st order kinetics.

All measurements for the mutant proteins were made at 5µM protein, 1mM calcium and 10mM EGTA. The F105W/130X mutants, except for 130V, could not be studied by this method as the change in fluorescence upon removing calcium was too small to detect two rates. The only observation noted was a slight increase in fluorescence as the calcium was removed by the EGTA. The data set was fit to the following double exponential equation with floating end point:

$$y = P(1) \times \exp(-P(2) \times X) + P(3) \times \exp(-P(4) \times X) + P(5) \quad (11)$$

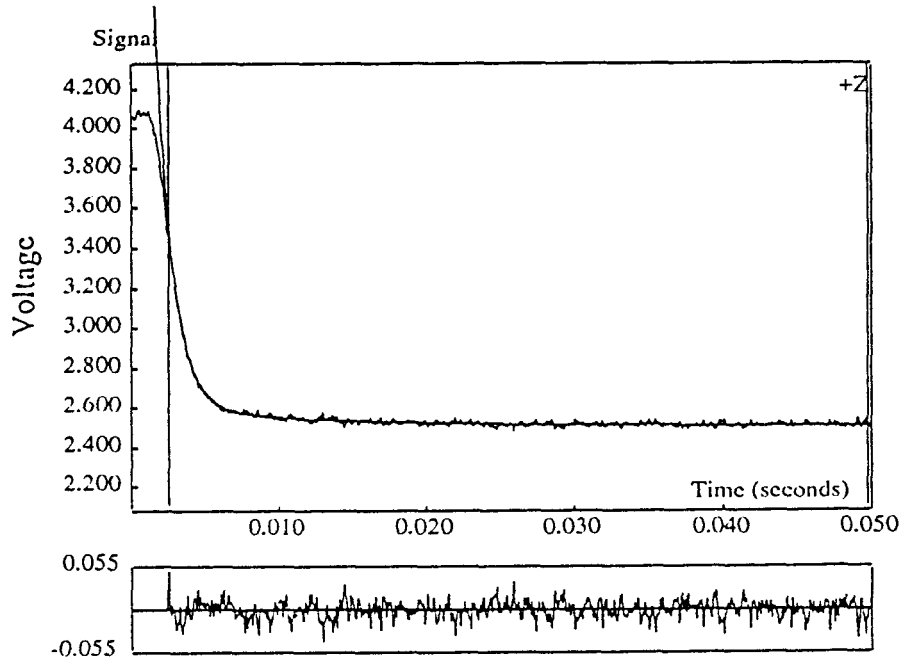
where P(2) and P(4) are the two rates and P(1) and P(3) are the associated changes in amplitude. P(5) is the end point (minimum) fluorescence reading and X is time in seconds (Figure 3.27).

Two calcium off-rates were observed with the addition of EGTA to the calcium saturated protein samples. There was a fast rate ($P(2)$) of approximately 900 per second and a slow rate ($P(4)$) of 100 per second. The fast rate was observed to increase up to 50% with the valine mutant protein. The fast rate was also associated with the largest change in fluorescence. This creates some ambiguity as to the identity of the loop associated with each rate since the Trp probe is most closely associated with loop I while the mutation should be directly impacting upon loop II. The two rates were interchanged in equation 11, so that $P(2)$ was set as the slow rate and $P(4)$ was set as the fast rate. If the exchange of rates produced an invalid mathematical solution, that is, a negative fluorescence value, the rates could then be assigned to the appropriate loop. However the same fluorescence intensity was associated with the fast rate regardless of the order of the two rates.

FIGURE 3.27. Non-Linear Regression Analysis of the Stopped-Flow Data for the F29W/54T Protein.

These graphs are samples of the non-linear regression analysis of the entire data set acquired in a single stopped-flow experiment at 21°C. Panel A shows a sample curve for the F29W/54T protein. The two dissociation rates were calculated using a double exponential function (equation 10) with floating end point. The residuals were evenly distributed indicating a good fit of the data to the equation. Panel B shows the fit of the same data set to a single exponential function. Note the poor fit for the rate calculation in the first half of the curve. The residuals are not evenly distributed about the line verifying the poor fit of the data to this equation.

PANEL A



PANEL B

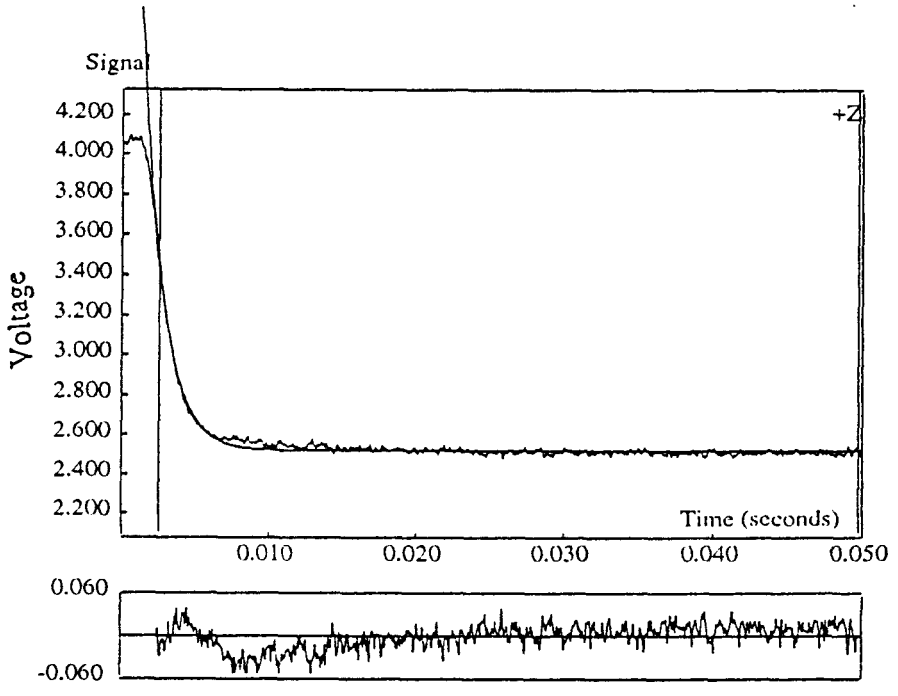


Table 3.3: The Rate of Release of Calcium Ions from Calcium-Loaded Troponin C Studied by Stopped-Flow

Mutant Protein	Rate 1 * P(2) (sec ⁻¹)	Amplitude P(1)	Rate 2 * P(4) (sec ⁻¹)	Amplitude P(3)
54T	900 +/- 20	8.25	94 +/- 9	.111
54A	1190 +/- 50	13.14	100 +/- 22	.073
54G	1260 +/- 100	11.48	100 +/- 14	.094
54V	1470 +/- 100	22.72	123 +/- 23	.102
130V	920 +/- 50	5.37	130 +/- 23	.07

* The error reported with Rate 1 and Rate 2 is the average error reported in fitting the data set with a non-linear regression analysis with floating end point.

** The standard deviation was calculated using 10 runs for each mutant protein.

All data was collected at 21°C.

Table 3.4: The Rates of Release of Calcium Ions from Calcium-Loaded F29W/54V Mutant Protein Studied at varying Protein, Calcium and EGTA Concentrations.

Reaction conditions	Rate 1P(2) (sec-1)	Amplitude P(1)	Rate 2 P(4) (sec-1)	Amplitude P(3)
2.5 μ M TnC 1mM Ca ²⁺ 10mM EGTA	810 +/-30	7.36	82 +/- 20	.092
2.5 μ M TnC 0.5mM Ca ²⁺ 10mM EGTA	810 +/- 30	7.11	86 +/- 20	.097
5 μ M TnC 0.5mM Ca ²⁺ 5mM EGTA	800 +/- 30	5.50	84 +/- 10	.061

Error determination was the same as outlined in the legend of Table 3.3. The data set for the experiments with 2.5 μ M TnC, 0.5mM Ca²⁺ and 10mM EGTA is the average of four runs instead of 10. Data was collected at 16°C.

3.8. Stability of the Calcium-free Mutant Proteins Measured by Urea

Denaturation

3.8.1 Unfolding of the Calcium-free Mutant Proteins Followed by Far UV

Circular Dichroism

The unfolding of the calcium-free F29W and F105W mutant proteins in urea was monitored by Far UV CD spectroscopy to compare the change in secondary structure of the whole protein due to mutation of the N-cap residue. The negative ellipticity was measured as the concentration of urea was increased from 0.1M to 8M urea. The data set was fitted with the non-linear regression analysis program GraFit (Erithacus Software Limited) by using equation 6 described in section 1.4.3 (Figures 3.28 and 3.30). The $\Delta G_{\text{unf}}^{\text{H}_2\text{O}}$ values are summarized in Table 3.5. The data in the transition region were fit with equation 3 described in section 1.4.3 to obtain ΔG_{unf} values which were plotted against [urea] (Figures 3.29 and 3.31). The $\Delta G_{\text{unf}}^{\text{H}_2\text{O}}$ and "m" values determined by this method are summarized in Table 3.6. The decreasing order of stability for the calcium-free F29W/54X mutant proteins was found to be:

Ser > Thr > Gly > Ala > Val

The decreasing order of stability for the calcium-free F105W/130X proteins was found to be:

Val > Ser > Asn > Gly > Asp > Ile > Thr.

The placement for the threonine and valine proteins were unexpected and so the experiments were repeated several months later with the same results. The interpretation of these results is believed to be dependent on the domain in

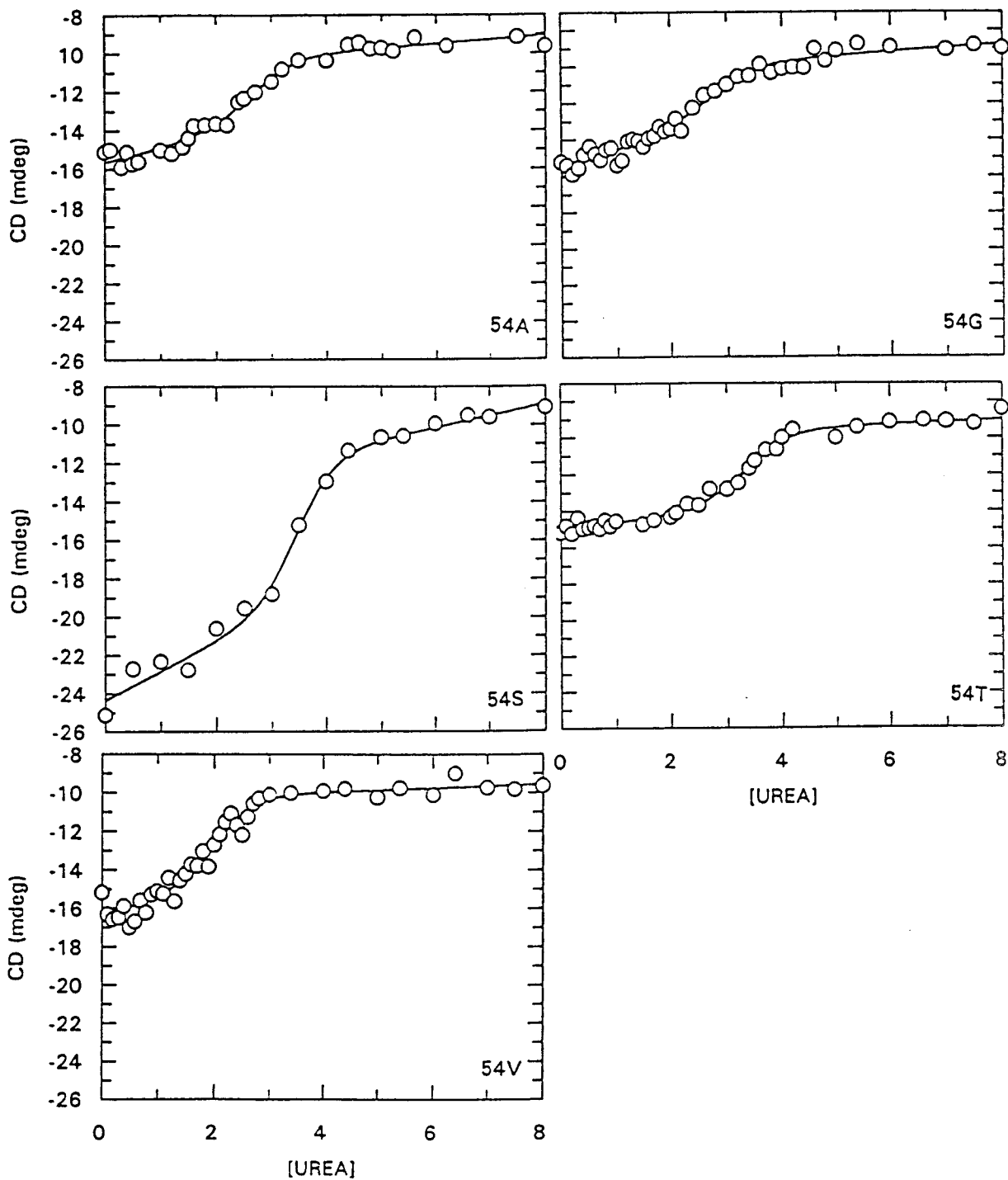
which the mutation is found and relates to the different function each domain has within the protein as a whole. The ΔG versus [urea] curves for the Ser, Asn, Gly, Asp and Ile and Val run close to parallel with their "m" values (the slope of the lines) being the same within experimental error. The slope of the threonine residue diverges which is diagnostic of a significant change in structure for the mutant proteins compared to the wild type (Serrano et al, 1992).

The $\Delta\Delta G_{\text{unf}}$ was also calculated using the [urea]_{50%} values are listed in Table 3.7. The [urea]_{50%} values themselves provided an immediate picture as to how easily the protein unfolded; the larger the [urea]_{50%} value, the more stable the protein. The $\Delta\Delta G_{\text{unf}}$ values calculated by this method (section 1.4.3, equation 7) are closer to the values calculated with equation 6 using non-linear regression analysis than those calculated by means of extrapolated data.

The change in free energy associated with the folding of each protein is tabulated in Table 3.8. All of the low- affinity domain mutant proteins except serine are less stable than the wild-type (Thr). All of the high-affinity domain mutants are more stable than the wild-type (Thr).

FIGURE 3.28. Urea Denaturation of Calcium-free, F29W/54X Mutant Proteins Followed by Far UV CD Spectroscopy.

Mutant proteins were unfolded in the presence of 0M to 8M urea. These graphs represent the change in molar ellipticity, $[\theta]$, at 222nm, as the concentration of urea was increased from 0.1M to 8M urea. The data set was fit to equation 6 using the GraFit software program. The solid line represents the computer generated fit of the observed data points (o). Data is summarized in Table 3.5.



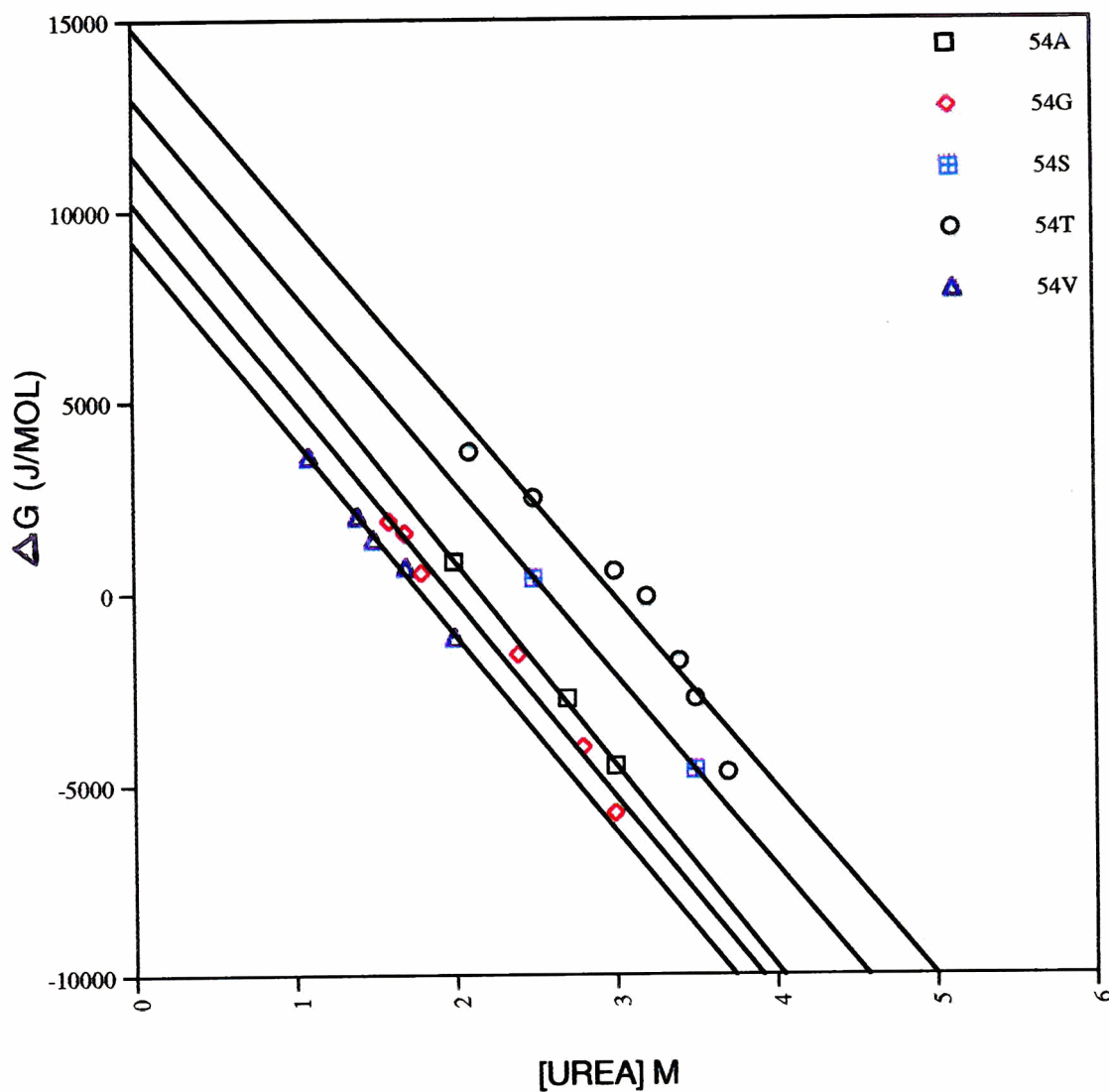
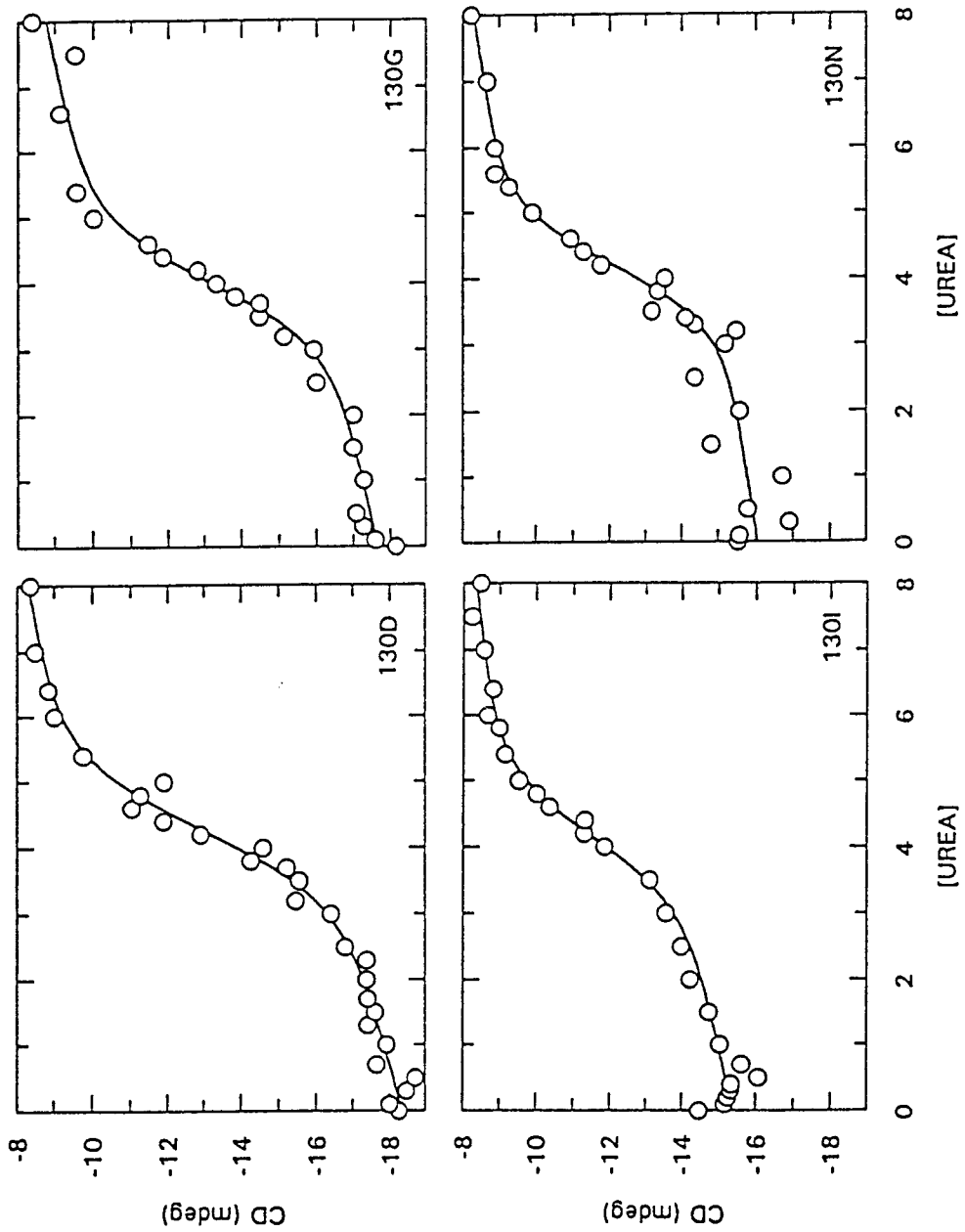


FIGURE 3.29. Free Energy Change of Unfolding of Calcium-free, F29W/54X Mutant Proteins Measured by CD Spectroscopy.

The $\Delta G_{\text{unf}}^{\text{H}_2\text{O}}$ was determined by plotting the free energy change calculated with equation 3 (section 1.4.3) versus the concentration of urea for the unfolding of the mutant proteins in the transition region. The y-intercept values are tabulated in Table 3.6.



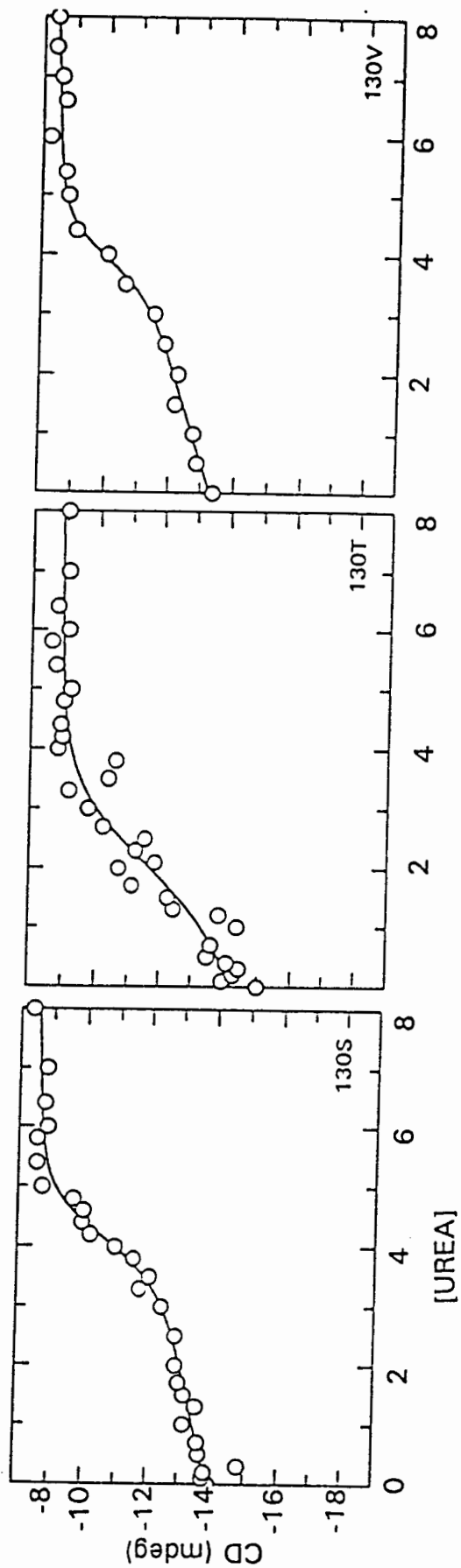


FIGURE 3.30. Urea Denaturation of Calcium-free, F105W/130X Mutant Proteins Followed by Far UV CD Spectroscopy.

Mutant proteins were unfolded in the presence of urea. These graphs represent the change in molar ellipticity, $[\theta]$, at 222nm, as the concentration of urea was increased from 0.1M to 8M urea. The data set was fit to equation 6 using the GraFit software program. The solid line represents the computer generated fit of the observed data points (o). Data is summarized in Table 3.5.

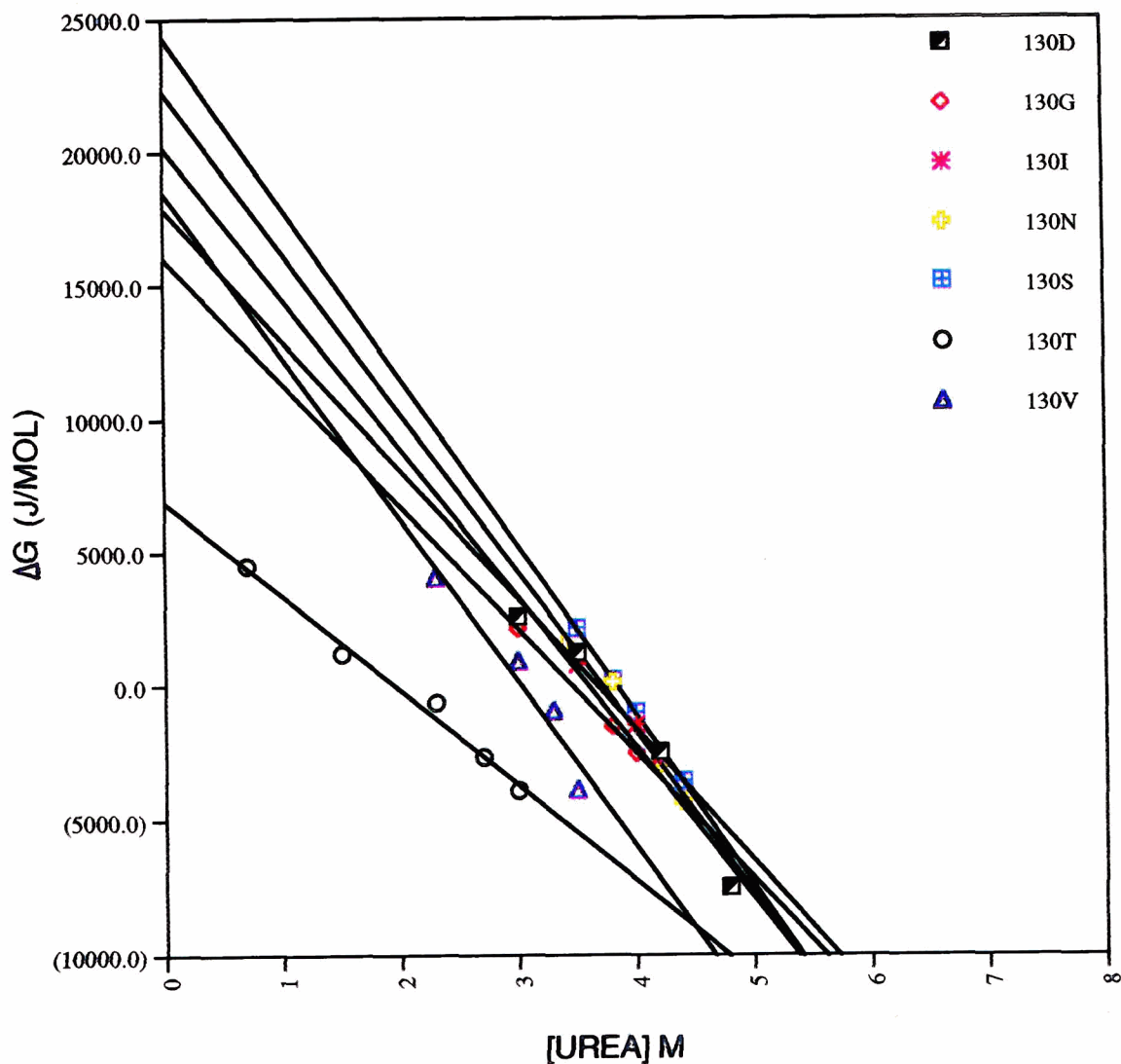


FIGURE 3.31. Free Energy Change of Unfolding of Calcium-free, F105W/130X Mutant Proteins Measured by CD Spectroscopy

The $\Delta G_{\text{unf}}^{\text{H}_2\text{O}}$ was determined by plotting the free energy change calculated with equation 3 (section 1.4.3) versus the concentration of urea for the unfolding of the mutant proteins in the transition region. The y-intercept values ($\Delta G_{\text{unf}}^{\text{H}_2\text{O}}$) are tabulated in Table 3.6.

3.8.2. Unfolding of Calcium-free Mutant Proteins Followed by Steady State Fluorescence Emission Spectroscopy

The calcium-free F29W/54X and F105W/130X mutant proteins were unfolded in the presence of urea. The change in fluorescence for the F29W proteins was large enough to measure an observable transition as the protein unfolded (Figure 3.32 and Table 3.5). Figure 3.33 is a plot of the change in free energy in the transition region versus urea concentration. The "m" value (ie. the slope of the line) is the same, within experimental error, for all of the mutant proteins. This suggests that the mutation did not affect the folding pathway.

The change in fluorescence for the F105W mutant proteins was very small. With an average change of 0.2 voltage units over the entire titration, it was difficult to accurately measure the effect of a change in urea concentration on the environment of the tryptophan probe. Several data points fluctuated between the maximum and minimum fluorescence within a 0.1M change in the urea concentration (Figure 3.34).

Using the $[\text{urea}]_{50\%}$ values from the fluorescence data, the $\Delta\Delta G_{\text{unf}}$ was calculated for the low-affinity domain mutants. The values are listed in Table 3.7. The $\Delta\Delta G_{\text{unf}}$ values calculated by this method (section 1.4.3, equation 7) are in agreement with the values calculated with equation 6 using non-linear regression analysis. The glycine residue was found to be more destabilizing when looking at the protein as a whole when compared to the destabilizing effect on the low-affinity domain only. An alanine residue at the N-cap of the C-helix was less destabilizing to the protein as a whole when compared to the low-affinity domain.

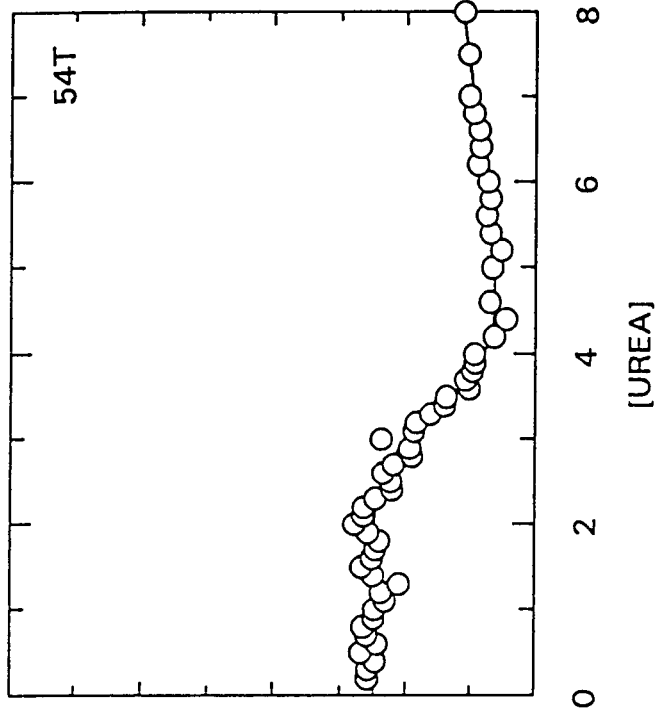
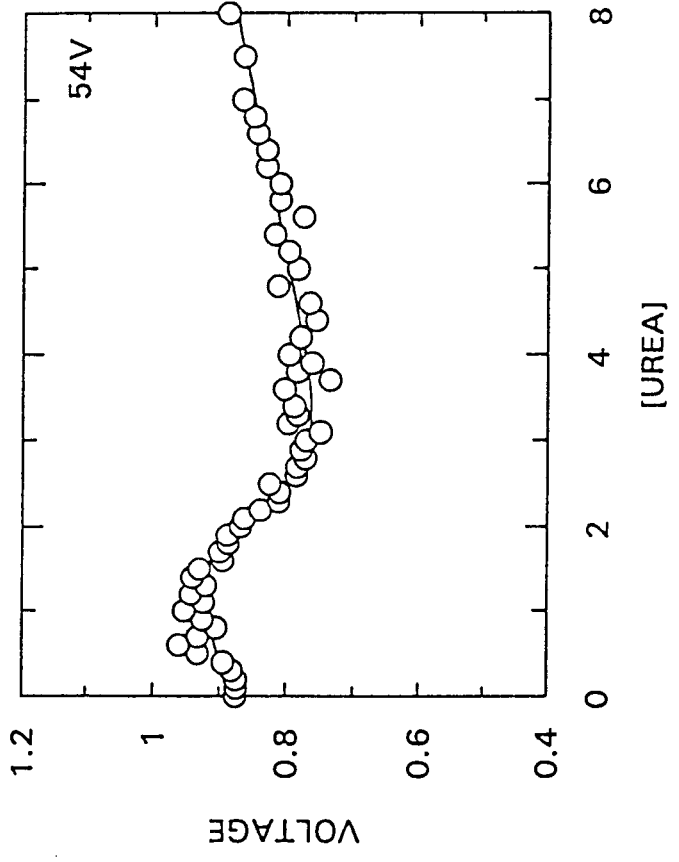
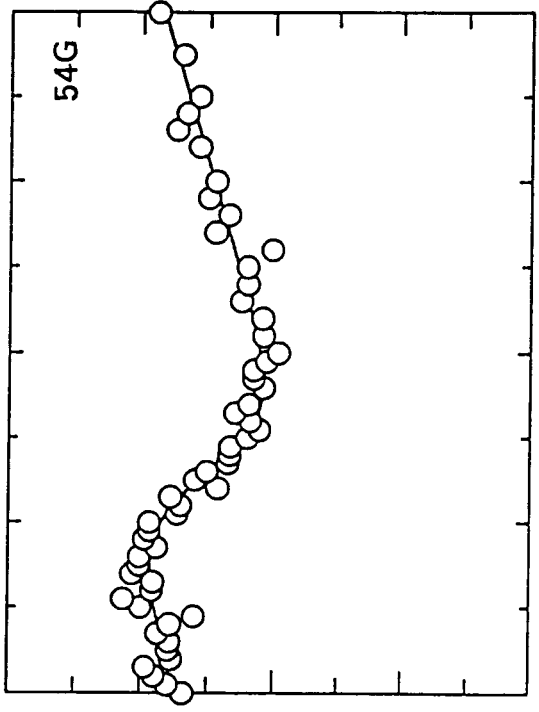
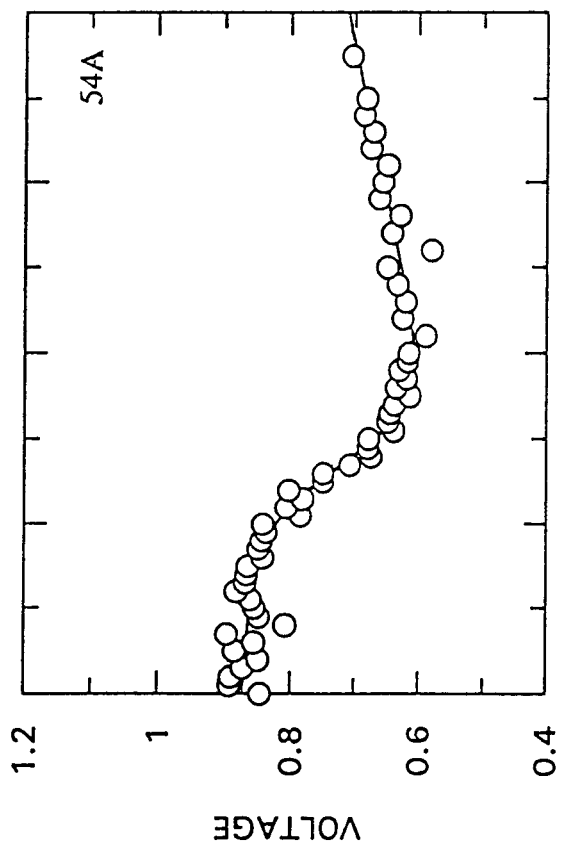


FIGURE 3.32. Urea Denaturation of Calcium-free, F29W/54X Mutant Proteins Followed by Steady State Fluorescence Emission Spectroscopy

Calcium-free mutant proteins were unfolded in the presence of urea. The fluorescence intensity was measured at 335nm after excitation at 278nm. Protein concentrations were 5 μ M. The pre- and post transition baselines were calculated using a linear regression analysis with GraFit. The Y-intercept values ($\Delta G_{\text{unf}}^{\text{H}_2\text{O}}$) were used for the non-linear regression analysis of the transition region using equation 6 (section 1.4.3). The solid line represents the fitted curve for the entire data set.

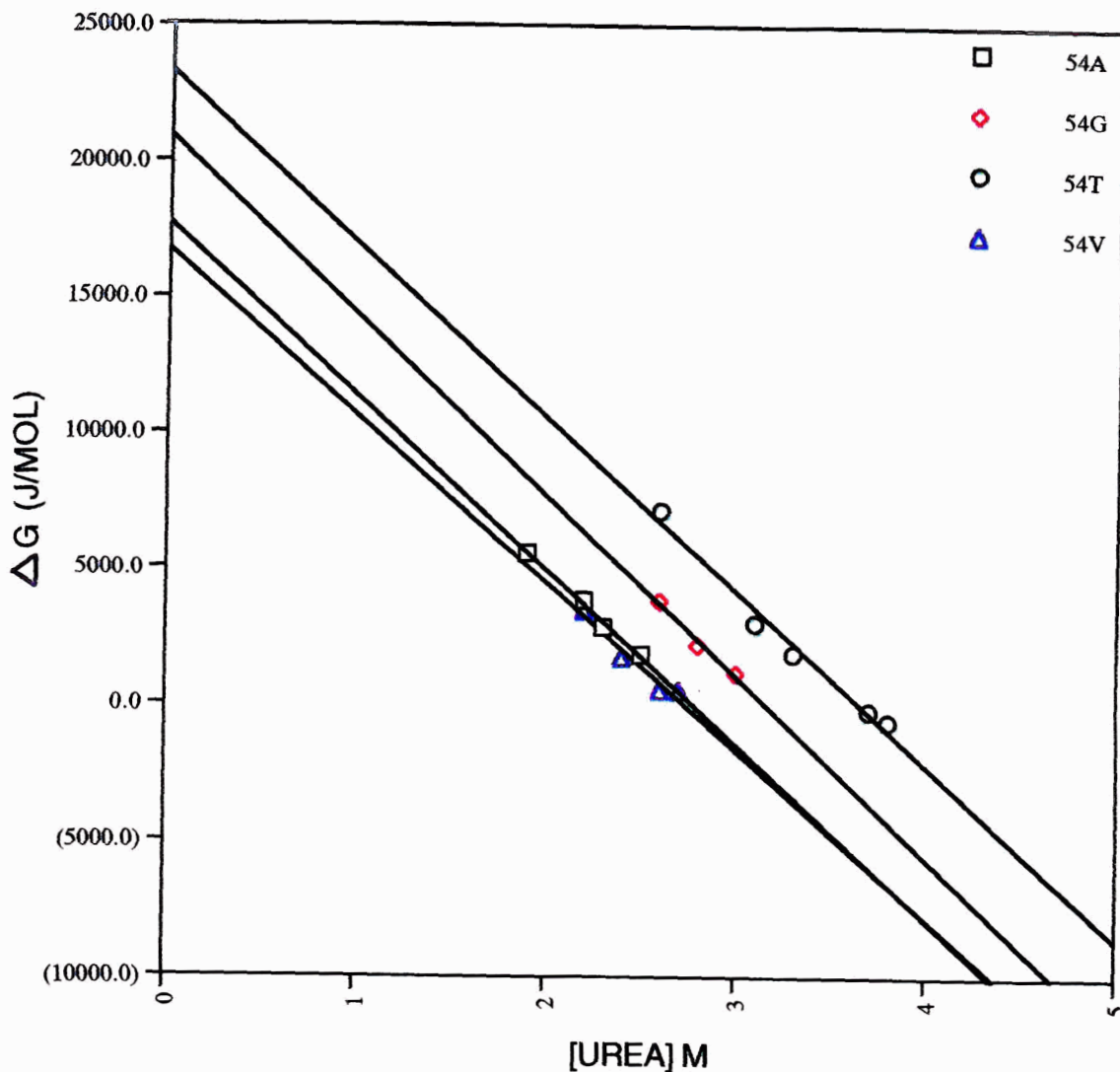


FIGURE 3.33. Free Energy Change of Unfolding of Calcium-free, F29W/54X Mutant Proteins Determined by Steady State Emission Fluorescence Spectroscopy

The $\Delta G_{\text{unf}}^{\text{H}_2\text{O}}$ was determined by plotting the free energy change calculated with equation 3 (section 1.4.3) versus the concentration of urea for the unfolding of the mutant proteins in the transition region. The y-intercept values ($\Delta G_{\text{unf}}^{\text{H}_2\text{O}}$) are tabulated in Table 3.6.

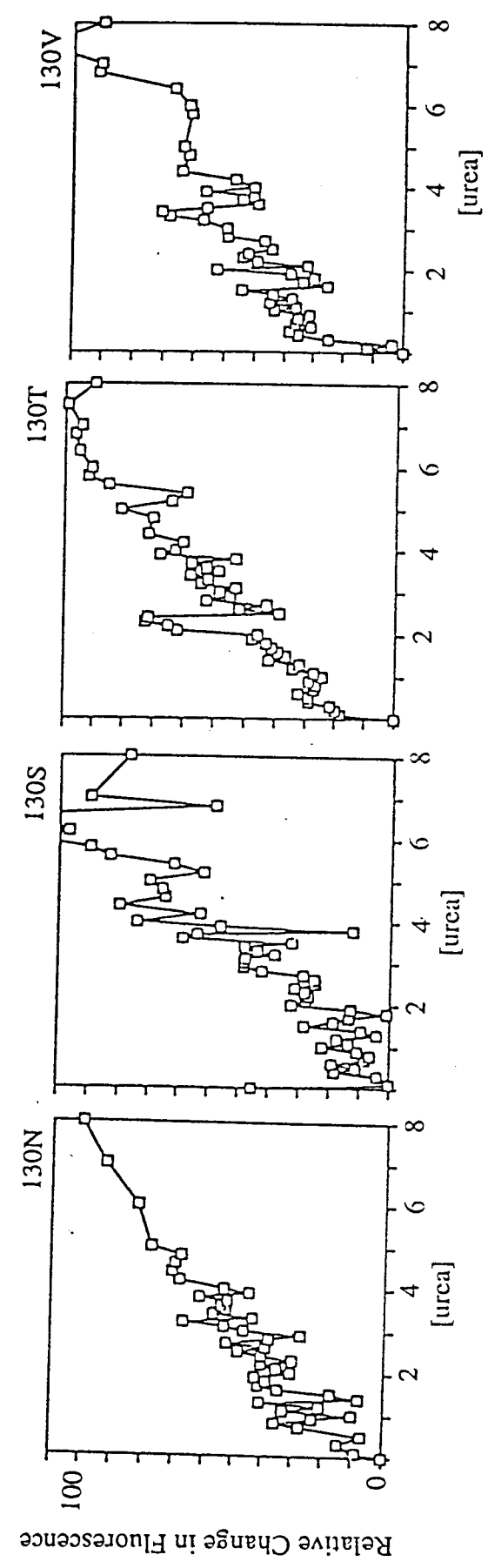
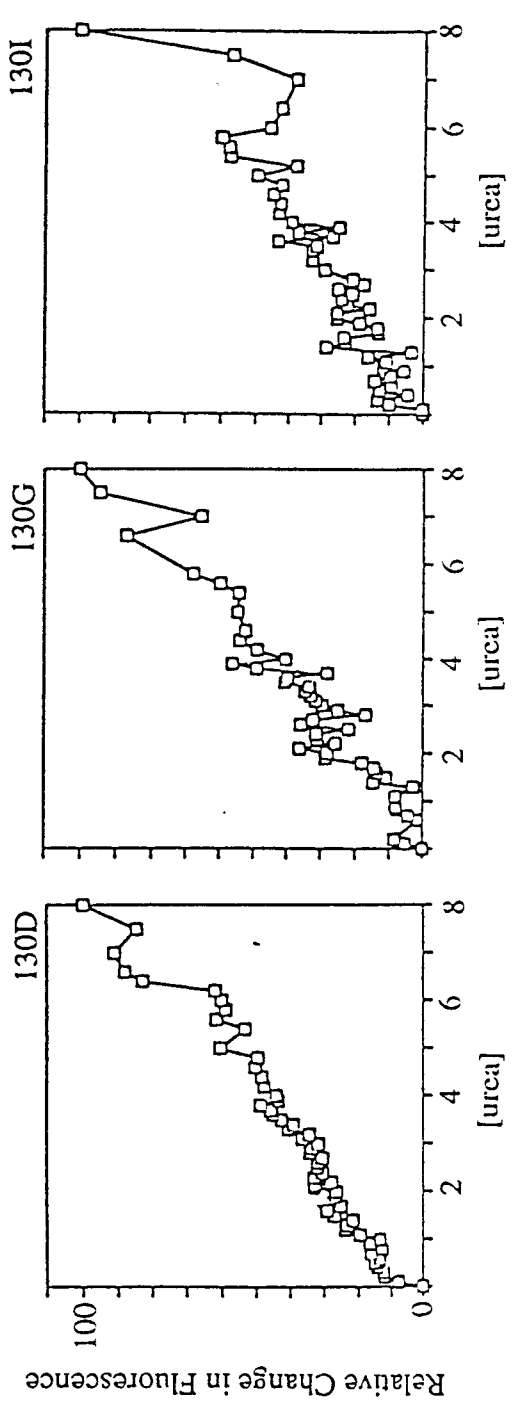


FIGURE 3.34. Urea Denaturation of Calcium-free, F105W/130X Mutant Proteins Followed by Steady State Fluorescence Emission Spectroscopy. Calcium-free mutant proteins were unfolded in the presence of 0.1M to 8M urea. These curves represent the relative change in the steady state fluorescence emission at 355nm. The proteins were excited at 278nm. Protein concentration was 5 μ m.

Table 3.5 Summary of Data for the Free Energy of Unfolding of the Calcium Free Form of Troponin C with Urea

Mutant Protein	CD		$\Delta\Delta G_{unf}^{H_2O}$ (kcal/Mol)	Steady State Fluorescence		$\Delta\Delta G_{unf}^{H_2O}$ (kcal/Mol)
	Slope "m"	$-\Delta G_{unf}^{H_2O}$ # (kcal/Mol)		Slope "m"	$-\Delta G_{unf}^{H_2O}$ # (kcal/Mol)	
54T	1.49+/-0.15	4.97+/-0.52	0.00	1.59+/-0.12	5.41+/-0.40	0.00
54A	1.46+/-0.23	3.96+/-0.60	1.01	1.53+/-0.11	4.23+/-0.29	1.18
54G	1.46+/-0.23	4.12+/-0.62	0.85	1.62+/-0.13	4.21+/-0.35	1.2
54S	1.62+/-0.26	5.66+/-0.91	-0.69	N/A**	N/A**	N/A
54V	1.61+/-0.20	3.32+/-0.41	1.65	1.62+/-0.13	3.48+/-0.28	1.93
130T	0.89+/-0.14	2.03+/-0.32	0.00	N/A*	N/A*	N/A
130D	1.09+/-0.10	4.68+/-0.45	-2.65	N/A*	N/A*	N/A
130G	1.23+/-0.12	4.95+/-0.47	-2.92	N/A*	N/A*	N/A
130I	1.11+/-0.14	4.61+/-0.63	-2.58	N/A*	N/A*	N/A
130N	1.29+/-0.18	5.41+/-0.76	-3.38	N/A*	N/A*	N/A
130S	1.43+/-0.22	6.00+/-0.91	-3.97	N/A*	N/A*	N/A
130V	1.60+/-0.25	6.42+/-0.99	-4.39	N/A*	N/A*	N/A

- * The free energy of unfolding could not be determined by fluorescence. A distinct transition between the folded and unfolded states was not observable as the change in fluorescence between the two states was too small to measure accurately.
- ** Due to an insufficient quantity of protein available, only 17 data points were recorded which failed to provide an accurate transition using fluorescence.
- # Calculated using non-linear regression analysis using GraFit with equation 6 (section 1.4.3)

Table 3.6 Free Energy of Unfolding of the Calcium-free Troponin C Mutants Using the Linear Extrapolation

Method

Mutant Protein	Circular Dichroism		Steady State Fluorescence	
	Slope "m"	$-\Delta G_{\text{unf}}^{\text{H}_2\text{O}}$ (kcal/Mol)	Slope "m"	$-\Delta G_{\text{unf}}^{\text{H}_2\text{O}}$ (kcal/Mol)
		$\Delta\Delta G_{\text{unf}}^{\text{H}_2\text{O}}$ (kcal/Mol)		$\Delta\Delta G_{\text{unf}}^{\text{H}_2\text{O}}$ (kcal/Mol)
54T	1.18+/-0.14	3.53+/-0.42	1.52+/-0.03	5.57+/-0.12
54A	1.27+/-0.08	2.74+/-0.18	1.53+/-0.06	4.23+/-0.13
54G	1.23+/-0.07	2.44+/-0.16	1.58+/-0.30	5.00+/-0.83
54S	1.20+/-0.28	3.09+/-0.80	N/A**	N/A**
54V	1.23+/-0.05	2.20+/-0.07	1.46+/-0.28	4.00+/-0.71
130T	0.84+/-0.055	1.64+/-0.12	N/A*	N/A*
130D	1.34+/-0.19	4.82+/-0.77	N/A*	N/A*
130G	1.11+/-0.17	3.83+/-0.063	N/A*	N/A*
130I	1.16+/-0.08	4.27+/-0.30	N/A*	N/A*
130N	1.37+/-0.035	5.06+/-0.14	N/A*	N/A*
130S	1.51+/-0.033	5.77+/-0.13	N/A*	N/A*
130V	1.31+/-0.45	3.97+/-1.59	N/A*	N/A*

- * The free energy of unfolding could not be determined by fluorescence.
- ** Due to an insufficient quantity of protein available , only 17 data points were recorded which failed to provide an accurate transition using fluorescence.
- # Calculated using equation 3 (section 1.4.3).

Table 3.7. Free Energy of Unfolding of the Calcium-free Form of Troponin C Mutant Proteins using the [urea]_{50%} values .

Mutant Protein	CD [θ] _{222nm}			Fluorescence		
	Slope "m"	[urea] _{50%} (M)	*ΔΔG[urea] _{50%} (kcal/Mol)	Slope "m"	[urea] _{50%} (M)	*ΔΔG[urea] _{50%} (kcal/Mol)
54T	1.18	2.98	0.00	1.52	3.65	0.00
54A	1.27	2.16	1.09	1.53	2.77	1.34
54G	1.23	1.98	1.21	1.58	3.16	0.75
54S	1.20	2.58	-0.48	N/A	N/A	N/A
54V	1.23	1.80	1.42	1.46	2.73	1.40
130T	0.84	1.95	0.00	N/A	N/A	N/A
130D	1.34	3.60	-2.15**	N/A	N/A	N/A
130G	1.11	3.46	-1.96**	N/A	N/A	N/A
130I	1.16	3.67	-2.24**	N/A	N/A	N/A
130N	1.37	3.70	-2.28**	N/A	N/A	N/A
130S	1.51	3.83	-2.44**	N/A	N/A	N/A
130V	1.31	3.04	-1.42**	N/A	N/A	N/A

* The $\Delta\Delta G[\text{urea}]_{50\%}$ values were calculated using the average slope, $\langle m \rangle$, calculated from the "m" values for the N-cap variants within one domain.

** These values of $\Delta\Delta G[\text{urea}]_{50\%}$ a value of $\langle m \rangle = 1.3$ was used which was calculated from the slopes for the amino acid substitutions excluding 130T. All of the substitutions in this domain result in an unknown change in the structure at the N-terminal end of the G-helix.

Table 3.8. Summary of the Change in Stability with N-cap Mutation in Going from a Threonine Residue to Mutant X For Each Domain.

Mutant Protein	$-\Delta G$ U to F-Ca (kcal/Mol)	$-\Delta G$ F-Ca to F+Ca (kcal/Mol)	$-\Delta G$ U to F+Ca (kcal/Mol)	$\Delta\Delta G$ Thr to Mutant (kcal/Mol)
54T	5.19**	7.90	13.09	0.00
54A	4.10**	7.43	11.53	1.56
54G	4.17**	7.23	11.40	1.69
54S	5.66	7.91	13.57	-0.48
54V	3.40**	7.59	10.99	2.10
130T	2.03	10.69*	12.72	0.00
130D	4.68	10.35*	15.03	-2.31
130G	4.95	10.24*	15.19	-2.47
130I	4.61	10.04*	14.65	-1.93
130N	5.41	10.44*	15.85	-3.13
130S	6.00	10.69*	16.69	-3.97
130V	6.42	7.41	13.83	-1.11

* Values taken from previous work on the high affinity domain (Trigo-Gonzalez, 1993).

** Average value from the Fluorescence and CD data.

3.9. Analysis of Polyclonal Antibody Raised Against cII-Fusion-Chicken Skeletal Troponin C.

3.9.1 Western Blot Analysis of Polyclonal Antibody

The polyclonal antibody was tested against cII-fusion chicken skeletal TnC, purified chicken skeletal TnC (cII fusion peptide removed) (Figure 3.35) and rabbit TnC (Figure 3.36). The Western Blot showed strong binding of the antibody to the fusion protein as expected. A much lighter band was observed for the purified TnC. Binding to rabbit skeletal TnC was not observed. A Western Blot was performed as above but a more sensitive chemiluminescent system of detection (USB) was used. Binding of purified chicken skeletal TnC was more pronounced but no band was observed for rabbit skeletal TnC. Since the proteins are unfolded on an SDS gel another method was used to detect antibody binding to the proteins.

3.9.2. Enzyme Linked Immunosorbant Assay of Polyclonal Antibody

Antibody binding to the purified chicken skeletal TnC was detected even when the antibody was diluted 1/3,000. Binding to fusion TnC was stronger with the signal for the 1/3,000 dilution being two times as strong as seen for the purified chicken skeletal TnC. No binding was observed in wells coated with rabbit skeletal TnC.

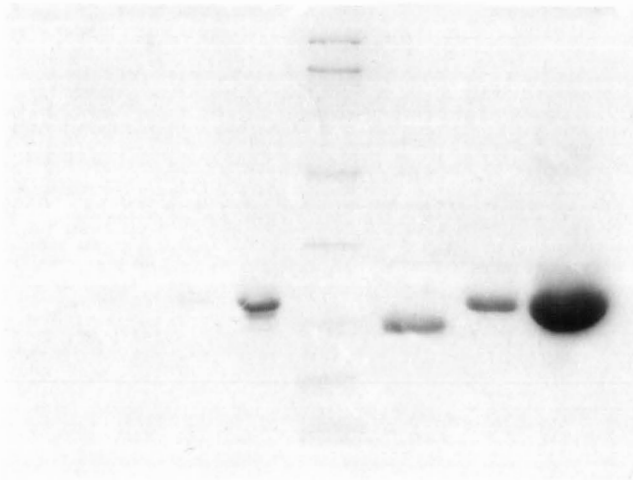
FIGURE 3.35 Western Blot Analysis of Polyclonal Antibody

Panel A: Coomassie stained SDS gel Lane 1: 1ng of Fusion TnC. Lane 2: 10ng of Fusion TnC. Lane 3: 100ng of Fusion TnC. Lane 4: 500 ng of Fusion TnC. Lane 5: 1000 ng of Fusion TnC. Lane 6: Low Range Molecular Weight Marker (Biorad). Lane 7: Purified Chicken Skeletal TnC Standard. Lane 8: cII Fusion chicken skeletal TnC standard. Lane 9: cII Fusion Chicken Skeletal TnC before FPLC purification.

Panel B: Western Blot of duplicate gel showing the binding of the polyclonal antibody to both the cII-fusion chicken skeletal TnC and chicken skeletal TnC.

PANEL A

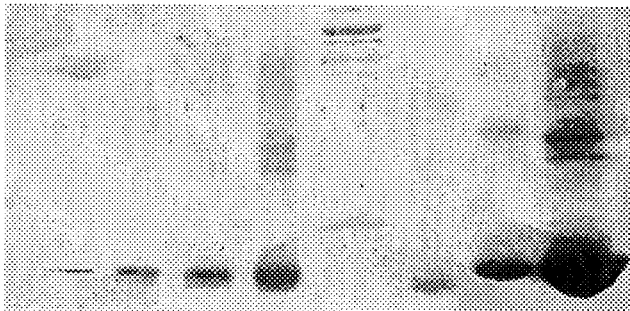
1 2 3 4 5 6 7 8 9



Fusion TnC
TnC

P A N E L B

1 2 3 4 5 6 7 8 9



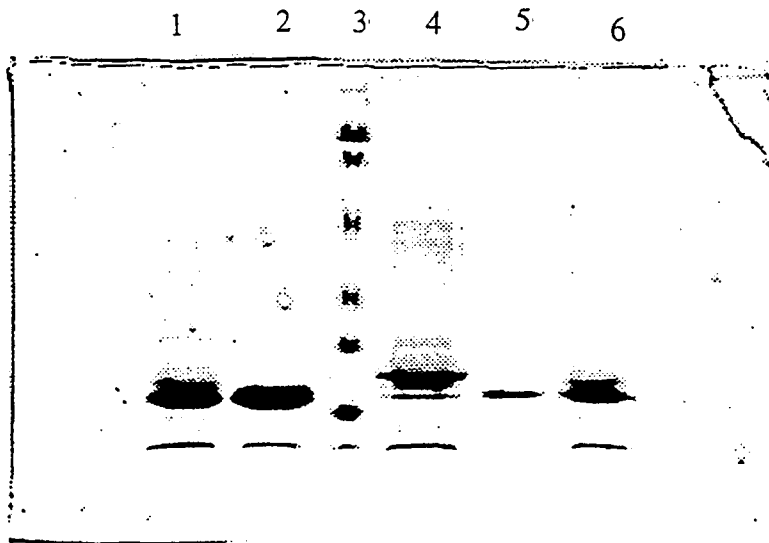
— Fusion TnC
— TnC

FIGURE 3.36. Western Blot Analysis of Rabbit Skeletal TnC and cII-Fusion Skeletal TnC.

Panel A: Coomassie stained SDS gel. Lane 1: Chicken skeletal TnC . Lane 2: Rabbit skeletal TnC. Lane 3: Molecular weight marker (Biorad). Lane 4: cII-Fusion chicken skeletal TnC. Lane 5: Rabbit skeletal TnC. Lane 6: Chicken skeletal TnC.

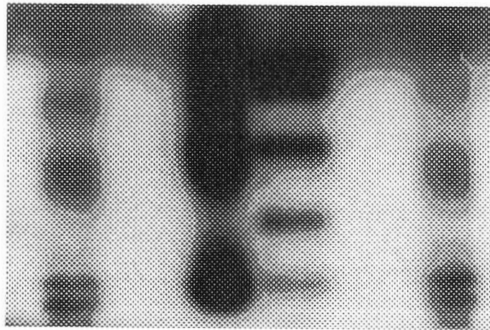
Panel B: Western Blot of duplicate gel (inverted) Lane 1: Chicken skeletal TnC. Lane 2: Rabbit skeletal TnC. Lane 3: cII-Fusion chicken skeletal TnC. Lane 4: Molecular weight marker (Biorad). The markers are available from Amersham with the biotin-streptavidin system to generate a signal upon development of the Western Blot . Lane 5: Rabbit skeletal TnC. Lane 6: Chicken skeletal TnC . The gel was developed using the ECL Detection System and exposure of the luminescent product on blue-light sensitive autoradiography film (Hyperfilm, ECL).

PANEL A



P A N E L B

1 2 3 4 5 6



— Fusion TnC
— TnC

4. DISCUSSION

Troponin C is a predominantly α -helical, calcium-binding protein arranged in four helix-loop-helix motifs (Figure 1.5). In the formation of an α -helix, hydrogen bonding occurs between the helix backbone NH group (donor) and the helix backbone CO group (acceptor) located 4 residues away (Figure 4.1). However, the first four residues of the helix are unable to form these "main chain" bonds. Instead, the side chains of these residues interact with the backbone of the helix to form hydrogen bonds whenever possible. Another residue involved in stabilizing the helix is called the N-cap; that is the residue immediately preceding the helix. The side chain of the N-cap forms a hydrogen bond with the backbone NH of the third residue of the helix which may in turn form a hydrogen bond between its side chain and the NH group of the N-cap. Statistically, the most favourable interaction occurs when a serine residue is the N-cap and N3 is a glutamic acid residue. The N-cap residues of the C- and G-helix of native chicken skeletal troponin C are threonine residues. The N3 residue of the C-helix is Glu 57 while N3 of the G-helix is Asp 133 (Figure 1.4).

Previous studies of troponin C (Trigo-Gonzalez et al, 1993) examined the paired calcium-binding sites of the high-affinity domain. It was shown that the calcium-affinity of the protein could be modified by changing the N-cap residue of the G-helix. A serine residue, which has one less methyl group in its side chain than the wild type threonine residue, had the same calcium-affinity, while the large hydrophobic side chain of an isoleucine residue produced a four-fold decrease in affinity. Aspartic acid and glycine both decreased the calcium-affinity, but not as much as the isoleucine residue. Asparagine, which is often found as the N-cap of a helix, decreased the calcium-affinity of TnC. We wished to examine whether this was a general feature of paired calcium-binding sites providing information on how these proteins bind their ligands. If it was a

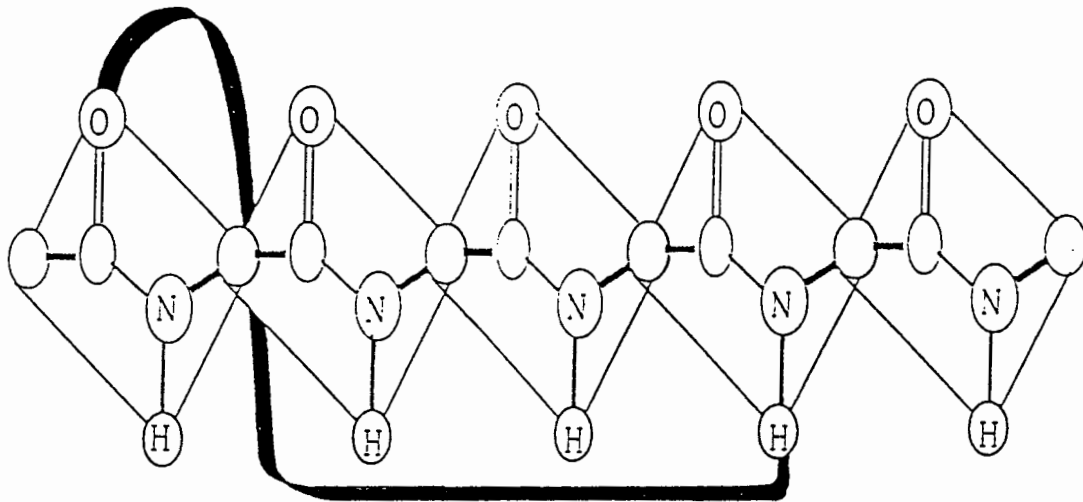


FIGURE 4.1. Hydrogen Bonding Pattern of the α -helix.

This figure is a diagrammatic representation of the hydrogen bonding pattern of the backbone of the α -helix. Including the groups involved in the formation of the hydrogen bond, there are 13 atoms between the NH donor and CO acceptor in an α -helix. Figure adapted from Mathews and vanHolde, 1990.

general feature, other calcium-binding proteins could be modified in a similar way to optimize their calcium-binding properties.

To determine the mechanism by which the calcium-affinity was attenuated, the protein was examined from three identifiable folded states: the unfolded state (U), the folded but calcium-free state (F-Ca) and the folded, calcium saturated state (F+Ca) with 4 calcium ions bound. Does the N-cap residue influence calcium affinity by an effect on the stability of the folded states, by an effect on the unfolded state or both? For example, when a substitution increases the affinity of a pair of sites, did it do so because of an increased stability of the folded state or a decreased stability of the unfolded state?

Urea denaturation was used to measure the change in the free energy of stabilization from the unfolded state (U) to the folded calcium-free state (F-Ca). The unfolding of the protein was monitored by Far UV CD and steady state fluorescence spectroscopy. The change in the free energy between the F-Ca and the F+Ca state was measured by calcium titration.

The amino acid substitutions of the N-cap of the C-helix were selected for comparison to the N-cap residues of the G-helix. Would the same residue at the N-cap of both helices produce the same change in stability, secondary structure and calcium-affinity?

4.1 Mutagenesis

The goal of the PCR mutagenesis was to substitute the threonine residue at the N-cap position of the C-helix with the following seven amino acids: Alanine (Ala), Aspartic acid (Asp), Glycine (Gly), Isoleucine (Ile), Asparagine (Asn), Serine (Ser) and Valine (Val). We were unable to isolate the Asn, Ile and Asp residues. The aspartic acid residue was the only mutant from the GXC and GXC2 oligonucleotides which could not be isolated. The reason for this is

unknown but it is possible that the product was lethal to the host cell. In previous work with the G-helix, this same mutation at the N-cap was difficult to isolate. The AXC primer included the wild type sequence (ACC) in the mixture. A new oligonucleotide was made excluding the substitution X=C and G since the serine mutant (AGC) had already been isolated. Nevertheless, the ACC sequence predominated in later clones. Sequencing verified the presence of the ACC sequence in a sample PCR reaction mixture. The problems may have occurred in either the PCR synthesis or in the transformation of the bacteria.

The expression of the gene for cII-fusion TnC is under the control of the temperature sensitive cII repressor protein. The K12 strain of *E. coli* synthesizes the cII repressor protein constitutively whereas the DH5 α strain of *E. coli* does not. Since the repressor protein was not present in the latter strain the fusion protein would be expressed uncontrollably. The bacterial cells responded by deleting portions of the plasmid DNA resulting in DNA fragments of varying sizes when screened by restriction digestion. To prevent expression of the gene in the transformed cells, the PCR fragments were ligated into pUC18 as per section 3.2.5. This would reduce selective pressure on particular mutations within the TnC sequence.

The difficulties in isolating certain sequences from heterogeneous primers suggests that future experiments to isolate mutants should use one oligonucleotide specific for each mutant. The PCR fragments generated should be ligated into pUC18 for sequencing. Once identified, the mutant PCR fragment could then be cloned into the pLcII vector and using the method of electroporation, the K12 strain of *E. coli* should be transformed.

For this thesis, the following mutant proteins were studied:

- 1) in the low-affinity domain, the alanine, glycine, serine and valine N-cap substitutions were constructed for comparison to the native threonine N-cap

residue and 2) in the high-affinity domain, the threonine, glycine, aspartic acid, isoleucine, asparagine, serine and valine N-caps were examined. Stock clones were sequenced prior to expressing the mutant proteins.

4.2 Mutations at the N-cap Position of the Helix

4.2.1. Studying the Proteins by Fluorescence

In previous work (Pearlstone et al, 1992, Trigo-Gonzalez et al, 1992), spectral probes were inserted into Troponin C by site-directed mutagenesis. A phenylalanine residue was replaced with a tryptophan residue at either position 29 or position 105 in the amino acid sequence. The tryptophan reporters precede the first co-ordinating residue of binding loops 1 and 3 respectively. The two domains of TnC were studied separately using one tryptophan probe at a time. The changes associated with a mutation at the N-cap position of either the C- or G-helix were monitored by measuring the relative change in steady state fluorescence. The change in spectral properties was due to conformational changes in the vicinity of the tryptophan probe as the protein unfolded or bound calcium. A small perturbation in the environment of the reporter group generally resulted in a large change in fluorescence. However, the tryptophan residues were only expected to report on their local environment (Smith, C.J. et al, 1991). If a mutation affected the low-affinity domain but not the high-affinity domain, a difference should be observed in the environment of Trp 29 but not Trp 105. Only those changes which are in close proximity to the tryptophan residue should affect the orientation of the indole ring which will vary the degree of quenching of the fluorescence by the solvent or by neighbouring residues through charge transfer. An example of this type of quenching was observed with the 54V and 54G mutants in the low-affinity domain between 0.1M and 2M urea. There was an initial increase in fluorescence intensity when urea was

added to the valine and glycine mutant proteins. The side chain of a neighbouring aspartate residue (such as Asp 30 which in loop I is not hydrogen bonded in the calcium-free state (Krudy et al, 1992)) may be quenching the fluorescence of the tryptophan in the folded state but as the protein begins to unfold, the carboxyl group may not be in the correct orientation to do so. This effect was not observed for all of the mutant proteins suggesting that the mutations produced subtle variations in the 2^o structure around the tryptophan residue. At higher concentrations of urea (2M - 4M) , all of the F29W mutant proteins showed a decrease in fluorescence due to the quenching of the tryptophan fluorescence on exposure to the solvent. A 10nm red shift was associated with the unfolding of the protein. In the second part of the denaturation curve there was an increase in fluorescence intensity. Because the change varied linearly with denaturant concentration, a simple solvent effect was indicated. The F105W/130X proteins have little structure associated with the high-affinity domain in the absence of calcium (Tsalkova & Privalov, 1985). Except for the F105W/130V mutant, the fluorescence intensity of the F105W/130X proteins increased without the large red shift of the F29W/54X proteins. This would suggest that the tryptophan residue was already exposed to the solvent in the calcium-free state. The observed linear increase in fluorescence intensity for all but the 130V mutant indicated a simple solvent effect.

The calcium titration of the F29W/54X mutant proteins was followed by the change in the fluorescence intensity of the tryptophan probe at 335nm. The small blue shift associated with the binding of calcium along with an increase in fluorescence intensity suggested that the tryptophan residue became more buried within the protein as calcium ions were bound. The large blue shift associated with the binding of calcium to the F105W/130X mutant proteins

together with a decrease in the fluorescence intensity suggested that the tryptophan residue was buried as the protein bound calcium and that the fluorescence was quenched by the side chain of nearby residues such as aspartic acid and glutamic acid (Dryden & Pain, 1989, Garcia et al, 1995).

The fluorescence emission spectra of all the F29W/54X proteins were the same in the calcium-free state. The tryptophan probe was in a similar environment for all of the mutants of the low-affinity domain at saturating calcium concentrations as well, which suggests that the mutation at the N-cap did not drastically alter the folded state of TnC (Figure 3.21).

The fluorescence emission spectra of all the F105W/130X proteins (Figure 3.22), except for the F105W/130V mutant (Figure 3.23), were the same in the calcium-free state. A similar change in the environment of the tryptophan probe was observed for the calcium-saturated state of the mutant proteins except for the F105W/130V mutant.

Compared to the F105W/130T, the calcium-affinity of the F105W/130V mutant decreased by two orders of magnitude (refer to the legend of Table 3.2.) The calcium off-rates of the F105W/130V mutant were the same as the rates observed for the F29W/54T protein (Table 3.3). The valine in the high-affinity domain may have altered the properties of binding loop IV to resemble those of binding loop II. This suggests that the function of a calcium-binding protein could be modified by a substitution of the N-cap residue.

The Hill co-efficients calculated from the calcium titrations were observed to be excessively high. Since the F29W probe only measures a change in the environment of the low-affinity domain, the maximum value expected should have been close to 2. ie. equal to the number of binding sites. A value of 3.85 for threonine and 3.75 for serine were calculated. The destabilizing mutants however, showed a decrease in the Hill coefficient ranging from 3 for the valine

residues down to 2.12 for glycine. The reason for the steepness of the curve is not known however this result has been observed by other groups working with the low-affinity domain fragment (residues 1-90) of chicken skeletal TnC with an F29W or an F22W probe inserted into the sequence (Li et al, 1995). Titrations of the N-terminal fragment without a tryptophan probe, monitored by NMR, have also shown steep binding curves which cannot as yet be explained (Li et al, 1995). The high values for the Hill coefficients could be concentration dependent. Since the protein concentration was 5 μ M, it is unlikely that aggregation was the problem.

While steady state fluorescence emission spectroscopy reported a decrease in the affinity for calcium it gave no information on the number of intact binding sites. The decrease in the Hill coefficient for the valine mutants could have been indicative of a decrease in the co-operativity of calcium-binding or as a result of the loss of a functional binding site. The flow dialysis experiments confirmed that the protein still had four functional binding sites. These experiments also showed a stepwise binding of calcium to the valine mutants (Figure 3.26) whereas the threonine N-cap proteins showed a single transition in the binding of calcium. These results can be interpreted to mean that the decrease in the Hill coefficient for the valine mutant was due to a decrease in the cooperativity of binding.

4.2.2 Studying the Proteins by Far UV CD Spectroscopy

Far UV CD spectroscopy was used to monitor the global changes in conformation associated with a mutation at either of the N-cap positions. This method was used to monitor the unfolding of the protein in urea. The change in secondary structure was measured by monitoring the change in helical content for each of the three folded states of the protein. All of the mutant proteins had

similar values when fully unfolded. For the calcium-free folded state, two of the N-cap mutants in the high-affinity domain, aspartic acid and glycine, showed a higher helical content than with the threonine residue as judged by their $[\theta]_{222\text{nm}}$ values (Table 3.1). In the low-affinity domain, the serine mutant showed a significant increase in helical content even without binding calcium. The calcium-saturated proteins were varied in their helical content.

Three N-cap mutants of the C-helix were available with the tryptophan probe at position 105 instead of at position 29. The CD spectra of the F29W/54T/G/and V mutant proteins (Figure 3.19) were compared to the spectra of the F105W/54T/G or V mutant proteins (Figure 3.20). We wished to examine the contribution made by the tryptophan probe to the 2° structure. The 3 spectra for each of the glycine mutant proteins were compared. The unfolded state and the folded states were the same regardless of which tryptophan probe was present in the sequence. The spectra for the wild type protein (54T) showed a small increase in the negative ellipticity (approximately 1.5mdeg) for the 2 folded states with the tryptophan probe at position 105 when compared to the wild type proteins with a tryptophan at position 29. (Table 3.1). The 54V mutant protein showed a very large increase in the negative ellipticity of the 2 folded states with the probe at position 105 when compared to the protein with a tryptophan residue at position 29. This suggests that with a valine at position 54 and a tryptophan at position 105 an interaction may have been introduced between the two domains as the protein folds. This interaction cannot be defined at this time. Further CD studies of the F105W/54X proteins is required.

4.2.3. Urea Denaturation

Urea was selected as the denaturant. It is known that urea binds to the surface of the protein. It is also able to access the interior of a folded protein

because it is uncharged. The exact nature of the interaction however is not known. It is predicted that urea interacts with both nonpolar and polar surfaces of proteins more favourably than water does (Creighton, 1993).

The method of analysis is outlined in the introduction (section 1.4.3). It was observed that the baselines in the pre- and post-transition region were not flat. Therefore F_N and F_U were obtained by extrapolating the initial and final baselines to the Y-axis. This procedure corrected for the fluorescence from the buffer and urea solutions used in the denaturation process (Pace, 1992). The data set was then fit to equation 6 with GraFit using non-linear regression analysis. The $\Delta G_{\text{unf}}^{\text{H}_2\text{O}}$ value obtained by this analysis was a measure of the conformational stability of each mutant protein. By comparing the $\Delta G_{\text{unf}}^{\text{H}_2\text{O}}$ values of the mutants to the wild-type protein (ie. with a threonine at the N-cap position of the C- or G-helix) the $\Delta\Delta G_{\text{unf}}^{\text{H}_2\text{O}}$ value was obtained.

The values of ΔG for the points in the transition region of each unfolding curve were plotted against the urea concentration (Figure 3.29, 3.31, 3.33). The long extrapolation to 0M urea tended to seriously underestimate the value of $\Delta\Delta G_{\text{unf}}^{\text{H}_2\text{O}}$ because a small error in the slope, "m", can produce a large error in the value of $\Delta\Delta G_{\text{unf}}^{\text{H}_2\text{O}}$. The calculations using [urea]50% (equation 8) were in the same range as those obtained from the non-linear regression analysis of the F29W/54X proteins .

The $\Delta\Delta G_{\text{unf}}^{\text{H}_2\text{O}}$ values determined by plotting ΔG versus [urea] for the F105W/130X proteins, were inconsistent with those calculated using equation 6. The "m" values were similar for all the mutant proteins except 130V, but they were all larger than the "m" value of the wild-type protein. A large change in the "m" value is an indication that the mutation has resulted in a structural change in the protein (Serrano, 1992). While fluorescence spectroscopy did not reveal a change in the structure as a result of the mutations at the N-cap (except for the

valine), it appears that the increased stability in the high-affinity domain is related to a change in the folded structure of the protein. All of these mutant proteins (F105W/130 D/G/N/I/S) have slopes which are within 0.33 units of each other (comparable to variations in "m" values of 0.31 units reported by Serrano and Fersht in their study of Barnase) suggesting that the method was not the reason for the divergent "m" value.

Fluorescence spectroscopy revealed a change in the structure of the protein when a valine residue was inserted at position 130. The change in structure was confirmed by an "m" value which diverged not only from the wild-type protein but also from the other substitutions made at this position.

The free energy difference, $\Delta\Delta G_{\text{Thr to Mut}}$ for U \rightarrow F-Ca, as a result of the substitution at the N-cap of the C-helix (F29W/54X) ranged from 1.79 kcal/mol less stable to 0.47 kcal/mole more stable than the wild type (Table 3.8). The mutants, in decreasing order of stability were:

Ser > Thr > Ala / Gly > Val.

The free energy difference, $\Delta\Delta G_{\text{Thr to Mut}}$ for U \rightarrow F-Ca, as a result of the substitution at the N-cap of the G-helix (F105W/130X) ranged from 4.39 kcal/mol to 2.58 kcal/mol more stable than the wild-type (Table 3.8). The mutants in decreasing order of stability were:

Val > Ser > Asn > Gly > Asp / Ile >> Thr.

4.2.4. Calcium Binding Studies

The calcium-affinity of the C-helix mutant proteins in decreasing order of affinity was as follows:

Ser/Thr > Val > Ala > Gly.

The calcium affinity of the valine mutant of the G-helix was measured in this study. The calcium-affinity of the G-helix mutant proteins reported in a previous study, together with the valine from this study, in decreasing order, are as follows :

Ser / Thr > Asn > Asp > Gly > Ile >>> Val.

The calcium off-rates measured for the F29W/54X proteins (Table 3.3) were related to the $\Delta\Delta G_{\text{Thr to Mut}}$ for $U \rightarrow F_{+Ca}$, listed in table 3.8 as follows:

Thr > Ala > Gly > Val

Referring to table 3.3, the rate at which calcium is lost increases in the same order. The order in which calcium is removed from the two loops of the low-affinity domain cannot however be assigned conclusively. Since the variable calcium off-rate is directly dependent on the identity of the N-cap residue it is likely that the calcium is removed from loop II and then loop I. It should be noted that the largest change in the fluorescence signal is associated with the fast rate. But the tryptophan probe is located next to the first calcium co-ordinating residue of loop I. Referring to the crystal structure of chicken skeletal TnC, it appears that the tryptophan probe may be very close in space to binding loop II because of a short β -sheet joining the two loops. This could explain the large decrease in fluorescence intensity associated with the loss of the calcium ion from loop II. However, recent NMR studies have shown a larger perturbation of loop II on binding the first equivalent of calcium to the N-terminal fragment of TnC

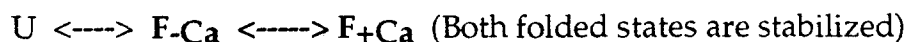
(residues 1-90) (Li et al, 1995). This inconsistency may be due to the fact that the NMR studies are using only a fragment of TnC rather than the whole protein.

4.2.5. Analysis of each N-cap mutation

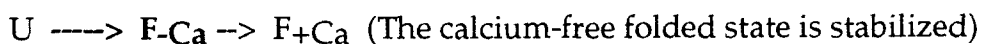
(a) The Serine Mutation

In the low-affinity domain, the serine N-cap induced a large change in the secondary structure of the protein in the calcium-free state (Figure 3.17). This stabilization of the secondary structure was expected since the serine/glutamic acid combination for the N-cap/N3 positions of a helix are reported as the most frequently occurring pairing and the most stable in the formation of a helix (Richardson and Richardson, 1988). The orientation of the serine in relation to the glutamic acid residue allows the reciprocal binding between the side chains and main chain NH groups of the two residues forming a stabilizing structure which has been termed the "capping box" (Harper and Rose, 1988).

A large free energy change (-5.66 kcal/mol) was observed for the folding of the calcium-free state with a $\Delta[\theta]_{222\text{nm}}$ of 16.02. A second large structural change, seen as a large increase in the negative ellipticity ($\Delta[\theta]_{222\text{nm}}$ of 5.18) was observed upon binding calcium producing a free energy change of -7.91 kcal/mol. Therefore, a serine residue at the N-cap position of the C-helix stabilizes both the calcium-free and the calcium saturated folded states of the protein, with the largest contribution to the 2° structure observed for the calcium-free folded state. This is illustrated using the same equilibrium described in section 1.3.



In the high-affinity domain, the serine N-cap does not induce as large a change in the helical content in either of the folded states when compared to the wild-type protein. This residue however results in a large free energy of stabilization (Table 3.8) upon folding. The free energy change from the calcium-free to the calcium-saturated state is essentially the same as for the threonine N-cap. The N3 residue of the G-helix is an aspartate residue instead of the glutamate residue found at the same position of the C-helix. Since the Glu and Asp side chains differ by only one methyl group, it has been speculated that the latter is not in close enough proximity to form a "capping box" with the serine residue as described above (Harper and Rose, 1988, Zhou et al, 1994). The interaction between Ser130 and Asp133 of the C-helix is still more stabilizing than the Thr130/Asp133 hydrogen bonding interaction observed in the crystal structure of the wild-type protein (Satyshur et al, 1988). It may be that this interaction only occurs for the threonine residue once the calcium ion is bound whereas the longer side chain of the glutamate can form a hydrogen bond to the serine residue in the calcium-free state. This mutation produced the smallest change in the secondary structure on binding calcium (Figure 3.18) but once folded this residue forms the most stable interaction observed in the high-affinity domain. Since the largest degree of stabilization is observed for the calcium-free folded state (Table 3.8) this state is highlighted in the equilibrium.

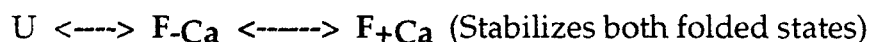


(b) Analysis of the Asparagine Mutation

Asparagine is often found as an N-cap but its presence depends on the backbone conformation of the protein. A large side chain must be accommodated and more degrees of freedom are lost for Asn compared to Thr in

the N-cap position. Asparagine is speculated to be well suited as the N-cap because it not only has a side chain that mimics a peptide but the entire residue mimics a dipeptide. Asparagine would help specify the location of the N-terminal end of the helix because it stabilizes the first turn of the helix while providing an additional interaction equal to that of a residue (Richardson and Richardson, 1988).

In the high-affinity domain, Asn produced the most pronounced change in secondary structure when compared to the other polar amino acids (Table 3.1). It was more stable than the threonine residue, but less stable than serine, in both the calcium-free and calcium-saturated folded states. While both folded states are stabilized, the calcium-free state showed a larger stabilizing effect as a result of the Asn substitution, with a larger change in secondary structure when compared to the calcium-saturated state. An asparagine residue at the N-cap of the C-helix was not available for comparison.

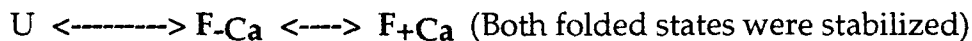


(c) Analysis of the Aspartic Acid Mutation

The aspartate N-cap induced a higher degree of helical content than the threonine residue but with a ΔG_U to $F\text{-Ca}$ of -4.68 kcal/mol, it was not the best choice of N-cap as observed by Forood's group. It was only slightly more stable than isoleucine, the least stable amino acid substitution for the folding of TnC to the calcium-free folded state. The Asp residue carries a negatively charged side chain which interacts favourably with the partial positive charge of the helix dipole (Creighton, 1987, Forood et al, 1993). The N1, N2 and N3 residues of the G-helix however, are negatively charged (Glu, Glu and Asp) and so the presence

of an aspartic acid residue at the N-cap was expected to be destabilizing due to electrostatic repulsion.

The largest calcium-induced change in secondary structure occurred with the Asp N-cap residue (Table 3.1). In other proteins, the Asp residue has been observed to form a hydrogen bond to the amino-terminal NH group forming a stable structure (Forood et al, 1993). This type of interaction may occur early in the folding pathway accounting for the large increase in helical content from the unfolded state to the calcium-free folded state. From the ΔG values in Table 3.8, we see that aspartate stabilized the folded calcium-free state a little more than the calcium-saturated state and that overall, it is more stabilizing to the helix when compared to threonine.

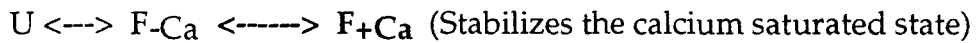


(d) Analysis of the Glycine Mutation

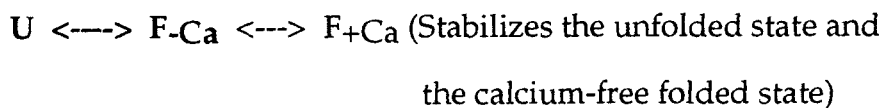
Glycine was more stable than threonine as the N-cap of the G-helix. Other studies have also reported that glycine has a stabilizing effect on helices (Chakrabartty, 1993, Serrano et al, 1992). However, with glycine at the N-cap of the G-helix, there is no side chain to form an interaction to Asp 133. The N-cap residue itself also has an exposed NH group which needs to form a hydrogen bond with the solvent or a neighbouring residue for stability. With a glycine residue, there is no steric hindrance to solvation which contributes to the observed stability.

It has been observed by other groups that the side chain of a glutamate residue at the N2 position of the helix can rotate along χ_1 to form a weak interaction with the NH group of the N3 residue. This interaction may serve as a surrogate N-cap as was observed for Chymotrypsin Inhibitor 2, T4 lysozyme and

Barnase (Chen & Fersht, 1994). Since glycine does not contribute to steric hindrance at the N-cap position, a similar arrangement may be possible between Glu 132 and the NH group of Asp 133 providing a larger measure of stabilization ($\Delta\Delta G = -2.47$) than that observed for the wild-type TnC.

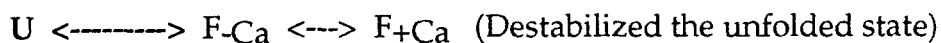


In the low-affinity domain, glycine was less stable than threonine with a smaller change in secondary structure on binding calcium. However, it provided a greater degree of stability than a substitution with a larger hydrophobic side chain in the calcium-saturated state. Glycine cannot form a stabilizing interaction with the side chain of Glu 57. The longer side chain of a glutamate residue at N3 may inhibit the interaction between N2 and N3 described above. The helix may also be destabilized by the two Glu side chains side by side which may inhibit solvation of the NH group at N3. Of all the residues, glycine loses the greatest amount of entropic freedom on folding which also contributing to its destabilization relative to threonine in the low-affinity domain. Of the two folded states, the glycine substitution provided the least amount of stabilization for the calcium saturated state. There is evidently some kind of helix-forming propensity associated with Gly at the N-cap since the calcium-free folded state was observed to have a substantial change in 2^o structure (Figure 3.17)



(e) Analysis of the Alanine Mutation

The NH group of the alanine residue does not appear to be stabilized by solvation as it was for glycine, probably due to the bulkier side chain. As the N-cap of the C-helix, alanine does not suffer a loss in entropic freedom, but the exposure of its more hydrophobic side chain to solvent was expected to be more destabilizing. In the low-affinity domain, the large lysine side chain at N1 may provide some shielding of the side chain from the solvent which may account for its slightly higher stability when compared to glycine (Table 3.8). This same shielding may also prevent the solvation of the NH group of the alanine residue itself which is expected to be a destabilizing factor. As explained for the glycine N-cap, Glu 56 could be favorably oriented to form a surrogate N-cap. The negative charge of the Glu side chain could also form a stabilizing interaction with the positive charge on the lysine side chain. The combination of potentially stabilizing and destabilizing factors resulted in very similar helix forming tendencies, calcium affinities and stabilities for the alanine and glycine N-caps in the low-affinity domain. A slightly higher calcium-affinity was observed for alanine compared to glycine. The alanine side chain may become less exposed to solvent in the calcium-saturated state, making it more stable. In the high-affinity domain we did not have an alanine N-cap to compare to glycine. Overall, the alanine residue may not contribute to the stabilization of a folded state. It is more likely that it is destabilizing the unfolded state.



(f) Analysis of the Valine Mutation

As the N-cap of the C-helix, valine was the most destabilizing substitution ($\Delta\Delta G = 2.10$) but it resulted in the largest increase in negative ellipticity when

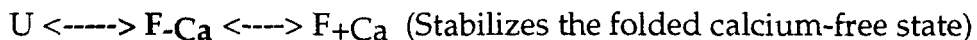
compared to the other hydrophobic residues examined in the low-affinity domain (Table 3.1). There are a number of possible destabilizing factors associated with a larger hydrophobic residue inserted at the N-cap position. A valine residue exposes a larger hydrophobic side chain to the solvent. The amide NH group at Asp 133 has no hydrogen bonding partner through the N-cap residue. The larger side chain of the valine residue may contribute to steric crowding with the side chains of the first four residues of the helix. This could counter any stabilizing effect from the charge-charge interaction of the positively charged lysine side chain and the 2 negatively charged glutamate side chains at position N1, N2 and N3 of the C-helix.

The calcium-free folded state was the least stable with a valine at the N-cap position. The binding of calcium to the calcium-free folded state stabilized the valine mutant by 4.19 kcal/mol which was more than that observed for any of the other amino acid substitutions (Table 3.8). The effects of this mutation are speculated to be a destabilizing effect on the unfolded state with a stabilization of the calcium-saturated state which may be due to the side chain becoming buried within the hydrophobic core.

$U \rightleftharpoons F_{-Ca} \rightleftharpoons F_{+Ca}$ (destabilizes the unfolded state
with some stabilization of the calcium saturated folded state)

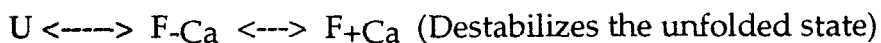
As the N-cap of the G-helix in the high-affinity domain, the valine mutant produced the least change in 2° structure on binding calcium (Table 3.1). It was the most stable variant in the folded calcium-free state (Table 3.8). This is the opposite of what was observed for the valine substitution at the N-cap of the C-helix. This stabilization may be due to a new hydrophobic interaction within the protein which reduced solvent exposure of the side chain early on in the folding

pathway rather than later with the binding of calcium. Compared to the threonine residue, on binding calcium, the valine substitution at position 130 destabilized the protein by 3.27 kcal/mol, with a drastic reduction in the calcium-affinity of the paired calcium binding sites in the high affinity domain (Figure 3.25).



(g) Analysis of the Isoleucine Mutation

The isoleucine residue was only available at the N-cap of the G-helix in the high-affinity domain. Isoleucine has a large hydrophobic side chain which is destabilizing. Due to steric hindrance, the side chain is probably exposed to solvent. The lysine side chain is not likely able to shelter the isoleucine side chain from interactions with the solvent. The hydrophobic side chain is again unable to form a stabilizing interaction with the N3 residue of the helix. TnC with an isoleucine at the N-cap had a lower calcium-affinity than threonine but it was more stable than threonine in both the calcium-free and calcium-saturated folded states. This increased stability may be due to an altered folded structure identified by the "m" value in the plot of ΔG versus [urea] (Figure 3.31 and Table 3.5).



To summarize, steady state fluorescence spectroscopy of the low-affinity domain revealed a decrease in stability as the size of the hydrophobic side chain increased. These results can be interpreted to mean that the side chain is exposed to solvent. However, in the high-affinity domain the valine residue was

unexpectedly stable when compared to glycine and isoleucine. The valine and isoleucine residues differ by one methyl group. It is possible that while the isoleucine side chain cannot be accommodated within the folded structure of the protein, the valine may be small enough to "fit" but in doing so has distorted the structure of the folded state. The formation of a new, stabilizing, hydrophobic interaction within the protein may have reduced the exposure of the side chain to the solvent but it has also resulted in a decrease in the ion-binding affinity of the protein. The calcium-affinity of the valine mutant in the high-affinity domain decreased by 2 orders of magnitude when compared to the other N-cap mutants of the same domain.

The threonine at the N-cap of the G-helix, had the lowest energy requirement to fold to the F-Ca conformation and has nearly the highest calcium-binding affinity. It is known that TnC can also bind magnesium at the high-affinity binding sites and that magnesium bound to loops III and IV is sufficient for the binding of TnC to the thin filament. Recent work demonstrated that there is a change in conformation associated with the exchange of magnesium ions for calcium ions (Trigo-Gonzalez et al, 1992). It would be interesting to measure the free energy change associated with magnesium ions binding to the high-affinity domain and compare this to the binding of calcium ions. This may provide a possible explanation for the small free energy change associated with the folding of the calcium-free form of the wild-type protein. The threonine residue was observed to provide the largest degree of stabilization in going from the F-Ca to the F₊Ca folded states (Table 3.8).

4.4 Polyclonal Antibody to chicken skeletal Troponin C

The polyclonal antibody was raised against the cII-fusion chicken skeletal TnC protein using rabbits. The sequence of chicken skeletal TnC and rabbit

skeletal TnC are almost identical. Chicken TnC has 6 residues at the beginning of its sequence, (M, A, S, M, T, D) which are not found in the rabbit sequence. From residue seven for chicken, which is residue 3 in rabbits, the sequences diverge at 8 residues with remaining differences mostly being conserved substitutions. ie. Glu to Asp (2), Lys to Arg, Trp to Phe, Val to Thr, Gly to Ser, Ser to Asp and Ala to Ile. If the antibody had been made to a region within the TnC sequence, binding to rabbit TnC would have been observed. The production of antibody to an epitope within the sequence of chicken TnC would likely have been deleterious to the rabbit. The antibodies were probably generated against the cII fusion portion of the protein inoculum. Since the antibody recognized the purified chicken TnC (minus the fusion peptide) but did not recognize rabbit TnC, the recognition site is suggested to involve the 5 residues at the beginning of the chicken Tnc sequence. This will be advantageous in future work with rabbit muscle fibers stripped of native rabbit TnC and reconstituted with chicken TnC. With this antibody, it may be possible to accurately measure the quantity of TnC associated with the thin filament in the reconstituted fiber.

5. Conclusion

This study showed that the calcium ion affinity can be tailored by inserting different residues at the N-cap position. However, the same mutation, located at equivalent positions but in separate domains within the protein, affected the formation of the helix and the stability of the protein to different extents. The tertiary structure of the protein must be considered in the selection of the N-cap residue if we wish to engineer calcium binding proteins with new ion affinities.

REFERENCES

1. Ausubel, F.M., Brent, R., Kingston, R.E., Moore, D.D., Seidman, J.G., Smith, J.A. & Struhl, K., *Current Protocols in Molecular Biology*, Volume 2 Greene Publishing Associates and Wiley-Interscience, 1992.
2. Armstrong, K.M. & Baldwin, R.L., Charged 9- Affects α -helix Stability at All Positions in the Helix by Interacting with the Backbone Charges, *Proc. Natl. Acad. Sci. U.S.A.*, **90**, 11337-11340, 1993.
3. Bell, J.A., Becktel, W.J., Sauer, U., Baase, W.A. & Mathews, B.W., Dissection of Helix Capping in T4 Lysozyme by Structural and Thermodynamic analyses of Six Amino Acid Substitutions at Thr 59, *Biochemistry*, **31**, 3590-3596, 1992.
4. Cantor, R.C. & Schimmel, P.R., *Biophysical Chemistry, Part II: Techniques for The Study of Biological Structure and Function*, W.H. Freeman and Co. New York, 1980.
5. Chakrabartty, A., Doig, A.J., & Baldwin, R.L., Helix Capping Propensities in Peptides Parallel Those in Proteins, *Proc. Natl. Acad. Sci. U.S.A.*, **90**, 11332-11336, 1993.
6. Chakrabartty, A., Kortemme, T., Padmanabhan S., & Baldwin, R.L., Aromatic Side-Chain Contribution to Far-Ultraviolet Circular Dichroism of Helical Peptides and Its Effect on Measurement of Helix Propensities, *Biochemistry*, **32**, 5560-5565, 1993.
7. Chen, Y.W. & Fersht, A.R., Stability and Solvation of Thr/Ser to Ala & Gly Mutations at the N-cap of α -helices, *FEBS Letters*, **347**, 304-309, 1994.
8. Colowick, S.P. & Womack, F.C., Binding of Diffusible Molecules by Macromolecules: Rapid Measurement by Rate of Dialysis, *J. Biol. Chem.*, **244**, 774-777, 1969.
9. Colowick, S.P. & Womack, F.C., Rapid Measurement of Binding of Ligands by Rate of Dialysis, *Methods Enzymology*, **27**, 464-471, 1973.
10. Creighton T.E., Stability of α -helices, *Nature*, **326**, 547-548, 1987.
11. da Silva, A.C.R., Araujo, A.H.B., Herzberg, O., Moulton, J., Sorenson, M., Reinach, R.C., Troponin-C Mutants with Increased Calcium Affinity, *Eur. J. Biochem.*, **213**, 599-604, 1993.

12. Dotson, D.G. and Putkey, J.A., Differential Recovery of Calcium Binding Activity in Mutated EF-Hands of Cardiac Troponin C. *J. Biol. Chem.*, **268**, 24067-24073, 1993.
13. Drake, A.F., Circular Dichroism, Methods in Molecular Biology, Microscopy, Optical Spectroscopy and Macroscopic Techniques, Humana Press, Totowa, New Jersey, 219-244, 1994.
14. Dryden, D.T.F. & Pain, R.H., Assignment of the Heterogeneous Static and Time-Resolved Tryptophan Fluorescence of 3-Phosphoglycerate Kinase, *Biochimica et Biophysica Acta*, **997**, 313-321, 1989.
15. Edwin T. Harper E.T., & Rose, G., Helix Stop Signals in Proteins and Peptides: The Capping Box, *Biochemistry*, **32**, 7605-7609, 1993.
16. Feldmann, K., New Devices for Flow Dialysis and Ultrafiltration for the Study of Protein-Ligand Interactions. *Analytical Biochemistry*, **88**, 225-235, 1978.
17. Forood, B., Feliciano, E.J., & Nambiar, K.P., Stabilization of α -helical structures in short peptides via end capping, *Proc. Natl. Acad. Sci. U.S.A.*, **90**, 838-842, 1993.
18. Gagne, S.M., Tsuda, S. Li, M.X., Chandra, M., Smillie, L.B. & Sykes, B.D., Quantification of the Calcium-Induced Secondary Structural Changes in the Regulatory Domain of Troponin C, *Protein Science* **3**: 1961-1974 (1994).
19. Garcia, P., Desmadril, M., Minard, P. & Yon, J.M., Evidence for Residual Structures in an Unfolded Form of Yeast Phosphoglycerate Kinase, *Biochemistry*, **34**, 397-404, 1995.
20. Harpaz, Y., Elmasry, N., Fersht A.R. and Henrick, K., Direct Observation of Better Hydration at the N-terminus of an α -helix with Glycine Rather Than Alanine as the N-cap Residue, *Proc. Natl. Acad. Sci. U.S.A.*, **91**, 311-315, 1994.
21. Krudy, G.A., Brito, R.M.M., Putkey, J.A. & Rosevear, P.R., Conformational Changes in the Metal-Binding Sites of Cardiac Troponin C Induced by Calcium Binding, *Biochemistry*, **31**, 1595-1602, 1992.
22. Lapanje, S., Physicochemical Aspects of Protein Denaturation, Wiley-Interscience Publication, John Wiley & Sons, New York, 1978.

23. Li, M.X., Gagne, S.M., Tsuda, S., Kay, C.M., Smillie, L.B., & Sykes, B.D., Calcium Binding to the Regulatory N-Domain of Skeletal Muscle Troponin C Occurs in a Stepwise Manner, *Biochemistry*, **34**, 8330-8340, 1995.
24. Lyu, P.C., Zhou, H. X., Jelveh, N., Wemmer, D.E., & Kallenbach, N.R., Position-Dependent Stabilizing Effects in α -Helices: N-Terminal Capping in Synthetic Model Peptides, *J. Am. Chem. Soc.*, **114**, 6560-6562, 1992.
25. Marqusee, S., Robbins, V.H., & Baldwin, R.L., Unusually stable helix formation in short alanine-based peptides, *Proc. Natl. Acad. Sci. U.S.A.*, **86**, 5286-5290, 1989.
26. Mathews, C.K. & van Holde, K.E., *Biochemistry*, The Benjamin/Cummings Publishing Company, Inc. 1990.
27. Mathews C.R. & Crisanti, M.M., Urea-Induced Unfolding of the α Subunit of Tryptophan Synthase: Evidence for a Multistate Process, *Biochemistry*, **20**, 784-792, 1981.
28. Nagai, K. & Thogersen, H.C., Synthesis & Sequence-Specific Proteolysis of Hybrid Proteins Produced in *Escherichia coli*, *Methods in Enzymology*, **153**, 461-481, 1987.
29. Pace, C.N., Determination and Analysis of Urea and Guanidinium Hydrochloride Denaturation Curves, *Methods in Enzymology*, **131**, 266-279, 1986.
30. Pace C.N., Laurents, D.V. & Erickson, R.E., Urea Denaturation of Barnase: pH Dependence and Characterization of the Unfolded State. *Biochemistry*, **31**, 2728-2734, 1992.
31. Pearlstone, J., Borgford, T., Chandra, M., Oikawa, K., Kay, C., Herzberg, O., Moulton, J., Herklotz, A., Reinach, F.C., & Smillie, L.B., Construction and Characterization of a Spectral Probe Mutant of Troponin C: Application to Analyses of Mutants with Increased Calcium Affinity, *Biochemistry*, **36**, 6545-6553, 1992.
32. Porumb, T., Determination of Calcium-Binding Constants by Flow Dialysis, *Analytical Biochemistry*, **220**, 227-237, 1994.
33. Robertson, S.P., Johnson, J.D. & Potter, J.D., The Time-Course of Ca^{2+} Exchange with Calmodulin, Troponin, Parvalbumin and Myosin in Response to Transient Increases in Ca^{2+} , *Biophys. J.*, **34**, 559-569, 1981.

34. Presta, L.G. & Rose, G.D. Helix Signals in Proteins, *Science* **240**, 1632-1641, 1988.
35. Procyshyn, R.M. & Reid, R.E., A Structure/ Activity Study of Calcium Affinity and Selectivity Using a Synthetic Peptide Model of the Helix-Loop-Helix Calcium Binding Motif, *J. Biol. Chem.*, **269**, 1641-1647, 1994.
36. Reid, R.E., Gariepy, J., Saund, A.K. & Hodges, R.S., Calcium Induced Protein Folding, *J. Biol. Chem.*, **256**, 2742-2751, (1981).
37. Richardson J.S., & Richardson, D.C., Amino Acid Preferences for specific locations at the ends of α -helices *Science*, **240**, 1988, 1648-1652.
38. Sambrook, J., Fritsch, E.F., Maniatis, T., *Molecular Cloning, A Laboratory Manual*, 2nd Edition, Cold Spring Harbor Laboratory Press, 1989.
39. Santoro, M.M. & Bolen, D.W., Unfolding Free Energy Changes Determined by the Linear Extrapolation Method. 1. Unfolding of Phenylmethanesulfonyl α -Chymotrypsin Using Different Denaturants *Biochemistry*, **27**, 8063-8068, 1988.
40. Santoro, M.M. & Bolen, D.W., A Test of the Linear Extrapolation of Unfolding Free Energy Changes over an Extended Denaturant Concentration Range, *Biochemistry*, **31**, 4901-4907, 1992.
41. Satyshur, K.A., Rao, S.T., Pyzalska, D., Drendel, W., Greaser, M. & Sundaralingam, M., Refined Structure of Chicken Skeletal Muscle Troponin C in the Two-Calcium State at 2\AA Resolution, *J. Biol. Chem.*, **263**, 1628-1647, 1988.
42. Szczesna, D., Guzman, G., Miller, T., Zhao, J., Farohkhi, K., Ellemberger, H., & Potter, J.D., The Role of the Four Ca^{2+} Binding Sites of Troponin C in the Regulation of Skeletal Muscle Contraction, *J. Biol. Chem.* **271**, 8381-8386, (1996)
43. Selkirk, E.E., *Physiology*, Fourth Edition, Little, Brown and Company, Boston, 1976.
44. Serrano, L. & Fersht, A.R., Capping and α -helix stability, *Nature*, **342**, 296-299, 1989.
45. Serrano, L., Kellis Jr., J.T., Cann, P., Matouschek, A. & Fersht, A.R., The Folding of an Enzyme: Substructure of Barnase and the Contribution of Different Interactions to Protein Stability, *J. Mol. Biol.*, **224**, 783-804, 1992.

46. Serrano, L., Sancho, J., Hirshberg, M. & Fersht, A.R., α -Helix Stability in Proteins: Empirical Correlations Concerning Substitution of Side-Chains at the N- and C-Caps and the Replacement of Alanine by Glycine or Serine at Solvent Exposed Surfaces, *J. Biol. Chem.*, **227**, 544-559, 1992.
47. Shaw, G.S., Hodges, R.S. & Sykes, B.D., Probing the Relationship between α -Helix Formation and Calcium Affinity in Troponin C: ^1H NMR Studies of Calcium Binding to Synthetic and Variant Site III Helix-Loop-Helix Peptides, *Biochemistry*, **30**, 8339-8347, 1991.
48. Shoemaker, K.R., Kim, P.S., York, E.J., Stewart, J.M. & Baldwin, R.L. Tests of the Helix Dipole Model for Stabilization of α -helices, *Nature* **326**, 563-567, 1987.
49. Smith, J., Clarke, A.R., Chia, W.N., Irons, L.I., Atkinson, T. & Holbrook, J.J., Detection and Characterization of Intermediates in the Folding of Large Proteins by the Use of Genetically Inserted Tryptophan Probes, *Biochemistry*, **30**, 1028-1036, 1991.
50. Sorenson, M.M., de Silva, A.C.R., Gouveia, C.S., Sousa, V.P., Oshima, W., Ferro, J.A. & Reinach, F.C., Concerted Action of the High Affinity Calcium Binding in Skeletal Muscle Troponin C., *J. Biol. Chem.*, **270**, 9770-9777, 1995.
51. Stryer, L., *Biochemistry*, Second Edition, W.H. Freeman and Company, San Francisco, 1981.
52. Trigo-Gonzalez, G., Structure and Function Relationships in Troponin C Probed by Site-Directed Mutagenesis, Master's Thesis, Simon Fraser University, 1992.
53. Trigo-Gonzalez, G., Racher, K., Burtnick, L., & Borgford, T., A Comparative Spectroscopic Study of Tryptophan Probes Engineered into High-Affinity and Low Affinity Domains of Recombinant Chicken Troponin C, *Biochemistry*, **36**, 7009-7015, 1992.
54. Trigo-Gonzalez *et al*, *Biochem.* **37**, 9826-9831, 1993).
55. Tsalkova, T.N. & Privalov, P.L., Thermodynamic Study of Domain Organization in Troponin C and Calmodulin, *J. Mol. Biol.*, **181**, 533-544 (1985).
56. van Holde, K.E., *Physical Biochemistry*, Second Edition, Prentice-Hall, Inc. Englewood Cliffs, N.J., 1985.

57. Varley, P.G., *Fluorescence Spectroscopy, Methods in Molecular Biology, Microscopy, Optical Spectroscopy and Macroscopic Techniques*, Humana Press, Totowa, New Jersey, 203-218, 1994.
58. Yao, M. & Bolen, W., How Valid are Denaturant-Induced Unfolding Free Energy Measurements? Level of Conformation to Common Assumptions over an Extended Range of Ribonuclease A Stability. *Biochemistry*, **34**, 3771-3781, 1995.
59. Zhou, H.X., Lyu, P., Wemmer D.E. & Neville R. Kallenbach, Alpha Helix Capping in Synthetic Model Peptides by Reciprocal Side Chain-Main Chain Interactions: Evidence for an N Terminal "Capping Box", *Proteins: Structure, Function and Genetics*, **18**, 1-7 1994.
60. Zhou, H. X., Pinker, R.J., & Kallenbach, N.R., Capping Interaction in Isolated α -Helices: Position-Dependent Substitution Effects and Structure of a Serine-Capped Peptide Helix, *Biochemistry*, **32**, 421-425, 1993.
61. Zot, H.G. & Potter, J.D., A Structural Role for the Ca^{2+} - Mg^{2+} Sites on Troponin C in the Regulation of Muscle Contraction: Preparation and Properties of Troponin C Depleted Myofibrils, *J. Biol. Chem.*, **257**, 7678-7683, 1982.